

## **DISCLAIMER**

**This report was prepared as an account of work sponsored by an agency of the United States Government. Neither the United States Government nor any agency thereof, nor any of their employees, makes any warranty, express or implied, or assumes any legal liability or responsibility for the accuracy, completeness, or usefulness of any information, apparatus, product, or process disclosed, or represents that its use would not infringe privately owned rights. Reference herein to any specific commercial product, process, or service by trade name, trademark, manufacturer, or otherwise does not necessarily constitute or imply its endorsement, recommendation, or favoring by the United States Government or any agency thereof. The views and opinions of authors expressed herein do not necessarily state or reflect those of the United States Government or any agency thereof. Reference herein to any social initiative (including but not limited to Diversity, Equity, and Inclusion (DEI); Community Benefits Plans (CBP); Justice 40; etc.) is made by the Author independent of any current requirement by the United States Government and does not constitute or imply endorsement, recommendation, or support by the United States Government or any agency thereof.**

## ARM Aerial Instrument Workshop Report

F Mei	D Dexheimer
J Fast	M Diao
B Geerts	A Bucholtz
L Riihimaki	C Flynn
T Thornberry	T Campos
S Springston	C Kuang
J Tomlinson	B Schmid

July 2020



## **DISCLAIMER**

This report was prepared as an account of work sponsored by the U.S. Government. Neither the United States nor any agency thereof, nor any of their employees, makes any warranty, express or implied, or assumes any legal liability or responsibility for the accuracy, completeness, or usefulness of any information, apparatus, product, or process disclosed, or represents that its use would not infringe privately owned rights. Reference herein to any specific commercial product, process, or service by trade name, trademark, manufacturer, or otherwise, does not necessarily constitute or imply its endorsement, recommendation, or favoring by the U.S. Government or any agency thereof. The views and opinions of authors expressed herein do not necessarily state or reflect those of the U.S. Government or any agency thereof.

## **ARM Aerial Instrument Workshop Report**

F Mei, Pacific Northwest National Laboratory (PNNL)  
D Dexheimer, Sandia National Laboratories  
J Fast, PNNL  
M Diao, San Jose State University  
B Geerts, University of Wyoming  
A Bucholtz, U.S. Naval Postgraduate School  
L Riihimaki, Cooperative Institute for Research in Environmental Sciences/National Oceanic and Atmospheric Administration (NOAA)  
C Flynn, University of Oklahoma  
T Thornberry, NOAA  
T Campos, National Center for Atmospheric Research  
S Springston, Brookhaven National Laboratory (BNL)  
C Kuang, BNL  
J Tomlinson, PNNL  
B Schmid, PNNL

July 2020

Work supported by the U.S. Department of Energy,  
Office of Science, Office of Biological and Environmental Research

## **Acknowledgments**

The workshop conveners and the co-authors of this report thank all the scientists who energetically participated in the workshop discussions and generously contributed their time and ideas to the Atmospheric Radiation Measurement user facility. We especially appreciate the workshop white paper authors who presented the most exciting instrumentation in various research areas and the workshop speakers who gave the insightful presentations. We also appreciate report preparation by the ARM Communications Team at Pacific Northwest National Laboratory.

## Acronyms and Abbreviations

2D	two-dimensional
2D-S	two-dimensional stereo probe
3D	three-dimensional
4STAR	Spectrometer for Sky-Scanning Sun Tracking Atmospheric Research
AAE	absorption Ångström exponent
AAF	ARM Aerial Facility
ACAPEX	ARM Cloud Aerosol Precipitation Experiment
ACE-ENA	Aerosol and Cloud Experiments in the Eastern North Atlantic
ACTIVATE	Aerosol Cloud Meteorology Interactions Over the Western Atlantic Experiment
ACUASI	Alaska Center for UAS Integration
ADI	Aerosol Dynamics Inc.
AERONET	Aerosol Robotic Network
AIMMS	aircraft integrated meteorological measurement system
AMF	ARM Mobile Facility
APS	aerodynamic particle sizer
ARM	Atmospheric Radiation Measurement
ASR	Atmospheric System Research
ATOM	Atmospheric Tomography Mission
ATOMIC	Atlantic Tradewind Ocean-Atmosphere Mesoscale Interaction Campaign
BBOA	biomass burning organic aerosol
BBOP	Biomass Burning Observation Project
BC	black carbon
BER	Biological and Environmental Research
BNL	Brookhaven National Laboratory
BrC	brown carbon
CACTI	Cloud, Aerosol, and Complex Terrain Interactions
CAPS	cloud, aerosol, and precipitation spectrometer; cavity enhance phase-shifted
CARES	Carbonaceous Aerosol and Radiative Effects Study
CAS	cloud and aerosol spectrometer
CCN	cloud condensation nuclei
CDS	cloud drop spectrometer
CFDC	continuous flow diffusion chamber
CHAPS	Cumulus Humilis Aerosol Process Study
CIRES	Cooperative Institute for Research in Environmental Sciences
CLD	chemiluminescence detection

CLIVAR	Climate and Ocean: Variability, Predictability and Change
CPC	condensation particle counter
CPI	cloud particle imager
CSI	cloud spectrometer and impactor
CVI	counterflow virtual impactor
DC	direct current
DFB TDL	distributed feedback tunable-diode laser
DLR	Deutsches Zentrum fur Luft- und Raumfahrt (German Aerospace Center)
DMT	Droplet Measurement Technologies
DOE	U.S. Department of Energy
DTS	distributed temperature sensing
EBSD	Earth and Biological Sciences Directorate (PNNL)
EC	elemental carbon
ECC	electro-chemical cell
ECL	elastic cloud lidar
EESSD	Earth and Environmental Systems Sciences Division
ELVOC	extremely low-volatility organic compounds
EMSL	Environmental Molecular Sciences Laboratory
FAA	Federal Aviation Administration
FAAM	Facility for Airborne Atmospheric Measurements
FCDP	fast cloud droplet probe
FFRDC	Federally Funded Research and Development Center
FIMS	fast integrating mobility spectrometer
G-1	Gulfstream-159
GAW	Global Atmosphere Watch
GNSS	Global Navigation Satellite Systems
GoAmazon	Observations and Modeling of the Green Ocean Amazon
GPS	Global Positioning System
HAMSR	high-altitude MMIC sounding radiometer
HARP	HIAPER Airborne Radiation Package
HIAPER	high-performance instrumented airborne platform for environmental research
HIMIL	HIAPER modular inlet
HIPPO	HIAPER Pole-to-Pole Observations
HIS	hyperspectral imaging
HI-SCALE	Holistic Interactions of Shallow Clouds, Aerosols, and Land-Ecosystems
HOLODEC	Holographic Detector for Clouds
HR-AMS	high-resolution aerosol mass spectrometer
HR-ToF-AMS	high-resolution time-of-flight aerosol mass spectrometer

HR-ToF-CIMS	high-resolution time-of-flight chemical ionization mass spectrometer
HSRL	high-resolution spectral lidar
HVPS	high-volume precipitation spectrometer
ICL	interband cascade laser
IN	ice nuclei
INFLAME	In situ Net Flux with the Atmosphere of Earth
INP	ice nucleating particle
IR	infrared
IRISS	Integrated Remote and In Situ Sensing
IRT	infrared thermometer
IWC	ice water content
JPL	Jet Propulsion Laboratory (NASA)
LAS	laser aerosol spectrometer
LBL	Lawrence Berkeley National Laboratory
LED	light-emitting diode
LIF	laser-induced fluorescence
LVOC	low-volatility organic compound
LW	longwave
LWC	liquid water content
MFR	multifilter radiometer
MILAGRO	Megacities Initiative: Local and Global Research Observations
miniSPLAT	miniaturized single-particle mass spectrometer
MMIC	monolithic microwave integrated circuit
MOSAiC	Multidisciplinary Drifting Observatory for the Study of Arctic Climate
MPL	micropulse lidar
MW	microwave
NAIS	neutral air ion spectrometer
NASA	National Aeronautics and Space Administration
NCAR	National Center for Atmospheric Research
NDVI	Normalized Difference Vegetation Index
NightFOX	Nighttime Fire Observations eXperiment
NOAA	National Oceanic and Atmospheric Administration
NPF	new particle formation
NRC	National Research Council Canada
NSF	National Science Foundation
OAP	optical array probe
OASIS	Optical Array Shadow Imaging Software
OPALS	open-path ammonia laser sensor

OVOC	oxygenated volatile organic compound
PAMR	profiling airborne microwave radiometer
PCASP	passive cavity aerosol spectrometer
PHIPS	Particle Habit Imaging and Polar Scattering
PI	principle investigator
PILS	particle-into-liquid sampler
PILS-IC	particle-into-liquid sampler with ion chromatograph
PM	particulate matter
PMF	positive matrix factorization
PMS	Particle Measuring Systems
PNNL	Pacific Northwest National Laboratory
POA	primary organic aerosol
POPS	printed optical particle spectrometer
PSAP	particle soot absorption photometer
PSL	polystyrene latex
PTI	photothermal interferometer
PTR-MS	proton transfer reaction mass spectrometer
PTR-ToF-MS	proton transfer reaction time-of-flight mass spectrometer
PVM	particle volume monitor
QCL	quantum cascade later
SAE	scattering Angstrom exponent
SAFIRE	Service des Avions Francais Instrumentés pour la Recherche en Environnement
SAIL	Surface Atmosphere Integrated Field Laboratory
SBIR	Small Business Innovation Research (DOE)
SEA	Science Engineering Associates
SGP	Southern Great Plains
S-HIS	scanning high-resolution interferometer sounder
SMPS	scanning mobility particle sizer
SOA	secondary organic aerosol
SP2	single-particle soot photometer
SP2-XR	single-particle soot photometer – extended range
SPARTAN	Surface PARTiculate mAtter Network
SPEC	Stratton Park Engineering Company
SSA	single-scattering albedo
SSFR	solar spectral flux radiometer
SST	sea surface temperature
STAP	single-channel tricolor absorption photometer
SW	shortwave

SWaP	size, weight, and power
TBS	tethered balloon systems
TCAP	Two-Column Aerosol Project
TDCIMS	thermal desorption chemical ionization mass spectrometry
TDL	tunable-diode laser
TRAC	time-resolved aerosol collector
TRACER	Tracking Aerosol Convection Interactions ExpeRiment
TSI	Trust Scientific Innovation
UAS	unmanned aerial systems
$\mu$ COPP	micro combined optical particle probe
UCPC	ultrafine condensation particle counter
UHSAS	ultra-high-sensitivity aerosol spectrometer
UIOOPDS	University of Illinois/Oklahoma Optical Array Probe Processing Software
UK	United Kingdom
UPS	uninterruptible power supply
URL	Universal Resource Locator
USB	universal serial bus
UV	ultraviolet
VAC	volts alternating current
VCSEL	vertical cavity surface emitting laser
VOC	volatile organic compound
WCL	Wyoming cloud lidar
WCM	water content monitor
WIBS	Wideband Integrated Bioaerosol Sensor
WMO	World Meteorological Organization
WRF	Weather Research and Forecasting model
WRF-SFIRE	Weather Research and Forecasting fire-spread model
WSOC	water-soluble organic carbon

## Contents

Acknowledgments.....	iv
Acronyms and Abbreviations .....	v
1.0 Introduction .....	1
2.0 Workshop Structure.....	2
2.1 Objectives and Goals.....	4
2.2 Organization of the Workshop .....	4
2.3 Community Participation .....	5
3.0 Workshop Discussion .....	6
3.1 Science Drivers .....	6
3.2 Measurements from Piloted Aircraft.....	7
3.2.1 Research Infrastructure .....	7
3.2.2 Aircraft and Atmospheric State Measurements.....	11
3.2.3 Radiation Measurements .....	14
3.2.4 Aerosol Measurements.....	19
3.2.5 Cloud Measurements.....	33
3.2.6 Gas-Phase Measurements.....	39
3.3 Measurements from Tethered Balloon System (TBS) .....	41
3.3.1 Current ARM TBS Capabilities .....	41
3.3.2 Proposed ARM TBS Capabilities.....	42
3.4 Measurements from Unmanned Aerial System (UAS).....	47
3.4.1 UAS Platform – ARM ArcticShark Versus Other Platforms .....	48
3.4.2 Current ARM UAS Instruments.....	50
3.4.3 Proposed ARM UAS Instruments .....	51
4.0 Recommendations .....	54
4.1 Recommendations for Measurements from Piloted Aircraft.....	55
4.1.1 Atmospheric State Measurements .....	55
4.1.2 Radiation Measurements .....	55
4.1.3 Aerosol and Gas-phase Measurements.....	56
4.1.4 Cloud Measurements.....	56
4.2 Recommendations for Measurements from Unmanned Platforms .....	57
5.0 References .....	57
Appendix A – Workshop Advisees and Invitees .....	A.1
Appendix B – ARM Aerial Instrumentation Workshop Agenda.....	B.1
Appendix C – White Papers.....	C.1

## Figures

1	The AAF's new Bombardier Challenger 850.....	2
2	Group photo from ARM Aerial Instrumentation Workshop at Discovery Hall, PNNL.....	3
3	ARM's tethered balloon systems can go into and above clouds to collect data related to horizontal wind, ice microphysics, turbulence, thermodynamic state, aerosols, and the cloud-top environment.....	4
4	Distribution of workshop white papers by field of study.....	5
5	Distribution of invited participants.....	6
6	Instruments mounted under G-1 wing.....	9
7	A notional installation for the wing pylons.....	9
8	Computational fluid dynamic along the fuselage at the first window position.....	10
9	Jason Tomlinson speaks at the ARM Aerial Instrumentation Workshop.....	13
10	Adjusting the instruments in flight aboard the G-1 aircraft.....	15
11	Troy Thornberry participates at the ARM Aerial Instrumentation Workshop.....	17
12	Discussion of network configuration improvements at the AAF Instrumentation Workshop.....	20
13	The G-1 flying above the clouds during the 2018-2019 CACTI field campaign in Argentina.....	21
14	Albert Mendoza, ARM engineer, takes the floor at the ARM Aerial Instrumentation Workshop.....	27
15	Minghui Diao discusses instrumentation and measurements at the AAF workshop.....	29
16	Inlet on G-1 aircraft.....	31
17	View from the G-1 aircraft during the HI-SCALE field campaign at the SGP in 2016.....	32
18	ARM technical director Jim Mather and Radiance Calmer at the workshop.....	35
19	TBS in flight at the ARM SGP CF in 2019.....	42
20	ARM TBS winch.....	42
21	Size-dependent detection efficiency of ADI MAGIC 200 CPC using charged ammonium sulfate.....	44
22	Enclosure with MAGIC CPC and system peripherals installed.....	45
23	Vertically resolved number concentration (1–3 nm) and altitude at SGP.....	45
24	Schematic for offline AMS sample analysis.....	46
25	Component drawing of University of Houston SO <sub>2</sub> sonde.....	47
26	The AAF's ArcticShark on the tarmac.....	48
27	Overview of sUAS campaigns for the atmospheric studies by Radiance Calmer.....	49
28	The NightFOX in situ instrument package payload.....	50
29	The NightFOX remote-sensing instrument package payload.....	50
30	Sebastien Biraud speaks with colleagues at the AAF Instrumentation Workshop.....	55

## Tables

1	Summary of atmospheric state instruments and measurements.....	11
2	Comparisons of VCSEL and DFB open-path laser hygrometers.....	13
3	Comparisons between HAMSR and PAMR microwave radiometers.....	14
4	Broadband radiometer options.....	18
5	Spectral radiometer options.....	19
6	Instruments that measure total particle number and aerosol size distribution.....	21
7	Instruments that measure aerosol composition.....	23
8	Instruments that measure trace gases than are aerosol precursors or can be used to infer processes influencing aerosol formation.....	25
9	Instruments that measure aerosol optical properties.....	27
10	Instruments that measure CCN and IN.....	30
11	Aerosol and trace gas instruments used in the HU-25 Falcon during ACTIVATE.....	33
12	Current AAF cloud probes.....	34
13	Current sources of in situ cloud liquid/ice water estimation at AAF.....	34
14	Select next-generation in situ cloud probes.....	35
15	Select cloud lidars.....	36
16	Select airborne cloud and precipitation radars.....	38
17	Summary of aerosol precursor, aerosol processing, and air mass tracer present capabilities.....	39
18	Summary of emerging technologies and opportunities for improved capabilities.....	40
19	Summary of presented instrumentation and associated measurement, vendor source, operational modes, and status.....	43
20	Commercially available 1-nm CPC systems and relevant specifications and recommendations.....	44
21	Existing AAF ArcticShark instruments.....	51
22	Proposed instruments for the ArcticShark UAS.....	52
23	Sharkeye combination cloud probe measurement specifications.....	52
24	Compact, mid-IR methane sensor performance.....	54

## 1.0 Introduction

The mission of the U.S. Department of Energy's (DOE) Biological and Environmental Research (BER) program is to “support transformative science and scientific user facilities to achieve a predictive understanding of complex biological, earth, and environmental systems for energy and infrastructure security, independence, and prosperity.” (<https://science.osti.gov/ber>) Aligned with the BER central mission, the Earth and Environmental Systems Sciences Division (EESSD) plays a vital role in supporting the fundamental research to understand and predict Earth’s climate and environmental systems, and is also in a unique position to inform the development of sustainable solutions to the nation’s energy and environmental challenges.

Specifically, EESSD manages two scientific user facilities: the Atmospheric Radiation Measurement (ARM) user facility and the Environmental Molecular Sciences Laboratory (EMSL). These facilities provide the broader scientific community with scientific expertise, technical capabilities, and unique data sets to facilitate science in areas of importance to DOE. As a multi-platform scientific user facility, ARM aims to fulfill the needs predominantly within the EESSD Atmospheric System Research (ASR) and the Earth and Environmental System Modeling (EESM) mission areas, and provide the critical measurements required to improve understanding of aerosol and cloud life cycles and their interactions, and their coupling with the Earth’s surface.

Over the years, ARM has carried out piloted and unmanned aircraft campaigns under different organizational and operational paradigms (Schmid et al. 2014, 2016). Building on its success, the ARM Aerial Facility (AAF) continues to complement the ground-based observations with airborne in situ cloud, aerosol, and trace gas observations as well as measurements of atmospheric state and atmospheric radiation. During the past three years, ARM has managed field campaigns using unmanned aerial systems (UAS) and tethered balloon systems (TBS) at Oliktok Point in Alaska to improve understanding of atmospheric processes in the Arctic. In 2019, following a careful evaluation of scientific community needs, ARM acquired a Bombardier Challenger 850 regional jet to replace the vintage Grumman Gulfstream-159 turboprop aircraft previously used by AAF. With this new “laboratory in the sky”, AAF is evaluating its current and future aerial observation capabilities to continue satisfying the needs of the research community.



**Figure 1.** The AAF's new Bombardier Challenger 850.

Previous DOE workshop reports have identified that in situ measurements are desirable at both the surface and vertically through the atmosphere for any deployment. A piloted research aircraft beneficially allows for a comparably large payload, which expands potential deployment and validation opportunities for state-of-the-science instrumentation. The advantages of using the UAS or TBS platforms include improved temporal coverage and vertical measurement resolution, with limitations in sensitivity, accuracy, and capability. ARM announced a white paper call for researchers to identify additional airborne measurements that should be adopted as facility instruments due to their essential nature to the broad scientific community. This call was intended to guide the addition and implementation of measurement capabilities on its recently acquired piloted aircraft (the [Bombardier Challenger 850 regional jet](#)), its midsize unmanned aerial system ([the ArcticShark UAS](#)), and its tethered balloon systems ([TBS](#)) to enhance ARM's aerial observation capability and better link ARM airborne observations to the surface-based observatories. Over 40 white paper (see Appendix C) responses were received from the community, which spurred and informed discussion at an invitation-based ARM Aerial Instrumentation Workshop held in March 2020 at Pacific Northwest National Laboratory (PNNL). A list of workshop attendees is given in Appendix A, and those participants represent broad and balanced scientific expertise in the areas of meteorology, clouds, aerosol, trace gases, radiation and surface properties. The workshop agenda is in Appendix B. The summary of the planning process of the workshop is presented in the following section (Workshop Structure). All session chairs compiled inputs from the participants and responses from the white papers to synthesize high-level summaries of the discussion, which are presented in section 3 (Workshop Discussion). Input obtained through this workshop discussion and the breakout session during the joint ARM/ASR principal investigator (PI) meeting is prioritized in section 4 (Next Steps) to develop a roadmap of capability development for the next decade that involves choices of the recommended technologies and the timescale estimation to address each scientific need.

## 2.0 Workshop Structure

In June 2019 ARM purchased a Challenger 850 jet aircraft to conduct aerial missions that supplement and enhance ground-based observatories. At the time of the 2020 ARM Aerial Workshop, plans for the jet

were based on a variety of inputs including outcomes from the 2015 ARM Aerial Measurements Workshop (<https://www.arm.gov/news/publications/post/35806>). ARM also began conducting test flights of the ArcticShark UAS in 2017 in preparation for science deployments. In addition, ARM expanded flights of the TBS to the Southern Great Plains (SGP) Central Facility in 2019, as well as continuing flights at the third ARM Mobile Facility (AMF3) site in Oliktok Point, Alaska. Staff from ARM and EMSL are collaborating to measure aerosol properties through the instrumented TBS platform.

On March 2 and 3, Discovery Hall at PNNL was crowded with top U.S. experts in a corner of atmospheric science devoted to airborne measurement platforms. This 2020 ARM Aerial Instrumentation Workshop was held to inform the atmospheric research community regarding updated ARM aerial capabilities and to solicit input on instrumentation for the Challenger jet, ArcticShark, and TBS platforms and the operations of these platforms. In early January 2020 ARM requested white papers from the atmospheric research community regarding the addition and implementation of aerial measurement capabilities. The white papers were asked to elaborate on the science drivers as well as the value added beyond the existing measurements, and also to demonstrate that the desired data products could be readily obtained via published algorithms.



**Figure 2.** Group photo from ARM Aerial Instrumentation Workshop at Discovery Hall, PNNL.

Workshop organizers began creating an agenda and inviting potential attendees in February 2020. Potential attendees were invited with the intent to coalesce a broad and balanced sampling of scientific expertise in the areas of meteorology, clouds, aerosols, trace gases, radiation, and associated sensor technology. Forty-nine presentations from university, national laboratory, and other research agencies in the U.S. promoted in-depth discussions across the seven science topics. In each topical area the section began with a briefing of the current ARM aerial capability, followed with a highlight of the new capabilities, an overview of the research progress, and the introduction of the corresponding white paper ideas. By the end of each section attendees also identified opportunities for needs, collaborations, and future steps.

## 2.1 Objectives and Goals

The ultimate goal of the workshop was to collect atmospheric research community input to guide the addition and implementation of measurement capabilities for ARM's recently acquired piloted aircraft, its midsize unmanned aerial system, and its tethered balloon systems. The white papers were presented at the workshop to spur and inform discussion and identify additional or improved essential airborne measurement capabilities to answer a broad range of science questions that should be adopted as facility instruments.



**Figure 3.** ARM's tethered balloon systems can go into and above clouds to collect data related to horizontal wind, ice microphysics, turbulence, thermodynamic state, aerosols, and the cloud-top environment.

Outcomes of the workshop were planned to form the basis of an additional discussion for a breakout session during the Joint ARM User Facility/Atmospheric System Research PI Meeting in June 2020. The workshop report was also intended to be referenced in the 2020 ARM triennial review document. Presentations and findings from the workshop will also contribute to ARM's strategic plan for the next decade (2020 ARM Decadal Vision).

## 2.2 Organization of the Workshop

ARM received 41 white papers in response to the solicitation. As illustrated in Figure 4, the white papers were distributed in the following areas of study: 15 aerosol, 5 cloud, 4 gas phase, 12 remote sensing, and 5 related to UAS or TBS. The white paper topics prompted the creation of a two-day workshop agenda with the first day focusing on manned aircraft instrumentation and the second day on UAS and TBS instrumentation. Brief summaries of current capabilities for each aerial platform and area of study were

presented following an introduction to the current ARM aerial capability. Each white paper was summarized by the author or a designated representative with an opportunity for follow-on questions.

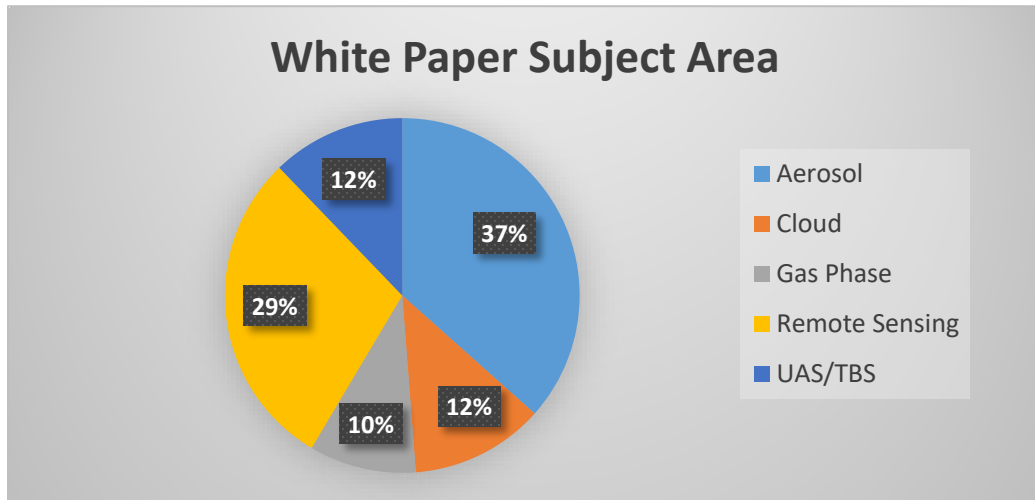


**Figure 4.** Distribution of workshop white papers by field of study.

## 2.3 Community Participation

Workshop attendees included invited participants, DOE ARM program managers, ARM Aerial Facility and TBS Facility staff, and AAF external mentors. Invited participants were composed of representatives of Federally Funded Research and Development Centers (FFRDCs) and other federal science agencies, universities, and scientific instrument industry vendors. The workshop focused on existing aerial instrumentation and what is on the horizon. Participants discussed how users of this instrumentation could get the best data on atmospheric components that create weather and can be used to model and predict future climate conditions. Attendees numbered 59, including seven who participated remotely. Presenters came from states including Hawaii, Alaska, California, Wyoming, Colorado, Maryland, and New York. They delivered 45 talks on aerial instrumentation, including ideas regarding instrumentation, science drivers, and mission design for the Challenger jet, ArcticShark, and TBS platforms. Workshop discussions were expected to identify and prioritize airborne instrumentation and measurement capabilities.

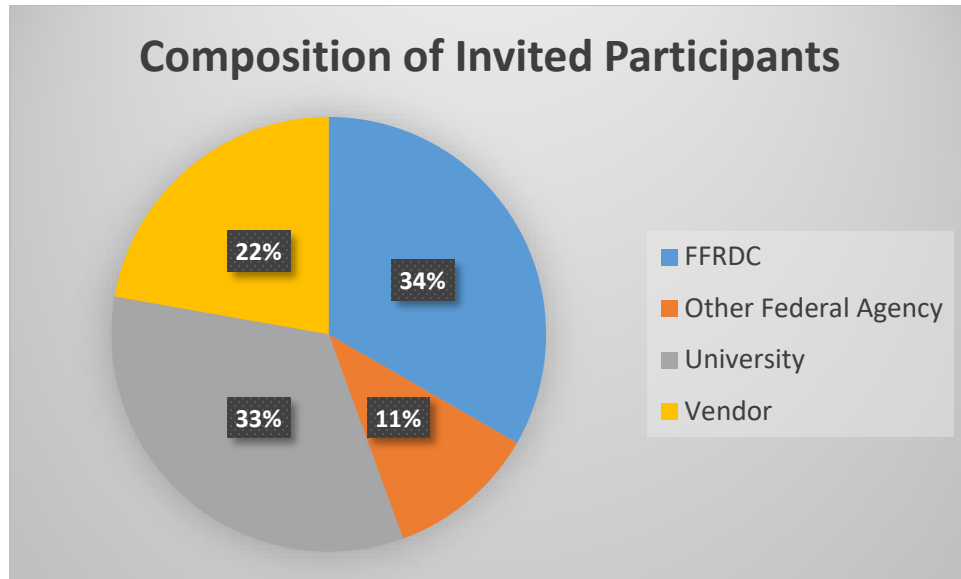


**Figure 5.** Distribution of invited participants.

## 3.0 Workshop Discussion

### 3.1 Science Drivers

In almost all atmospheric experiments, measurements require accurate specification of the atmospheric state, especially spatial information about water vapor mixing ratio, temperature, pressure, three-dimensional (3D) winds, and their turbulent structures. This drives the need to obtain more frequent measurements of the meteorological state of the atmosphere in high time resolution. Highly temporally resolved atmospheric observations are often needed as inputs in model parameterizations and act to modulate cloud and radiation processes.

The ARM science community has always recognized that solar and infrared (IR) radiation are the primary drivers of climate and weather. In fact, the initial thrust, and one of the ongoing efforts, of the ARM facility has been in making long-term measurements of solar and IR radiation from various surface sites around the world for over 25 years (remember that ARM stands for ‘Atmospheric Radiation Measurements’). However, it is not just the total amount of solar and IR radiation reaching the surface or entering/exiting at the top of the atmosphere that matters. The participants in the Radiation Measurements section of the workshop also stressed the importance of measuring the distribution of the radiative energy throughout the atmospheric column since these measurements reveal details of atmospheric composition and process dynamics including the physical and thermodynamic structure of the atmosphere, cloud and aerosol properties, cloud dynamics, and underlying surface properties.

Given that aerosols and their trace gas precursors are so heterogeneous in the vertical and horizontal dimensions due to their short lifetimes, frequent, high-time-resolution, spatially resolved measurements are needed to characterize their properties. Aerosols affect short-term climate forcing by perturbing radiation (via scattering and absorption) and cloud properties (e.g., albedo, lifetime, precipitation) by acting as cloud condensation nuclei (CCN) or ice nuclei (IN). But the ability of aerosols to perturb radiation and clouds is not simply a one-way process since aerosol formation, turbulent mixing and

transport, chemical processing, and removal is inherently influenced by many meteorology processes, including clouds. This coupling influences the overall lifetime of aerosols in the atmosphere that can be as long as several weeks. As with clouds, aerosol properties vary substantially in space and time. Therefore, the impact of aerosols on cloud radiative forcing and other cloud-aerosol interactions both depend upon the intersection of highly complex cloud and aerosol populations that are not adequately represented by Earth System Models. It is well known that Earth System Models poorly represent the vertical distribution of aerosols, especially in the remote troposphere, affecting calculations of clear-sky aerosol radiative forcing. In addition, errors in the simulated vertical aerosol distribution will lead to uncertainties in calculations of aerosol-cloud-precipitation interactions and thus cloud radiative forcing.

Improving cloud processes in models requires information not only on the cloud dynamical properties, such as the turbulence structures, but also the cloud microphysical properties, such as droplet size distribution. The capability of accurately and quantitatively measuring atmospheric cloud hydrometers can only be achieved by aerial measurements. The coincident aerosol and cloud measurements have significant impact on 1) improving our understanding of the role of aerosols and clouds in modulating radiative forcing and 2) unraveling the complex processes that lead to cloud glaciation through the evolution from supercooled liquid water, to ice formation and mixed-phase condition, to complete glaciation. Hence the two science drivers improve our understanding, observation, and modeling of 1) radiative forcing and 2) the hydrological cycle.

Different airborne platforms have their own unique specialties. The piloted aircraft – Challenger 850 – can fly longer with higher payload capacity and over expanded spatial ranges. UASs and TBSs provide three flight capabilities that are challenging for manned aircraft: long-term (> 12 hours for TBS and 6-8 hours for UASs) airborne measurements within remote areas, vertical profiles within the atmosphere, and deployments in dangerous environments for manned aircraft (within icing clouds, at low altitudes, or in very remote areas).

## 3.2 Measurements from Piloted Aircraft

Airborne measurements through the piloted aircraft has been widely applied in many aspects of environmental research and effectively provided the spatial coverage for the atmospheric study needs. The development, integration, and operation of in situ and remote instrumentation on a piloted aircraft platform require additional considerations to achieve the desired performance and must accommodate the rapid changes occurring in the environmental conditions. This session will start with the introduction of the research infrastructure of the DOE Challenger 850; then we summarize the current and proposed measurements capabilities for each measurement category.

### 3.2.1 Research Infrastructure

At the time of the workshop, the DOE Challenger 850 (registration number N850RJ) cabin was still in an executive configuration. The process to convert the aircraft over to a flying laboratory for atmospheric research started in June 2020. The aircraft is based on the 50-seat CRJ200 regional jet and thus offers copious room in the interior for the installation of the research infrastructure and the provisions for the installation of instrument racks. The aircraft operates at altitudes above 30,000 ft and has a range close to 3000 miles. These capabilities will allow the ARM Aerial Facility to expand its research portfolio.

The first step in building the flying laboratory entails maximizing the floor space for rack installations. During modifications, the contractor will remove all existing galley, entertainment equipment, executive seats, and the rear lavatory, leaving the forward lavatory. Durable Lonseal flooring will replace the executive flooring. Kydex will be used for the interior walls. Mission-style seats with at least a 4-point harness will be installed. Light-emitting diode (LED) lighting will replace the existing lighting, and an intercommunication system will be installed to facilitate communication between the pilots and scientists.

AAF focused the design for the science infrastructure around efficiency and ease of use. The goal is to enable rapid loading and unloading of instrument racks. Nine rack installation locations on the right side of the aircraft cabin are available. Each of these locations has a rack access panel that provides vacuum, compressed zero air, exhaust, ethernet, up to 20 A of 115 VAC power, and up to 20 A of 115 VAC uninterruptible power supply (UPS)-protected power. Additional rack access panels are in the baggage hold and in the avionics bay. The infrastructure for these systems is in raceways behind easily removable panels in the cabin. The baggage hold will contain the vacuum pump and compressed zero air bottles. This provides a clean cabin appearance. The left side of the cabin has eight seat locations for scientists. Each of these locations has an operator access panel that will provide 115 VAC power, ethernet, and a 5V USB plug. In addition, a single-bay rack installation could use these locations. All wiring for ethernet, fiber optics, and Global Positioning System (GPS) are routed to a system interface panel located in an aft-most location in the cabin. This is a patch panel that enables AAF to quickly change the routing of data signals to facilitate a flexible payload configuration.

The research power required to support a full payload has been determined to be 20 kVA. Four 5 kVA Nova Electric combined frequency converter and uninterruptible power supply (UPS) convert the 3-phase 400 Hz input power to single phase 60 Hz power. In addition, these frequency converters synchronize the research power with the input power source for a smooth power transfer. At least 80 amps of 28 VDC power (~ 2.3 kVA) is available for the instrumentation installed on the wing pylons. The remaining power is dedicated to 115 VAC research power. Each Nova electric frequency convertor provides 3 kVA of uninterruptible power for up to 4 minutes to protect sensitive instrumentation in the cabin. In total, 12 kVA (104 A) of uninterruptible power is available. DC power requirements have recently become diverse for instrumentation installed in the cabin. AAF will install a transformer rectifier, as needed, in a rack to accommodate a wide range of DC voltage requirements. AAF controls and monitors the power distribution system from a power panel at an aft-most location in the cabin. The panel provides control of both the cabin and wing receptacles. The power is automatically load-shredded if an engine generator fails. There are also manual switches for the load shedding located on the flight deck and main power panel. During ground operations, the research power is provided by the aircraft ground power unit and is separate from the aircraft bus for the avionics. If a ground power unit is not available, up to 10 kVA of research power is available from the aircraft's auxiliary power unit (APU).



**Figure 6.** Instruments mounted under G-1 wing.

The aircraft can carry up to six pylons (three on each wing), as shown in Figure 7. Two types of pylons are available for use. One type is a stub pylon designed to carry the 3-V cloud particle imager or similar instrument. The other type has two canister positions, which provide the aircraft with eight canister positions for external probes. The face of each canister is in a location where the airflow is laminar with a stable velocity. This location shall be directly below or preferably in front of the leading edge of the wing. The pylons have a manually adjustable canister pitch angle of  $+\/- 10$  degrees and toe angle of  $+\/- 5$  degrees to enable the alignment of the probe to be parallel to the airflow. Each pylon location has 20 A of 115 VAC, 20 A of 28 VDC, and four ethernet ports. The innermost hardpoint location on the left side has a connection for a fiber-optic cable. Each pylon location on the right side has a compressed air connection. The outermost pylon location on the right side has two GPS connections.



**Figure 7.** A notional installation for the wing pylons.

The aircraft fuselage has identical 20.5" nadir and zenith circular ports for the installation of radiometers, imagers, and infrared thermometers. The ports are on the centerline of the aircraft, directly above/below each other, and flat and level to the plane of the aircraft.

The inlets are a key component for the research aircraft. These anti-iced inlets decelerate and bring the aerosol, cloud droplets, and trace gases into the cabin via a manifold with minimal ram heating or sample

loss. The isokinetic aerosol inlet is located above the counterflow virtual impactor (CVI) cloud inlet on the inoperable galley service door on the right side of the aircraft behind the flight deck. The trace gas inlet(s) are located here or on a window plate. The meteorological state instrumentation is on the same door below the inlets. Computational fluid dynamics modeling of airflow around a Challenger 850 fuselage was performed for a conceptual design. As shown in Figure 8, at a true air speed of 190 kts, a sampling location of 6" from the fuselage is theoretically in the free airstream. The inlets and instrumentation are conservatively placed 10" from the fuselage.

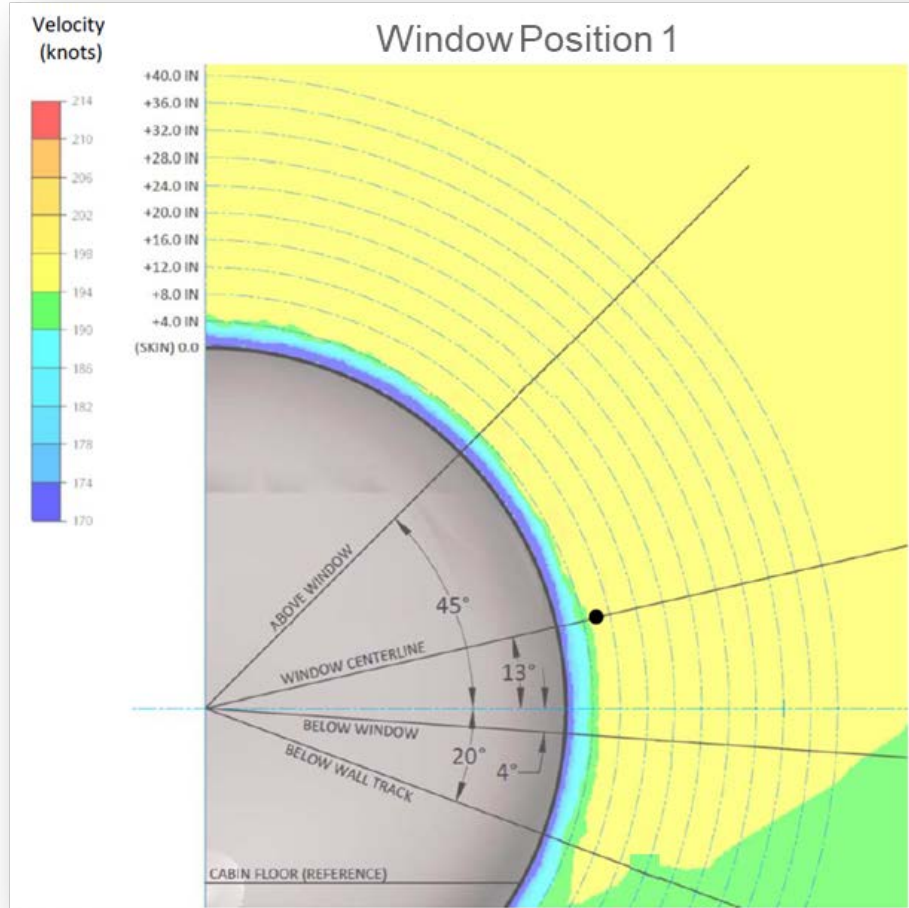


**Figure 8.** Computational fluid dynamic along the fuselage at the first window position.

The Challenger 850 can facilitate research that was not possible on the AAF Gulfstream-159. The aircraft has a faster cruise speed, longer flight durations, a higher maximum service ceiling, and large circular ports in the zenith and nadir direction. The ability to reach higher altitudes enables in situ measurements of cirrus clouds. In addition, it opens the door for a wide range of remote-sensing instrumentation. Joe Hardin et al. demonstrated that almost all of ARM's field campaigns have had a scientific objective that would benefit from the aerosol profiling, cloud kinematics, and microphysical measurements that aerial remote sensing can provide. It is desirable that the Challenger 850 can accommodate the installation of selected nadir- and zenith-pointed guest radars, lidars, radiometers, and imagers. In addition, it is

desirable for the aircraft to support the installation of the aforementioned instrumentation on the side of the aircraft, and/or at slanted angles. Alternatively, a heavy pod mount on the wing or a blister on the belly of the aircraft could hold the active and passive remote-sensing instrumentation.

If the aircraft infrastructure can support it, airborne measurements by lidars and radars can provide information on aerosol and cloud layers and their distribution. This information provides guidance to scientists onboard on where to conduct in situ measurements of aerosol and cloud layers. In addition, these instruments facilitate the remote measurements of the microphysical properties of clouds. The faster cruise speed and longer flight duration will facilitate a more efficient and simpler reposition flight plan for international research campaigns. In addition, it will greatly broaden the potential sampling area both vertical and horizontally.

### 3.2.2 Aircraft and Atmospheric State Measurements

This session started with the overview of the AAF current atmospheric state measurements and instruments, as listed below (Table 1). The table includes the key atmospheric state variables that are essential to aircraft observations, including temperature, static pressure, differential pressure, acceleration, air motion and air speed, in situ dew-point temperature, in situ absolute humidity, and in situ water vapor number concentrations, as well as microwave remote sensing of temperature and water vapor vertical profiles.

**Table 1.** Summary of atmospheric state instruments and measurements.

Measurement	Instrument	Source	Other configurations	Status
Temperature	Rosemount 102 probe	Rosemount		AAF-owned
Static pressure	Rosemount 1201F1	Rosemount		AAF-owned
Differential pressure	Gust probes, Rosemount 1221F2	Aircraft manufacturer; Rosemount		AAF-owned
Static pressure	Rosemount 1201F1	Rosemount		AAF-owned
Differential pressure; Acceleration; 5-port air motion sensing: true air speed, altitude, angle of attack, side-slip, temperature, relative humidity	Gust probes, Rosemount 1221F2; Accelerometer; Aircraft Integrated Meteorological Measurement System-20 (AIMMS-20)	Aircraft manufacturer; Rosemount Aventech		AAF-owned AAF-owned
Dew-point temperature (in situ)	Chilled-mirror hygrometer	General Eastern-1011B	Closed-path, delayed measurement of water vapor (not instantaneous)	AAF-owned

Measurement	Instrument	Source	Other configurations	Status
Absolute humidity (in situ)	Tunable-diode laser (TDL)	Port City Instrument	Lower accuracy and precision than other open-path hygrometers below	AAF-owned
Water vapor number concentrations (in situ, open-path)	Vertical cavity surface emitting laser (VCSEL) hygrometer	Zondlo group in Princeton	Measurement range: 1-40,000 ppmv; accuracy $\leq$ 6%; precision $\leq$ 1%; calibration provided by Minghui Diao (San Jose State University) and others at NCAR and Princeton	Deployed by other agency for 13 years
Water vapor number concentrations (in situ, open-path)	DFB tunable-diode laser (TDL) hygrometer	D. Sonnenfroh, Physical Sciences, Inc. and Zondlo group in Princeton	Measurement range is currently for mixed-phase clouds, but can be modified for wider range; accuracy and precision $\leq$ 2 ppmv; more lab calibrations can be conducted at Zondlo Princeton Lab.	Deployed by other agency for 1 year; test flights done on UND ScanEagles; can be deployed on both UAS and piloted aircraft
Microwave sounding of water vapor, T, and precipitation and cloud liquid water (remote sensing)	HAMSR (high-altitude MMIC sounding radiometer)	JPL, Caltech	1–3 km vertical resolution; see through clouds; validations by in-flight comparison with dropsondes	Built in 2001; flown on Global Hawk, ER-2, DC-8; can fly on UAS and piloted aircraft
Microwave sounding of water vapor, T, and precipitation and cloud liquid water (remote sensing)	PAMR (profiling airborne microwave radiometer)	Boulder Environmental Sciences & Technology	See through clouds; observe both above and below flight line	Not tested on flight; latest technology; fit on both UAS and piloted aircraft

One of the most challenging variables to be measured accurately on a research aircraft is water vapor (or humidity, depending on the types of measurements). A detailed comparison between two in situ, open-path, tunable-diode, laser-based hygrometers was introduced by Minghui Diao, as shown in Table 2. The National Science Foundation (NSF)/National Center for Atmospheric Research (NCAR) vertical cavity surface emitting laser (VCSEL) hygrometer has been flown on the NSF Gulfstream-V research aircraft since 2007 (Zondlo et al. 2010). The hygrometer was built by M. Zondlo while at Southwest Sciences Inc., with continued calibrations in the Zondlo group at Princeton and then transitioned to NCAR with calibrations now provided by M. Diao at San Jose State University (SJSU). Since 2008, the VCSEL hygrometer has been calibrated by M. Diao, M. Zondlo, J. DiGangi, and S. Beaton using the NCAR environmental chambers as well as the calibration chamber at Zondlo group. A series of publications have been based on the water vapor measurements obtained from the VCSEL hygrometer, including analysis on cloud macro- and microphysical properties of ice clouds (Diao et al. 2013a, b, 2014, 2015, Patnaude and Diao 2020), radiative transfer calculations (Tan et al. 2016), model validations for a cloud-resolving model (Diao et al. 2017), the WRF model (D'Alessandro et al. 2017), and a climate model (D'Alessandro et al. 2019, Wu et al. 2017).



**Figure 9.** Jason Tomlinson speaks at the ARM Aerial Instrumentation Workshop.

**Table 2.** Comparisons of VCSEL and DFB open-path laser hygrometers.

<b>Instrument</b>	Vertical cavity surface emitting laser (VCSEL) hygrometer (Zondlo et al. 2010)	DFB TDL open-path hygrometer
<b>Laser</b>	VCSEL laser	DFB laser
<b>Design</b>	Open-path; two absorption lines (1854.03 nm and 1853.37 nm; autonomous	Open-path; currently one absorption line (2.7 micron), but can add another line; autonomous
<b>Resolution</b>	25 Hz and 1 Hz	1 Hz
<b>Weight</b>	5 kg	0.9 kg
<b>Power</b>	10 W	49 W
<b>Dimension</b>	Pylon 24 × 6 × 30 cm; Housing 24 × 14 × 7 cm	5675 cm <sup>3</sup> (7-inch diameter × 9-inch length)
<b>Measurement range</b>	1–40,000 ppmv; -90°C to 35°C, operating in both clear-sky and cloudy conditions	High dynamic range (4–5 orders of magnitude); currently designed for mixed-phase cloud range, but can be modified for wider range; operating in both clear-sky and cloudy conditions
<b>Accuracy and precision</b>	Accuracy $\leq$ 6%; precision $\leq$ 1%	Accuracy and precision are 2 ppmv at 240 K, i.e., measurement uncertainty $<$ 10% at 240 K
<b>Calibration systems</b>	Environmental chambers at NCAR operated by M. Diao and S. Beaton; calibration chamber by M. Diao, M. Zondlo, J. DiGangi in Zondlo lab; can calibrate under a series of T, P, q conditions	Zondlo lab has a dilution flow system, chemical baths, the LAUDA bath temperature controller, and a chilled-mirror hygrometer (MBW-373LX); can calibrate under a series of T, P, q conditions
<b>Other measurements</b>	Temperature and pressure sensors	Temperature and pressure sensors
<b>Flight platform</b>	Flown on NSF G-V since 2007	Tested on UND ScanEagle in 2019; Can be deployed on both ArcticShark UAS and piloted aircraft

The distributed feedback tunable-diode laser (DFB TDL) open-path hygrometer was designed and built by D. Sonnenfroh (Physical Sciences, Inc.) and M. Zondlo (Princeton) for the ArcticShark UAS system. This hygrometer can also be operated on piloted aircraft, such as the Bombardier Challenger 850. Currently, the UAS DBF TDL hygrometer operates at 2.7 micron, but the system can be modified for dual absorption lines to achieve a wider measurement range. The VCSEL hygrometer is mounted with an aperture plate on the fuselage, and the pylon protrudes 29 cm above the fuselage of the aircraft. The UAS DBF TDL can be mounted in a wing pod.

Another comparison between two microwave sounding systems of water vapor is shown in Table 3. The HAMSR instrument was built in 2001 and has been flown on multiple platforms and field campaigns. The PAMR instrument uses the latest technology and has not been tested on a flight before. Both instruments can fly on UAS and piloted aircraft and can complement in situ measurements by providing vertical profiles of temperature, humidity, cloud liquid water, and total precipitable water.

**Table 3.** Comparisons between HAMSR and PAMR microwave radiometers.

Instrument	HAMSR (high-altitude MMIC sounding radiometer)	PAMR (profiling airborne microwave radiometer)
<b>Measurements</b>	T(z); q (z); cloud liquid water; precipitation; convection	T(z); q (z); cloud liquid water; precipitation; convection
<b>Weather condition</b>	Clear-sky and in-cloud; hurricane	Observe both above and below flight line, through clouds, fog, or drizzle.
<b>Resolution</b>	2 km for q(z) in vertical; 1–3.5 km for T(z)	
<b>Frequency, wavelength</b>		19–200 GHz; 15–1.5 mm
<b>Data processing</b>	Data can be transmitted to ground for real-time processing, and can provide real-time on-board processing	Power and ethernet connection to aircraft; autonomous
<b>Weight</b>	100 lbs	5.4 kg
<b>Power</b>	70 W	75 W
<b>Dimension</b>	36"×15"×14"	Length 83 cm × diameter 10 cm
<b>Calibration systems</b>	Validated in-flight against dropsondes	
<b>Flight platform</b>	Built in 2001; Flown on Global Hawk, ER-2, DC-8; can be flown on both UAS and piloted aircraft.	Not tested in flight; prefer 360° view such as at aircraft nose, tail; fit on both UAS and piloted aircraft.

### 3.2.3 Radiation Measurements

Radiation measurements from an aircraft provide the capability to quantify the vertical distribution of radiative energy. For example, altitude profiles of the downwelling and upwelling broadband and spectral solar and infrared (IR) irradiance can provide heating and cooling rate profiles due to water vapor, aerosols, and clouds. They can also provide the broadband and spectral albedo of the clouds and of the surface (including, for example, the Normalized Difference Vegetation Index [NDVI]).

Direct spectral solar radiation measurements can provide the aerosol optical depth and can be used to derive aerosol properties. Spectral solar irradiance measurements, combined with direct spectral solar radiation measurements, can be used to derive cloud properties and effects. Hyperspectral visual imagery can characterize the spatial heterogeneity of the surface. High-resolution, spectrally resolved IR radiance can be used to derive profiles of temperature, water vapor, and trace gases.

This session began with a presentation on the current AAF aircraft radiometer measurement capabilities by Laura Riihimaki. She gave an overview of the radiometers that flew on the G-1 aircraft and are available to fly on the Bombardier (see also Tables 4 and 5 below). Two SPN-Unshaded (SPN-U) radiometers, mounted on the top and bottom of the aircraft, can measure the down- and upwelling total solar radiative flux. An SPN-Shaded (SPN-S) radiometer, mounted on the top of the aircraft, can measure the downwelling total, direct, and diffuse solar radiative flux (with no moving parts, and no need to track the sun). Multifilter radiometers (MFRs) mounted on the top and bottom of the aircraft can measure the narrow-band solar spectral irradiance. Kipp & Zonen CGR4 pyrgeometers mounted on the top and bottom of the aircraft can measure the down- and upwelling IR irradiance. An infrared thermometer (IRT) mounted on the bottom of the aircraft can measure surface or cloud top temperatures.

The above combination of instruments can provide profiles of solar and IR fluxes and heating rates; surface albedo, surface temperature and surface properties; and radiative forcing due to aerosol, clouds, and other atmospheric constituents.



**Figure 10.** Adjusting the instruments in flight aboard the G-1 aircraft.

Laura Riihimaki also discussed the need to correct the downwelling shortwave measurements for the attitude of the aircraft. Total solar radiation measurements on the top of the aircraft are typically

dominated by the direct component of the radiation. As the aircraft pitches and rolls in flight the incident angle between the sun and the sensor changes, introducing offsets in the measured signal that have nothing to do with changes in the atmosphere but are only due to the changes in attitude of the aircraft. She described a method developed by Long et al. (2010) that uses the diffuse/direct solar measurements from the SPN-S to correct the direct component of the solar radiation for these attitude fluctuations.

In the presentation by Anthony Bucholtz, he presented a survey of current capabilities in the community for measuring broadband solar and IR radiation from aircraft, and an overview of the modified Kipp & Zonen CM22 pyranometers and CG4 pyrgeometers that he developed that amplify the signal at the sensor. These radiometers have flown on numerous research aircraft and Bucholtz collaborated with NCAR to mount similar radiometers on their research aircraft as facility instruments. A similar collaboration could be formed with ARM to deploy radiometers for the Bombardier and UAS. Anthony Bucholtz then presented a quick overview of the NCAR radiometers. In addition to the modified Kipp & Zonen radiometers mentioned above, NCAR also flies Zeiss spectrometers to measure the spectral solar irradiance, a Heitronics KT19 IRT to measure surface/cloud top temperatures, and the zenith- and nadir-mounted HIAPER Airborne Radiation Package (HARP) instrument to measure actinic flux.

The National Oceanic and Atmospheric Administration (NOAA) Lockheed Orion aircraft ('Hurricane Hunters') fly Eppley solar pyranometers and IR pyrgeometers. Similarly, the United Kingdom (UK) Facility for Airborne Atmospheric Measurements (FAAM) aircraft flies Eppley solar pyranometers and IR pyrgeometers.

Anthony Bucholtz also presented an overview of some of the challenges in making solar and IR radiation measurements from aircraft and ways to mitigate those effects. He discussed the need to correct uplooking solar measurements for the changing attitude of the aircraft by either using actively leveling platforms, or correction schemes using navigational data (e.g., the Long method discussed above).

Finally, Anthony Bucholtz presented an overview of the In situ Net Flux within the Atmosphere of the Earth (INFLAME) sensor developed by Mlynczak et al. at the National Aeronautics and Space Administration (NASA) Langley Research Center and the Lawrence Berkeley National Laboratory. INFLAME is a low-resolution Fourier transform spectrometer that directly measures the difference between the upwelling and downwelling visible, near-IR, and IR radiation streams from which the spectrally resolved radiative heating/cooling rate can be derived. This instrument has been flown on a Learjet and Mlynczak is interested in working with ARM to further develop INFLAME for the Bombardier.

Connor Flynn presented an overview of current possibilities for measuring spectral and hyperspectral solar radiation from aircraft. He described 4STAR (Spectrometer for Sky-Scanning Sun Tracking Atmospheric Research), an instrument developed at NASA's Ames Research Center that actively tracks the sun and measures the direct spectral solar radiance from which the spectrally resolved aerosol optical depth, aerosol Angstrom exponent, and the column O<sub>3</sub>, NO<sub>2</sub>, and water vapor can be derived. Under suitable conditions, it can also operate in sky scan mode for retrievals of aerosol intensive properties including aerosol size distribution, index of refraction, single-scattering albedo (SSA) and asymmetry factor (similar to Aerosol Robotic Network [AERONET] retrievals). When flying underneath clouds and fixed in zenith scanning mode, 4STAR, linked with spectral solar irradiance measurements (such as the University of Colorado solar spectral flux radiometer [SSFR] sensor), can also derive cloud properties

(e.g., optical depth, cloud droplet effective radius, and phase). 4STAR has flown on numerous research aircraft for NASA and DOE.

Connor Flynn also described 5STAR-Airborne, a new instrument in development that measures the hyperspectral and multispectral solar irradiance without the use of fiber optics. It would measure and derive similar quantities as 4STAR, but it is much smaller and lighter and would be suitable for a UAS.

Finally, Connor Flynn described two new SPN radiometers that are now commercially available. The SPN-532 is similar to the SPN-S instrument mentioned above except that it measures the total, direct, and diffuse solar irradiance in a narrow-band at 532 nm (instead of the broadband solar measured by the SPN-S). The SPN-Spectral uses fiber-optic cables connected to a grating spectrometer to measure the total, direct, and diffuse spectral solar irradiance. Both of these SPN variants have the capability to measure direct and diffuse spectral irradiances and thus potentially do retrievals of cloud and aerosol properties, although the absolute accuracy of these measurements and retrievals is not yet known.

Connor Flynn also discussed the need to actively level the zenith-mounted spectral solar radiation instruments to compensate for the changing attitude of the aircraft as it pitches and rolls in flight.

Laura Riihimaki then presented an overview of the hyperspectral imaging (HIS) camera (a presentation from Chand and Tagestad) proposed as a replacement for the RGB camera previously flown on the ARM G-1. This imager actually consists of two hyperspectral cameras (350-1000 nm; 1000-2500 nm) that would measure the solar reflective spectrum of the surface in several hundred bands. It would be used to characterize the spatial heterogeneity of the surface for land, atmospheric, and coastal research. It would be mounted on the bottom of the Bombardier and possibly the UAS.

Finally, Lambrightsen remotely presented an overview of the scanning high-resolution interferometer sounder (S-HIS), that measures the spectral IR radiance from 3.5-17.3 microns. This instrument is used to derive profiles of temperature, water vapor, CO, N<sub>2</sub>O, CH<sub>4</sub>, SO<sub>2</sub>, O<sub>3</sub>; total column CO<sub>2</sub>; and surface temperature and emissivity. It has flown on numerous research aircraft and it is proposed for the Bombardier.



**Figure 11.** Troy Thornberry participates at the ARM Aerial Instrumentation Workshop.

Tables 4 and 5 below summarize the radiometer instrumentation discussed in the workshop. Most of the radiometers are either commercially available, already developed, or could be collaboratively developed for ARM:

**Table 4.** Broadband radiometer options.

Name	Source	Manufacturer	Primary measurement	Piloted aircraft suitability	UAS suitability	Status
SPN-U: Unshadowed SPN	ARM facility instrument	Dynamax	Total broadband solar irradiance	Yes, previously flown on ARM G-1	Yes, size: ~4" x 4", wt: ~4 lbs	ARM owns
SPN-S: Shadowed SPN	ARM facility instrument	Dynamax	Total, direct, and diffuse broadband solar irradiance	Yes, previously flown on ARM G-1	Yes, size: ~4" x 4", wt: ~4 lbs	ARM owns
CM22 pyranometer modified for aircraft use	NPS	Kipp & Zonen	Broadband total solar irradiance	Yes, previously flown on numerous aircraft	Yes, size: ~3' x 3', wt: ~2 lbs	Could be developed by NPS for ARM
CGR4 pyrgeometer	ARM facility instrument	Kipp & Zonen	Broadband IR irradiance	Yes, previously flown on ARM G-1	Yes, size: ~3' x 3', wt: ~2 lbs	ARM owns
CGR4 pyrgeometer modified for aircraft use	NPS	Kipp & Zonen	Broadband IR irradiance	Yes, previously flown on numerous aircraft	Yes, size: ~3' x 3', wt: ~2 lbs	Could be developed by NPS for ARM
KT-19 IR pyrometer	ARM facility instrument	Heitronics	Surface temperature (e.g., SST), cloud top/bottom temp, sky temp	Yes, previously flown on ARM B-1 and numerous aircraft	Possibly, size: ~9" x 4", wt: ~5 lbs	ARM owns
PSP pyranometers and PIR pyrgeometers	ARM facility instruments	Eppley	PSP: total solar irradiance PIR: LW IR irradiance	Yes, many groups fly on aircraft	Yes, size: ~3' x 3', wt: ~2 lbs	Commercial off the shelf

**Table 5.** Spectral radiometer options.

Name	Source	Manufacturer	Primary measurement	Piloted aircraft suitability	UAS suitability	Status
MFR: multifilter radiometer	ARM facility instrument	Yankee	Narrow-bandpass spectral solar irradiance	Yes, previously flown on ARM G-1	Yes, Size: 2.5" x 2" Wt: <2lbs	ARM owns
SPN-532: narrow-band shadowed SPN	U. Colorado	Dynamax	Total, direct, and diffuse irradiance at 532 nm	Yes, previously flown on aircraft	Yes, size: ~4'x4', wt: ~5 lbs	Commercial prototypes available
SPN-Spectral: spectral shadowed SPN	U. Colorado	Dynamax	Total, direct, and diffuse spectral solar irradiance	Yes, previously flown on aircraft	Possibly, Size: ~9"x4", Wt: 5 lbs	Commercial prototypes available
4STAR: Spectrometer for Sky-Scanning Sun-Tracking	NASA Ames	Developed by NASA Ames	Spectral solar irradiance, aerosol AOD, cloud properties	Yes, flown on numerous aircraft	No, too big: Size: 26"x19" Wt:140lbs	Would need to contact NASA Ames
5STAR-Airborne	NASA Ames	Developed by NASA Ames	Hyperspectral +multispectral solar irradiance	Yes,	Possibly: Size: <2' high, Wt: 30 lbs	Would need to contact NASA Ames
INFLAME: in situ net flux within the atmosphere	NASA Langley	Developed by NASA Langley and Lawrence Berkeley Laboratory	Spectral net flux in visible, near-IR, and IR	Yes, previously flown on NASA Learjet	No, too big	Would need to contact NASA Langley
HARP	NCAR facility instrument	Developed by NCAR	Actinic fluxes	Yes, flies on NCAR G-V	No, spectrometers too big	Would need to contact NCAR
HIS: hyperspectral imaging cameras	PNNL	Do not know	Hyperspectral solar reflective spectrum (350-2500 nm)	Yes, to replace the RGB camera flown on ARM G-1	Possibly, Wt: ~10 lbs	Would need to contact PNNL
S-HIS: scanning high-resolution interferometer sounder	U. Wisconsin	Developed by U. Wisconsin	Spectral LW, MW, SW radiance; brightness temperature	Yes, previously flown on numerous aircraft	No, Size: 61"x14.5"x17" Wt: ~150 lbs	Would need to contact U. Wisconsin

### 3.2.4 Aerosol Measurements

This section describes instruments and their measurements of aerosol properties from the white papers and presentations that have been grouped into the following key topics: particle number and size distribution, aerosol composition, aerosol precursors, aerosol optical properties, cloud and ice nucleating properties, and inlets. Instrumentation currently used by the AAF as well as other instrumentation needed to assess science questions are included in these subsections. Finally, a brief overview of the instrument strategy used by previous and ongoing aircraft measurement campaigns is presented.



**Figure 12.** Discussion of network configuration improvements at the AAF Instrumentation Workshop.

### **3.2.4.1 Particle Number and Size Distribution**

Total particle number concentrations and size-resolved number concentrations are fundamental measurements needed to understand the life cycle of aerosols including emissions, new particle formation (NPF), condensational growth, and deposition. Aerosol size distribution is also a key factor that controls 1) aerosol optical properties that affect radiative transfer and 2) CCN concentrations that influence cloud properties. The AAF currently has several instruments used by past G-1 deployments that measure total particle number and size resolved concentrations as listed in Table 6. Each of these instruments can measure particle number and size distribution at 1 s intervals (1 Hz), making them suitable for aircraft deployments. The upper and lower size range limits vary among the instruments and it is important to note that the uncertainty in particle number at either the upper or lower size ranges may be relatively large. Most of the instruments are most suitable for obtaining aerosol size distribution in the Aiken- and Accumulation-mode size ranges. Additional instruments would be needed to fully characterize the number and size of ultrafine particles with diameters smaller than 10 nm. At a 1 Hz sampling rate, the number of particles in the coarse-mode size range will be small and longer averaging times may be needed to obtain meaningful concentrations. While the cloud, aerosol, and precipitation spectrometer (CAPS), cloud and aerosol spectrometer (CAS), and fast cloud droplet probe (FCDP) can measure coarse-mode particle concentration by size, they are normally used to measure droplet number concentration and it is not clear how well they characterize the number and size of large particles. ARM does have a TSI aerodynamic particle sizer (APS) designed to measure large particles between 0.5 and 20  $\mu\text{m}$  as part of its ground-based sampling that could be used for airborne deployments.



**Figure 13.** The G-1 flying above the clouds during the 2018-2019 CACTI field campaign in Argentina.

**Table 6.** Instruments that measure total particle number and aerosol size distribution.

Instrument	Measurement	Source/supplier	AAF-owned
Ultrafine condensation particle counter (UCPC), model 3025A	Total aerosol concentration > 3 nm	Trust Science Innovation (TSI) Inc.	Yes
Condensation particle counter (CPC), model 3772	Total aerosol concentration > 7 nm	Trust Science Innovation (TSI) Inc.	Yes
Scanning mobility particle spectrometer (SMPS)	Aerosol size distribution from 0.015 to 0.45 $\mu\text{m}$	BNL	Yes
Laser aerosol spectrometer (LAS) model 3340	Aerosol size distribution from 0.09 to 7.5 $\mu\text{m}$	Trust Science Innovation (TSI) Inc.	Yes
Passive cavity aerosol spectrometer 100X (PCASP)	Aerosol size distribution from 0.10 to 3 $\mu\text{m}$	Particle Measuring Systems (PMS)	Yes
Ultra-high-sensitivity aerosol spectrometer (UHSAS)	Aerosol size distribution from 0.060 to 1 $\mu\text{m}$	Droplet Measurement Technologies (DMT)	Yes
Cloud aerosol and precipitation spectrometer (CAPS), cloud aerosol spectrometer (CAS)	Aerosol size distribution from 0.5 to 50 $\mu\text{m}$	Droplet Measurement Technologies (DMT)	Yes
Fast cloud droplet probe (FCDP)	Aerosol size distribution from 2 to 50 $\mu\text{m}$	Stratton Park Engineering Technologies	Yes
Fast integrated mobility spectrometer (FIMS)	Aerosol size distribution from 0.010 to 0.5 $\mu\text{m}$	Washington University	No
Neutral cluster and air ion spectrometer (NAIS)	Aerosol size distribution from 0.002 to 0.040 $\mu\text{m}$	Airel Ltd.	No
1-nm condensation particle counter	Total aerosol concentration > 1 nm	Aerosol Dynamics Inc. (ADI) adapted by BNL	No

While the passive cavity aerosol spectrometer (PCASP) and ultra-high-sensitivity aerosol spectrometer (UHSAS) have been used extensively to measure aerosol size distribution, they have had performance issues at times and the size range is not large enough to answer all science questions. Given the importance of quantifying the aerosol size distribution, it is desirable to have alternative instruments to provide data redundancy and extend the capabilities of the AAF to the size range smaller than 60 nm. The fast integrating mobility spectrometer (FIMS), originally designed by Jian Wang, is one such instrument that measures aerosol size distribution between 10 and 500 nm in diameter at 1 Hz; therefore, it is suitable for rapid measurements needed on research aircraft that frequency samples large gradients in aerosol concentrations. The performance of FIMS has been established with side-by-side comparisons with scanning mobility particle sizer (SMPS) measurements. FIMS has been a guest instrument on past G-1 deployments, including the Biomass Burning Observation Project (BBOP), Observations and Modeling of the Green Ocean Amazon (GoAmazon), Holistic Interactions of Shallow Clouds, Aerosols, and Land-Ecosystems (HI-SCALE), and Aerosol and Cloud Experiments in the Eastern North Atlantic (ACE-ENA). It is particularly useful in detecting new particle formation (NPF) events and describing growth of ultrafine particles to Aiken- and accumulation-mode sizes. Efforts are also underway to develop a version that is smaller in size, lighter, and more robust.

It is desirable to have measurements of the aerosol size distribution down to at least 1 nm to fully understand new particle formation and growth; however, the AAF does not yet have this capability. The neutral air ion spectrometer (NAIS) is a commercial instrument that can address this need by measuring the size distribution of ultrafine particles between 2 to 40 nm at 1 Hz. NAIS has been deployed on research aircraft and a Zeppelin during recent field campaigns in Europe. However, the electrometer sensitivity may limit the NAIS for high aerosol concentration application only. There are now condensation particle counters (CPC) that can measure total aerosol number concentration down to 1 nm at 1 Hz. By combining this instrument with existing CPCs that measure concentrations for particles greater than 3 or 10 nm we can determine the particle number concentration at the smallest sizes. Because of its size and weight, an advantage of the 1-nm CPC is that it can also be used on TBS and UAS platforms. Testing of this instrument on the ARM TBS has already been performed during a two-week deployment at the SGP site in 2019.

### **3.2.4.2 Composition**

Aerosol composition is another fundamental measurement needed to understand the life cycle of aerosols. Composition is a signature of emissions and numerous chemical mechanisms associated with gas-to-particle partitioning that has occurred along the path of an air parcel. The hygroscopicity of specific compounds also influences the ability of aerosols to uptake water and act as CCN or IN. For example, sulfate ( $\text{SO}_4$ ) is formed from chemical reactions associated with  $\text{SO}_2$  that is often emitted by coal-fired power-plants. AAF currently only has two instruments, the particle-into-liquid sampler (PILS) and the single-particle soot photometer (SP2), to measure aerosol composition. PILS has not been used on recent aircraft deployments because of the long sampling time required and significant amount of effort needed to process the samples. The SP2 measures the total and size-resolved concentration of black carbon (BC). BC is emitted by anthropogenic sources as well as fires and has short-term climate impacts by absorbing atmospheric radiation and consequent atmospheric warming.

Previous G-1 aircraft deployments have relied on various guest instruments to obtain information on aerosol composition, including the high-resolution time-of-flight aerosol mass spectrometer

(HR ToF AMS, Aerodyne Research), miniaturized single-particle mass spectrometer (miniSPLAT), and time-resolved aerosol collector (TRAC) as listed in Table 7. Two deployment challenges were discussed during the workshop. One deployment challenge of the mass spectrometers is to maintain the critical low pressure inside of the mass spectrometer chamber. Thus, development of technologies and methodologies to significantly reduce the pump-down time or maintain the pressure condition is desirable. The other challenge is technical development needed to shield the mass spectrometer detector from the interference due to the background signals.

**Table 7.** Instruments that measure aerosol composition.

Instrument	Measurement	Source/supplier	AAF-owned
Particle-into-liquid sampler (PILS)	Bulk ionic concentration of Na, Chl, SO <sub>4</sub> , NH <sub>4</sub> , NO <sub>3</sub> , WSOC, K, Ca, Mg, and possibly other compounds	BNL build	Yes
Single-particle soot photometer (SP2)	Black carbon (BC) mass and number concentrations and size distribution at 1 s intervals	Droplet Measurement Technologies (DMT)	Yes
High-resolution time-of-flight aerosol mass spectrometer (HR-ToF-AMS)	Bulk concentration of SO <sub>4</sub> , NO <sub>3</sub> , NH <sub>4</sub> , OM, and Cl from 0.050 to 1 $\mu\text{m}$ as well as mass spectra at $\sim$ 10-15 s intervals	Aerodyne Research Inc.	No
miniSPLAT	Composition of refractory and non-refractory species, number concentrations, size and density of individual particles	PNNL-build	No
Time-resolved aerosol collector (TRAC)	Automated sampling on substrates for laboratory spectro-microscopy analyses	Environmental Molecular Science Laboratory (EMSL)	No
Wideband integrated bioaerosol sensor (WIBS)	Fluorescent and non-fluorescent size distributions from 0.5 to 30 $\mu\text{m}$ , classifications to discriminate particle type	Droplet Measurement Technologies (DMT)	No

The HR-ToF-AMS is the most common method in the atmospheric community to measure aerosol composition concentrations for particles as small as 40 nm and as large as 1  $\mu\text{m}$  in diameter at a sampling interval between 1 and 10 s. In addition to providing bulk concentration of primary non-refractory aerosol species (SO<sub>4</sub>, NO<sub>3</sub>, NH<sub>4</sub>, OM, Cl), the HR-ToF-AMS provides individual mass spectra that can be analyzed for signatures that reveal information on their source and secondary chemical processing. Statistical techniques, such as positive matrix factorization (PMF), have been frequently used to estimate the amount of primary organic aerosol (POA), biomass burning organic aerosol (BBOA), and secondary aerosol (SOA) species such as semi-volatile, low-volatility, and extremely low-volatility organic compounds (SVOCs, LVOCs, ELVOCs). The HR-ToF-AMS does not obtain information on non-refractory aerosol species such as BC, dust, and sea salt.

Amy Sullivan summarized the on-line and offline PILS measurements. Many research groups have their own versions of PILS that have been used on research aircraft to characterize aerosol composition, including PILS coupled with ion chromatograph (PILS-IC) and PILS coupled with a fraction collector.

PILS requires a relatively long sampling time, up to a few minutes; therefore, the measurements represent a spatial average when deployed on a research aircraft. A large number of tubes is also required to sample an aircraft flight period of a few hours. One advantage of PILS over the HR-ToF-AMS is its ability to measure water-soluble organic carbon (WSOC) as well as inorganic anions and cations of sodium (Na), potassium (K), magnesium (Mg), calcium (Ca), and many other species. These species can be used as markers for chemical aging, cloud processing, and biomass burning. WSOC accounts for 20 to 70 % of the total organic carbon in aerosols and it influences the aerosol's hygroscopicity and thus its ability to serve as CCN. Sources of WSOC can arise from combustion, industrial, and natural sources and/or be formed by secondary processes.

The relative concentration of aerosol species usually varies as a function of size. For example, BC is more prevalent at small particle sizes, OM is more prevalent at Aitken- and Accumulation-mode sizes,  $\text{SO}_4$  and  $\text{NO}_3$  are more prevalent at larger accumulation mode sizes, and dust and sea salt are more prevalent at coarse-mode sizes. This varying aerosol mixing state as a function of size will affect aerosol optical and cloud nucleating properties. However, there are far fewer field measurements of aerosol composition as a function of size. The HR-ToF-AMS can quantify aerosol composition as a function of size when the sampling interval is increased; however, this configuration would prevent the measurement of temporal variations in aerosol concentrations during aircraft flights.

In contrast to the bulk measurements from the HR-ToF-AMS, real-time mass spectrometry techniques can also be used to obtain information for individual particles including composition as a function of size. One such single-particle instrument, called miniSPLAT, has been used on past ARM aircraft campaigns such as the Two-Column Aerosol Project (TCAP) and HI-SCALE. In addition to composition, miniSPLAT obtains information on aerosol size (for diameters between 50 nm to 2  $\mu\text{m}$ ), number concentrations, size distribution, density, and sphericity at high time resolution. During a typical aircraft flight, the size of thousands of particles can be quantified per second, while composition can be characterized for up to 100 of those. By obtaining the relative contribution of various compounds in individual particles, the overall mixing state of the aerosol population can be characterized. In contrast to the HR-ToF-AMS, miniSPLAT can also characterize the presence of BC, dust, and sea salt.

A time-resolved aerosol collector (TRAC), designed by Alexander Laskin, is simply a filter sampler that collects particles on a substrate over predetermined time intervals. Up to 560 samples can be collected by TRAC using time intervals as short as two minutes. Various spectro-microscopy techniques in the laboratory can be applied to determined chemical composition, morphology, and phase of individual particles. Information is not available in real time and requires a significant effort to perform the various spectro-microscopy analyses and assemble the results. However, these analyses provide more detailed characterization of the chemical makeup of aerosols and their mixing state that cannot be obtained by bulk measurement techniques. They can also characterize the composition of larger particles than is possible by the HR-ToF-AMS. Similar sampling systems have been deployed on the TBS to characterize aerosol composition that would otherwise be impossible with heavier real-time mass spectrometry instruments, such as the HR-ToF-AMS and miniSPLAT.

It is increasingly recognized that aerosols of biological origin may contribute to CCN and IN; therefore it is important to better characterize their concentrations and characteristics. While the CCN and IN activity of bioaerosols is still poorly understood, some studies have shown that biological particles tend to act as IN at warmer temperatures than mineral dust. The wideband integrated bioaerosol sensor (WIBS, DMT) was discussed as one option to address this need. WIBS uses laser-induced fluorescence to infer the

presence of bioaerosols between 0.5 and 30  $\mu\text{m}$  and has been deployed on several aircraft campaigns since 2013 supported by NASA and NSF. Particles of biological origin can also be determined using spectro-microscopy analyses of filter samples, such as those obtained from TRAC.

### 3.2.4.3 Aerosol Precursors

In addition to measurements of aerosol properties, it is important to quantify gas-phase aerosol precursor species to fully understand chemical processes in the life cycle of aerosols. Organic aerosols are the largest fraction of aerosol mass in many regions of the world. While primary emissions contribute to a fraction of this mass, secondary organic aerosol (SOA) formation contributes to most of this mass that depends on chemical reactions associated with hundreds to thousands of volatile organic compounds (VOCs) and oxygenated VOCs (OVOCs). Products generated by ozone ( $\text{O}_3$ ) formation also contribute to the rate of SOA formation. Sulfate ( $\text{SO}_4$ ) is also a large fraction of aerosol mass that is controlled by the amount of sulfur dioxide ( $\text{SO}_2$ ) and dimethyl sulfide (DMS) in the atmosphere. Trace gases comprised of nitrogen, such as nitrogen oxide ( $\text{NO}$ ), nitrogen dioxide ( $\text{NO}_2$ ), ammonia ( $\text{NH}_3$ ), nitric acid ( $\text{HNO}_3$ ), and many others can contribute directly or indirectly to the formation for aerosol nitrate ( $\text{NO}_3$ ) and ammonium ( $\text{NH}_4$ ). The formation of ultrafine particles smaller than 1 nm in diameter occurs in the presence of sulfuric acid ( $\text{H}_2\text{SO}_4$ ) and/or certain organic compounds such as amines.

Numerous types of instruments deployed on past aircraft measurement campaigns quantify concentrations of trace gases. The proton transfer reaction mass spectrometer (PTR-MS) is one type of instrument frequently used over the past two decades to measure a range of VOCs. In the past, this instrument usually provided about 10 trace gases, but more recent developments have led to far more compounds. Two instruments were discussed at the workshop as listed in Table 8: the PTR-time-of-flight-MS (PTR-ToF-MS) and the high-resolution time-of-flight chemical ionization mass spectrometer (HR-ToF-CIMS).

**Table 8.** Instruments that measure trace gases than are aerosol precursors or can be used to infer processes influencing aerosol formation.

Instrument	Measurement	Source/supplier	AAF-owned
Proton-transfer-reaction time-of-flight mass spectrometer (PTR-ToF-MS)	Volatile organic compounds (VOCs) and oxygenated VOCs (OVOCs) at 20 Hz	Vocus	No
High-resolution time-of-flight chemical ionization mass spectrometer (HR-ToF-CIMS)	100's of multifunctional organics, nitrate precursors, biomass burning tracers, radical sources	U. Washington	No
Ozone analyzer	$\text{O}_3$ concentrations at 1 Hz	ThermoFisher Scientific model 49i	No
Enhanced trace level $\text{SO}_2$ analyzer	$\text{SO}_2$ concentrations at 1 Hz	ThermoFisher Scientific model 43i-TLE	No
NO- $\text{NO}_2$ - $\text{NO}_x$ Analyzer	NO and $\text{NO}_2$ concentrations at 1 Hz	ThermoFisher Scientific model 42i	No
$\text{N}_2\text{O}/\text{CO}$ Analyzer	$\text{CO}$ , $\text{N}_2\text{O}$ , and $\text{H}_2\text{O}$ concentrations at 1 Hz	Los Gatos Research Inc, N2O/COR-23r	No

The PTR-ToF-MS can quantify data hundreds of VOCs and OVOCs at sub parts-per-billion (ppb) levels up to 20 times per second. In addition to quantifying aerosol precursors, these measurements can be used to identify chemical tracers of air mass origins (e.g., biological versus anthropogenic), atmospheric processing (e.g., photo-oxidation, cloud-water chemistry), and new particle formation and growth events (e.g., via nucleation markers such as amines). The Vocus PTR-ToF-MS has been deployed on aircraft campaigns supported by NSF, NASA, NOAA, and the UK Met Office. The HR-ToF-CIMS can quantify the concentration of hundreds of multifunctional organics, nitrate precursors such as dinitrogen pentoxide ( $\text{N}_2\text{O}_5$ ) and  $\text{HNO}_3$ , biomass burning tracers such as hydroxy and nitro-aromatics, levoglucosan, hydroxy acetone, and radical sources such as nitrous acid (HONO) and nitryl chloride ( $\text{ClNO}_2$ ) up to 10 times per second. The University of Washington HR-ToF-CIMS has been deployed on the G-1 aircraft during the HI-SCALE campaign as well as other NSF aircraft campaigns.

Table 8 also lists other guest trace gas measurements that have been made on past G-1 deployments that are used to characterize air parcels of anthropogenic origin and determine the degree of photochemical activity in the atmosphere that influences secondary chemical aerosol mechanisms. The details of the AAF-owned trace gas instruments are discussed in section 3.2.6.

### **3.2.4.4      Aerosol Optical Properties**

Aerosols influence climate by scattering and absorbing solar and infrared radiation (also known as direct radiative forcing) and consequently perturbing the Earth's energy budget; therefore, it is important to quantify their optical properties. In general, scattering aerosols reduce the amount of radiation reaching the surface and consequently cool the atmosphere and partially offset atmospheric warming caused by increases in greenhouse gas concentrations. Some types of aerosols such as black (elemental) carbon (BC or EC), brown carbon (BrC), which is a form of organic matter, and certain types of dust absorb radiation that can warm the atmosphere. A key parameter used in radiative transfer calculations in Earth System Models is the single-scattering albedo (SSA or  $\omega_o$ ), which is the ratio of scattering efficiency to the total extinction efficiency (i.e., scattering plus absorption). The direct radiative effect of aerosols is very sensitive to SSA. For example, a change in  $\omega_o$  from 0.9 (less absorbing) to 0.8 (more absorbing) can change the sign of the direct effect (warming versus cooling) depending on the underlying surface albedo and the altitude of the aerosols. Radiative transfer calculations also usually employ Mie theory that uses refractive indices that describe how much of the light path is bent by spherical particles. The real and imaginary components of refractive indices depend on aerosol composition. In addition to composition, scattering also depends on the particle size and morphology.

Scattering and absorption measurements are usually made at select wavelengths, rather than for the entire solar and infrared spectrum. The Angstrom exponent is a parameter that is used to describe how optical properties vary as a function of wavelength. In general, there is less measurement uncertainty with scattering than with absorption. Typically,  $\omega_o$  is determined by combining scattering and absorbing measurements (e.g., from a nephelometer and particle soot absorption photometer [PSAP]) that usually measure the air stream at slightly different times. These sampling issues, combined with a higher uncertainty associated with absorption and different wavelengths sampled by the scattering and absorption instruments, will impact the derived  $\omega_o$ . Despite substantial advances in aerosol optical property instruments over the past five decades, measuring absorption and how it propagates into SSA calculation is still a major challenge.

The AAF has several types of instruments that measure scattering and absorption as listed in Table 9. The discussion at the workshop focused on newer instruments as possible replacements or additions, including the LED-based nephelometer, cavity attenuated phase shift – single scattering albedo (SSA) monitor (CAPS PM<sub>SSA</sub>), and photothermal interferometer (PTI). The LED-based nephelometer and Aurora nephelometer both measure scattering at three wavelengths (450, 532, 632 nm) and can be used to replace older TSI nephelometers being phased out by the manufacturer (and no longer supported). The AAF is conducting extensive testing on the Aurora version to compare its performance with the long deployed TSI version. The LED-based nephelometer is being deployed as a core component of the global Surface PARTiculate mAtter Network (SPARTAN) and the World Meteorological Organization's (WMO) Global Atmosphere Watch (GAW) program; therefore, the LED-based nephelometer will likely become a global standard in the near future. It will be advantageous for AAF to have such an instrument since its performance will be well characterized by the community. The advantage of the CAPS PM<sub>SSA</sub> is that it simultaneously measures both extinction and scattering of the same air volume at five wavelengths (405, 450, 530, 630, 660, 780 nm); therefore, there are no uncertainties associated with combining information from separate instruments and somewhat different sampling times. Absorption and  $\omega_o$  can then be obtained by combining the extinction and scatter measurements. The PTI measures absorption and scattering at the same two wavelengths, 405 and 532 nm, so that  $\omega_o$  can be derived at those wavelength as well as the absorption and scattering Angstrom Exponents (AAE and SAE). The AAE can be used to quantify and partition absorption between BC and BrC as well as between carbonaceous aerosols and dust.



**Figure 14.** Albert Mendoza, ARM engineer, takes the floor at the ARM Aerial Instrumentation Workshop.

**+Table 9.** Instruments that measure aerosol optical properties.

Instrument	Measurement	Source/supplier	AAF-owned
Humidigraph f(RH)	Scattering as a function of relative humidity	PNNL build	Yes
Integrating nephelometer, model 3563	Scattering at 450, 550, 700 nm	Trust Science Innovation (TSI) Inc.	Yes

Instrument	Measurement	Source/supplier	AAF-owned
Particle soot/absorption photometer (PSAP)	Absorption at 462, 523, 628 nm	Radiance Research	Yes
Single-channel tricolor absorption photometer (STAP)	Absorption at 450, 525, 624 nm	Brechel Manufacturing Inc.	Yes
LED-based nephelometer	Scattering at 450 nm, 532 nm and 632 nm	AirPhoton	No
Cavity attenuated phase shift – single scattering albedo (SSA) monitor (CAPS PM <sub>SSA</sub> )	Direct measurements of extinction and scattering at 405, 450, 530, 630, 660, or 780 nm with derivations of SSA and absorption	Aerodyne Research Inc.	No
Photothermal interferometer (PTI)	Absorption and scattering at 532 nm and 405 nm, derived SSA at each wavelength, and AAE/SAE	BNL build	No
Aerosol lidars such as the high-spectral-resolution lidar version 2 (HSRL-2)	Profiles of extinction, backscatter, and depolarization at 355, 532, and 1064 nm over 15-m intervals	NASA Langley	No

Aerosol optical properties often exhibit large vertical and horizontal variations, reflecting heterogeneities in the number, composition, size, and mixing state of aerosol populations, as well as boundary-layer properties, such as moisture controlling the uptake of water on aerosol surfaces. Airborne in situ sampling may miss or incorrectly represent these variations. Fortunately, downward- and/or upward-pointing remote-sensing instruments such as lidars obtain high-resolution measurements of aerosol optical property profiles. This wealth of spatiotemporal information on the local and regional scale of in situ sampling enables insights into processes responsible for spatial variability in aerosol properties. For these reasons, lidars are now commonly deployed during aerosol and cloud-aerosol interaction field campaigns. In addition to key aerosol science questions, lidars also provide logistical benefits to aircraft operations. For example, aerosol layers detected by lidars provide real-time guidance to direct research aircraft to perform detailed in situ sampling at appropriate locations and altitudes that might otherwise be missed. Remote sensing also reduces the need for aircraft to perform as many spirals or rising/descending maneuvers (which can comprise a significant portion of flight duration) to characterize vertical gradients in aerosols.

Jerome Fast's group collected a comprehensive list of aerosols and meteorological lidars. Some types of airborne lidars are designed to measure aerosol optical properties, while other types can measure profiles of aerosol optical properties as well as temperature and moisture (e.g., Raman lidars). While ARM has several ground-based lidars, it does not have a lidar available for airborne operations and special ports on a research aircraft are needed to accommodate lidars. One example lidar used for aircraft operations, the second generation of the high-resolution spectral lidar (HSRL-2) developed by NASA, is listed in Table 9. The first generation of NASA's airborne HSRL is similar in principal to ARM's ground-based HSRL. The HSRL-2 obtains extinction, backscatter, and depolarization at three wavelengths (355, 532, 1064 nm) over vertical intervals as small as 15 m. Data at horizontal intervals of 100 m are obtained assuming an aircraft flight speed of 100 m s<sup>-1</sup>. Raw measurements are often averaged in space (and thus in time) to minimize random errors. Other products can be derived from HSRL-2 measurements, including estimates of boundary-layer height as well as profiles of aerosol concentration, size, and type. Aircraft

deployments of HSRL-2 were made as part of ARM field campaigns, such as the Cumulus Humilis Aerosol Process Study (CHAPS), the Carbonaceous Aerosol and Radiative Effects Study (CARES), and TCAP, in collaboration with other organizations. In each of these campaigns, multiple aerosol layers above the boundary layer were often observed.

### 3.2.4.5 Cloud and Ice Nucleating Properties

Quantifying cloud droplet nuclei and ice nuclei concentrations is important to establish the link between aerosol populations and their effect on cloud properties. The ability of particles to act as CCN depends on aerosol size and chemical composition as well as the ambient supersaturation within clouds. Species such as  $\text{SO}_4$ ,  $\text{NO}_3$ ,  $\text{NH}_4$ , and sea salt are hydrophilic and species such as organic matter, BC, and dust are hydrophobic; however, the overall hygroscopicity depends on the mixture of chemical species in a particle. Field campaign and laboratory experiments have shown that aerosol chemical composition and morphology are factors controlling the ability of particles to serve as IN. Dust particles are particularly conducive to act as IN, likely because of their irregular shape. Recent studies have shown that particles of biological origin, such as fragments of pollen, bacteria, fungi, and insects, can also act as IN.

To address science questions associated with cloud-aerosol interactions, the AAF has a dual-column cloud condensation nuclei counter (CCN) as listed in Table 10. This instrument measures total CCN concentration simultaneously at two supersaturations that can be chosen by the user. ARM has other CCN instruments that obtain concentrations at multiple supersaturations, but the instruments cycle through one supersaturation at a time over a period of several minutes. This sampling frequency is problematic for aircraft deployments; therefore, these instruments are deployed at ground sites. This ability to simultaneously measure CCN at multiple supersaturations at high temporal frequency is a current instrument challenge. To address science questions regarding the impact of aerosols on cloud droplets, it would be desirable to deploy at least two dual-column CCN counters suitable for aircraft operations, with one of them running in a scanning-mode CCN, since knowing CCN at two supersaturations only may not be sufficient for all cloud conditions.



**Figure 15.** Minghui Diao discusses instrumentation and measurements at the AAF workshop.

**Table 10.** Instruments that measure CCN and IN.

Instrument	Measurement	Source/supplier	AAF-owned
Dual-column cloud condensation nuclei counter (CCN)	CCN concentration at two specified supersaturations	Droplet Measurement Technologies (DMT)	Yes
Automated airborne continuous flow diffusion chamber	INP concentration	Handix Sci. Inc.	No
Real-time ice nucleation chamber	INP concentration	PNNL	No

Ice formation in the atmosphere has significant impacts on cloud formation and/or electrification and on cloud properties, thereby influencing the Earth's changing energy balance. (Kanji et al. 2017) Field measurements of ice nucleating particles (INP) are essential for validating theoretical and laboratory studies. However, INP measurements are problematic since their concentrations are often several orders of magnitude lower than CCN concentrations. To determine the INP concentration, two approaches have been used, both at ground sites and in the AAF aircraft: Online (such as using a continuous flow diffusion chamber [CFDC]) and offline (where particles are collected on a hydrophobic substrate or a filter). For the offline method, to obtain statistically meaningful samples, either sampling periods need to be longer to obtain a sufficient number of particles to represent atmospheric conditions, or the sampling flow rate needs to be high enough to obtain sufficient particles. The longer sampling time also makes such measurements problematic for aircraft operations since the spatial averages may not reflect actual variability in INP that affects ice crystal formation in clouds. An online approach, such as CFDC, largely improves the spatial and temporal resolution limitation and provides the possibility of real-time ambient INP measurements, although the CFDC still has a limited in situ sampling period at one ice nucleation mode. Two CFDCs were presented in this workshop, as shown in Table 10. The version from Handix Scientific is currently funded by NASA to develop a commercial version of the instrument. Another version of CFDC proposed by Dr. Gourihar Kulkarni is currently listed as the EMSL capability for instrument users. While IN measurements have been collected at ground sites and by the AAF aircraft during ARM field campaigns, no such CFDC have been developed to sample aloft on the TBS or UAS platforms. Potential INP collection on TBS and UAS still relies on the offline method.

### 3.2.4.6 Inlets

Inlets are as important as instruments, since the inlet design characteristics regulate the size range of particles passed from the environment to aerosol instruments located within an aircraft. Past aircraft deployments, including those with the G-1, have used two types of inlets: isokinetic and CVI. The isokinetic inlet uses a two-stage diffuser assembly to deaccelerate the airflow into the aircraft. This inlet is used primarily to sample interstitial aerosols, although it is possible for cloud droplets to pass through the inlet. Aerosol instruments normally heat air to remove water condensed on aerosol surfaces, but they will also evaporate cloud droplets so that only aerosol residuals remain. In this case, aerosol measurements would contain both interstitial and cloud-borne aerosols that could have very different chemical signatures that are averaged together and cannot be distinguished. To obtain measurements of only the aerosol residuals, CVI inlets are designed to sample only cloud droplets. A counterflowing air stream is used to selectively remove nonactivated particles from the airflow entering the aircraft, while larger cloud

droplets are permitted to pass through. Thus, the aerosol instruments would quantify the size and composition of on the aerosol residuals when the CVI inlet is used.



**Figure 16.** Inlet on G-1 aircraft.

For future Bombardier missions, it is thus desirable to have both isokinetic and CVI inlets. The characteristics of the aerosol residuals will shed light on what type of material is being activated as cloud droplets and what in-cloud chemical processes occur that are both needed to better understand cloud-aerosol interactions and represent those processes in models.

### **3.2.4.7 Aircraft Field Campaign Examples**

Over the past several decades there have been many deployments of research aircraft by multiple national and international efforts that collected in situ and remote-sensing measurements of aerosol properties. Many of those also included cloud properties to investigate cloud-aerosol interaction processes. Past G-1 deployments include Megacities Initiative: Local and Global Research Observations (MILAGRO, 2006), CHAPS (2007), CARES (2010), TCAP (2012 and 2013), BBOP (2013), GOAmazon (2014), ARM Cloud Aerosol Precipitation Experiment (ACAPEX, 2015), Airborne Carbon Measurements V(ACME-V, 2015), HI-SCALE (2016), ACE-ENA (2017 and 2018), and Cloud, Aerosol, and Complex Terrain Interactions (CACTI, 2019). The scientific findings and logistical lessons learned from these deployments can be used to infer new instrumentation needed in future airborne campaigns to tackle outstanding science questions related to aerosol life cycle and its interaction with clouds.



**Figure 17.** View from the G-1 aircraft during the HI-SCALE field campaign at the SGP in 2016.

The instrument and sampling design of the Aerosol Cloud Meteorology Interactions Over the Western Atlantic Experiment (ACTIVATE) sponsored by NASA was presented by Luke D. Ziemba at the workshop as an example of current strategies used to sample coincident aerosol and cloud properties. The overall goal of ACTIVATE is to characterize aerosol-cloud-meteorology interactions using extensive, systematic, and simultaneous in situ and remote-sensing airborne measurements with two aircraft and a hierarchy of models. Sampling focuses on marine boundary-layer stratiform and cumulus clouds and post-frontal environmental conditions. The cloud types over the western Atlantic Ocean are representative of many regions of the world that comprise a large net cooling effect on the global atmosphere. Anthropogenic and biogenic aerosols from North American sources are frequently transported over the western Atlantic, potentially perturbing cloud properties. The HU-25 Falcon obtains in situ measurements of aerosol and cloud properties, while the King Air uses a HSRL to obtain time-height information on aerosol optical properties along the flight tracks of the Falcon. A summary of the aerosol properties and trace gas instrumentation on the Falcon is included in Table 11.

**Table 11.** Aerosol and trace gas instruments used in the HU-25 Falcon during ACTIVATE.

Instrument	Measurement	Source/supplier
Condensation particle counter (CPC, model 3772), and ultrafine CPC (model 3776)	Aerosol number concentration at 1 Hz	Trust Science Innovation (TSI) Inc.
Nano-SMPS (mobility)	Aerosol size distribution between 10 and 420 nm at 60 s intervals	Trust Science Innovation (TSI) Inc.
Laser aerosol spectrometer (LAS, optical)	Aerosol size distribution between 0.09 to 7.5 $\mu\text{m}$ at 1 Hz	Trust Science Innovation (TSI) Inc.
CCN spectrometer	CCN number concentration and spectra	Droplet Measurement Technology (DMT)
Nephelometers	Scattering coefficient, one at RH < 40% and the other at RH > 80%	Trust Science Innovation (TSI) Inc.
Particle soot/absorption photometer (PSAP)	Absorption coefficient	Radiance Research
HR-ToF-AMS – fast mode	Bulk aerosol composition at 1 Hz between 60 and 800 nm	Aerodyne Research Inc.
Particle-into-liquid sampler (PILS)	Bulk aerosol composition < 5 $\mu\text{m}$ at 7-minute intervals	PI build
G2301-m gas concentration analyzer	CO <sub>2</sub> , CH <sub>4</sub> , CO concentration at 0.4 Hz	PICARRO
Ozone monitor	O <sub>3</sub> concentration at 0.5 Hz	2B Technologies

The Falcon collects information along a series of constant altitude transects below, within, and above cloud layers over the western Atlantic, which is a sampling strategy similar to many past aircraft campaigns. The AMS and LAS are manually switched between the isokinetic and CVI inlets so that aerosol residual size and composition can be obtained within clouds.

### 3.2.5 Cloud Measurements

#### 3.2.5.1 In Situ Particle Probes

The array of cloud and precipitation particle probes currently available at the AAF is shown in Table 12. They capture the particle size distribution over a range of four orders of magnitude, from 2  $\mu\text{m}$  to 20 mm, with much redundancy in the 20-1000  $\mu\text{m}$  size range. Data are processed and variables such as effective radius, total surface area, and liquid water content (LWC) are derived using OASIS (Optical Array Shadow Imaging Software), UIOOPS (University of Illinois/Oklahoma Optical Array Probe [OAP] Processing Software), and software developed by Stratton Park Engineering Company (SPEC). Several probes are available to estimate the in situ LWC in clouds (Table 13). Two probes measure total condensed water content, so ice water content (IWC) can be isolated.

**Table 12.** Current AAF cloud probes.

Instrument name	Manufacturer	Measuring range	Size resolution	Technique	
<b>FCDP</b> – Fast cloud droplet probe	Stratton Park Engineering Company (SPEC)	2–50 $\mu\text{m}$	~ 1 $\mu\text{m}$	scattering	
<i>current: wide beam (low concentrations)</i>					
<b>2D-S</b> – Two-dimensional stereo probe	SPEC	20 $\mu\text{m}$ –3 mm	10 $\mu\text{m}$	shadow images	
<i>new: narrow beam (high concentrations)</i>					
<b>HVPS-3</b> – High-volume precipitation spectrometer	SPEC	0.3–19.2 mm	150 $\mu\text{m}$	shadow images	
<b>CPI</b> – Cloud particle imager – soon new <b>3V-CPI</b>	SPEC	4.6 $\mu\text{m}$ –2.3 mm	2.3 $\mu\text{m}$	shadow images	
<b>CAPS</b> – Cloud, aerosol, and precipitation spectrometer	<b>CIP</b> – Cloud imaging probe <b>CAS</b> – Cloud and aerosol spectrometer	Droplet Measurement Technologies (DMT)	25 $\mu\text{m}$ –1.55 mm 0.51 $\mu\text{m}$ –50 $\mu\text{m}$	20 $\mu\text{m}$ ~ 1 $\mu\text{m}$	shadow images scattering

**Table 13.** Current sources of in situ cloud liquid/ice water estimation at AAF.

Instrument name	Manufacturer	Range – droplet sizes	Range – LWC/IWC	Technique
<b>WCM-2000</b> – Water content monitor	Science Engineering Associates, Inc. (SEA Inc.)	<25/<30 $\mu\text{m}$ (two hotwires), LWC+IWC (scoop)	0–10 g/m <sup>3</sup> , TAS < 150 m/s, 0–6 g/m <sup>3</sup> , TAS < 230 m/s,	Hotwires and scoop
<b>PVM</b> – Particle volume monitor	Gerber Scientific, Inc.	3–50 $\mu\text{m}$	0.002–10 g/m <sup>3</sup> (LWC)	Light scattering
<b>CAPS</b> (Hotwire)	Droplet Measurement Technologies (DMT)	<30 $\mu\text{m}$	0 - 3 g/m <sup>3</sup> (LWC)	hotwire
<b>CSI</b> – Cloud spectrometer and impactor	DMT	NA	0.001–5 g/m <sup>3</sup> (Total condensed cloud water content)	spectrometer measuring evaporated water vapor
Cloud probes	<i>Integrated measurements (IWC/LWC differentiation somewhat possible)</i>	various	various	Integrated water content from size distributions

Paul Lawson (SPEC, Inc) presented three new instruments for consideration on the Challenger 850 (Table 14): the HVPS-4, with orthogonal views as for the HVPS-3, but with dual resolution; an improved 2D-Gray probe with four gray levels and 10- $\mu\text{m}$  pixel resolution; and the cloud drop spectrometer (CDS), which has a 40-times-larger sample volume than the CDP, and a range of 2-200  $\mu\text{m}$ . The CDS avoids drop coincidence errors. The HPVS-4 and 2D-Gray probes are in development; the CDS is at a conceptual stage.

**Table 14.** Select next-generation in situ cloud probes.

Name	Source	Size range	Size resolution	Status
HVPS-4	SPEC	0.3–19.2 mm	dual	in development
2D-Grey	SPEC	20 $\mu\text{m}$ –3 mm	10- $\mu\text{m}$	in development
CDS	SPEC	2–200 $\mu\text{m}$	~ 1 $\mu\text{m}$	conceptual
PHIPS	DFG (Schnaiter et al. 2018)	4–800 $\mu\text{m}$	2 $\mu\text{m}$	available
HOLODEC	MTU, NCAR, Mainz	~ 10–200 $\mu\text{m}$ or larger	~ 3 $\mu\text{m}$	available

A promising new cloud probe is the particle habit imaging and polar scattering (PHIPS) probe, which measures the angular light-scattering function of particles, provides stereo-graphic images of particles, and therefore allows better phase discrimination than any other cloud probe. Another very promising probe is the HOLODEC (holographic detector for clouds), which provides not only size distributions, but also the relative position of particles in a volume (~15 cc), through digital reconstruction. Such reconstruction used to be a computational nightmare but is becoming far less prohibitive for large sample sizes with the increase of data storage and HPC. A next-generation HOLODEC is being developed. Both PHIPS and HOLODEC are designed to fit in a standard PMS cannister.



**Figure 18.** ARM technical director Jim Mather and Radiance Calmer at the workshop.

### 3.2.5.2 Isotopic Measurements

Water isotope ratios help reveal water cycle processes and controls on clouds/precipitation. Measuring the isotopic composition of water vapor used to be a time-consuming logistical nightmare. Today, technology exists to make continuous gas-phase spectroscopic measurements at > 1 Hz frequency. Both ambient water vapor and vaporized condensed water can be analyzed. On the NCAR/NSF C-130, a combination of a CVI inlet and an isokinetic inlet has been used to separately sample condensed water and total water, respectively.

### 3.2.5.3 Cloud Lidars

The three most widely used airborne cloud and aerosol lidars in the U.S. are listed in Table 15. The mini-MPL is the least expensive (~\$100K), the least power and weight, the most compact, but also the least resolved in range and time, and less sensitive (limited to the planetary boundary layer or thin clouds). The ECL is a newer lidar designed for a FAA-certified aircraft, based on the multiple versions of Wyoming cloud lidar (WCL) currently available on the Wyoming King Air and NCAR C-130. The HSRL is the higher-power, heavier-weight lidar of the three, and was developed in 2005-2006 for the HIAPER (NCAR G5) aircraft.

**Table 15.** Select cloud lidars.

Name	Source	Properties	Variables	Status
Mini-micropulse lidar (MPL)	Hexagon	532 nm or 1047 nm, low-power, compact, eye-safe, ~10 kg, less sensitive, less range-resolved	backscatter power, depol ratio	available, low-cost
Elastic cloud lidar (ECL)	Alpenglow	355 nm, higher-power (12 mJ/pulse at 20 Hz), bi-static design, 5"x7" optical window port required, eye-safe beyond 134m, ~30 kg	backscatter power, depol ratio + derived variables	available
High-spectral-resolution lidar (HSRL)	U. Wisconsin	532 nm, high-power, eye-safe, 2"x2" optical window port required, large and heavy (~136 kg)	backscatter power, depol ratio + derived	uncertain (developed for the NCAR G-V)

Other airborne lidars exist or are under development, measuring water vapor (using Raman scattering or differential absorption) or air motion of scatterers (Doppler lidar), but these systems require clear air, although they typically have channels measuring the same as the lidars listed in Table 15 (backscatter power and depolarization ratio).

### 3.2.5.4 Cloud Radars

Airborne profiling cloud radar measurements have three main advantages. Firstly, they provide cloud vertical context used in the interpretation of in situ cloud microphysics data (e.g., Wang et al. 2012). Secondly, they allow retrieval of cloud properties in vertical profiles along the flight track, from close to the ground (even in complex terrain) to flight level and in some cases above flight level. Retrievals use single-frequency radars, multiple radar frequencies (e.g., W, Ka, Ku), and dual-polarization variables. Some retrieval algorithms combine radar data with lidar and/or passive microwave radiometer data. Thirdly, these data allow validation of retrieval algorithms designed for ground-based or spaceborne radars, by comparing close-range radar estimates against in situ (flight-level) data.

The most widely cited airborne cloud and precipitation radars are listed in Table 16. Almost all systems are Doppler, allowing the retrieval of vertical or 3D hydrometeor motions. Most systems are profiling; some are scanning across the flight track. The longer-wavelength systems are designed for precipitation estimation and/or for storm dynamics studies.

**Table 16.** Select airborne cloud and precipitation radars.

Operator	NCAR	U. Wyoming		NASA			NOAA	NRC Canada	SAFIRE France	DLR Germany
<b>Acronym</b>	HCR	WCR	KPR	HIWRAP	CRS	EXRAD	TDR, LFR	NAWX	RASTA	HAMP
<b>Platform</b>	G-V	UW King Air & NCAR C-130	UW King Air & others	Global Hawk & ER-2	ER-2	ER-2 & Global Hawk	P3 & G-IV	Convair 580	Falcon, ATR42	G-550
<b>Mounting location</b>	lead cone of underwing pod	fuselage inside cabin	PMS-compatible pod	fuselage	tail cone of wing pod	fuselage inside cabin	tail cone, fuselage inside cabin	fuselage cabin and blister radome	fuselage inside cabin	fuselage underbelly pod
<b>Frequency</b>	W-band	W-band	Ka-band	Ku/Ka bands	W-band	X-band	X-, C-band	W/X bands	W-band	Ka-band
<b>Transmitter</b>	Klystron	Klystron	SolidState	SolidState	SolidState	Klystron		Klystron/Magnetron	Klystron	Magnetron
<b>Antenna(s)</b>	1 antenna variable beam direction	up to 5 antennas multiple beams; up, dual-down, dual-side	2 antennas: ~nadir and ~zenith	GH: 2 antennas: conical scan. two dual-freq. feeds ER-2: nadir polarimetric antenna	1 nadir polarimetric antenna	2 antennas: nadir and conical scan (25°)	TDR: 2 antennas scanning 20° fore or aft LFR: 1 antenna	W/X: 3/2 antennas multiple beams	up to 6 antennas, up & down, u,v,w	1 antenna nadir beam
<b>Beam width</b>	0.7°	0.8°	4.2° (2.2°)	3°/1.2° for Ku/Ka	0.5°	3.3°	1.3°, 1.9°	0.7°/3.5° & 5.5°	0.5°	0.6°
<b>Best RangeRes</b>	38 m	15 m	30 m	38 m	38 m	75 m	75 m	15 m / 45 m	30 m	15 m
<b>Sensitivity</b>	-22 dBz at 10 km	-40 dBz at 1 km	-18 dBz at 1 km	0/-5 dBz for Ku/Ka at 10 km	-30 dBz at 10 km	-15 dBz at 10 km	-12 dBz at 10 km	-20/-30 dBz at 1 km	-35 dBz at 1 km	-25 dBz at 10 km
<b>Doppler</b>	yes	yes	yes	yes	yes	yes	yes, no	yes	yes	yes
<b>Polarization diversity</b>	alternating H, V	alternating/simultaneous H,V on transmit/receive	-	Nadir mode: LDR	LDR	LDR	-	W: H and V X: H and V LDR	-	LDR

### 3.2.6 Gas-Phase Measurements

The gas-phase piloted aircraft measurement capabilities and emerging technique white paper submissions were the primary focus of this session. A summary of instrumentation, performance, and support information is included in Tables 17 and 18. Current AAF gas-phase measurement capabilities provided by BNL and Lawrence Berkeley National Laboratory (LBNL) were summarized. The AAF gas-phase suite selection is prioritized to support ARM scientific investigations of aerosol precursors ( $\text{SO}_2/\text{NO}_x/\text{NO}_y$ ) and processing ( $\text{O}_3$ ), as well as air mass characterization ( $\text{CO}/\text{CO}_2/\text{CH}_4/\text{N}_2\text{O}/\text{O}_3$ ).

**Table 17.** Summary of aerosol precursor, aerosol processing, and air mass tracer present capabilities.

Measurand	Present method	Figures of merit	Comments/comparison
$\text{CO}/\text{N}_2\text{O}/\text{H}_2\text{O}$	QCL absorbance	8.75" x 32" 75 lbs ~200 W $2\sigma$ @ 0.2 Hz (CO) 1 ppbv	Well established with low operator overhead. Faster response (~10 Hz) on-line by 2021.
$\text{CO}_2/\text{CH}_4$	WS-CRD absorbance	8.75" x 23" 75 lbs 150W $2\sigma$ @ 0.3 Hz ( $\text{CO}_2$ ) 0.2 ppmv ( $\text{CH}_4$ ): 0.5 ppbv	Well established and state-of-the-art capability with minimal in-flight support requirements.
$\text{O}_3$	UV absorbance	8.75" x 23" 35 lbs 150 W $2\sigma$ @ 0.1 Hz 3-5 ppbv	UV absorbance is well established with low operator overhead. Response speed needs improvement.
$\text{SO}_2$	Pulsed fluorescence	8.75" x 23" 48 lbs 165 W 0.1 Hz $2\sigma$ : 0.6 ppbv	Well established with low operator overhead. Sensitivity and response time marginal for airborne platforms.
$\text{NO}/\text{NO}_2/\text{NO}_y$	3-channel chemiluminescence detection (CLD)	24" x 28" + pump + 2 cylinders 200 lbs (total) 500 W (total) $2\sigma$ @ 0.5 Hz (NO) 20 pptv ( $\text{NO}_2$ ) 60 pptv ( $\text{NO}_y$ ) 60 pptv	CLD well established. 2-h warm-up. High operator and calibration overhead. Consumables required. Complex data processing required.

**Table 18.** Summary of emerging technologies and opportunities for improved capabilities.

Measurand	Emerging technique or improvement opportunity	Figures of merit	Comments/comparison
CO/N <sub>2</sub> O/H <sub>2</sub> O	QCL absorbance	~ 10 Hz	Faster response from existing AAF instrument, expected online by 2021. Requires larger pump.
CO <sub>2</sub> /CH <sub>4</sub>	Improved WS-CRD (Model 2401-m)	8.75" x 23" 75 lbs; 150W 2 $\sigma$ @ 1 Hz [CO <sub>2</sub> ] 0.05 ppmv [CH <sub>4</sub> ]: 1 ppbv [CO]: 0.015 ppmv	Well established and state-of-the-art capability with minimal in-flight support requirements.
O <sub>3</sub>	Solid state CLD	3.5" x 10" 9 lbs 15 W 2 $\sigma$ @ 10 Hz 3-5 ppbv	Solid state C.L. is fast, light, but must be referenced to UV absorbance, meaning it is complementary to but does not replace the UV absorbance.
SO <sub>2</sub>	Laser-induced fluorescence (LIF)	Unk footprint 200 lbs 1400 W 1 $\sigma$ @ 1 Hz: 5-6 pptv Overall Uncy: ( $\pm 16\% + 0.9$ ) pptv	Rollins et al. 2016. <i>Atmospheric Measurement Techniques</i> 9(9): 4601–4613.
NO	LIF	20" H 110 lbs 400 W 2 $\sigma$ @ 1 Hz: 1 pptv @ 10 Hz: 0.3 pptv Accy: 6-10%	Rollins et al., 2020, AMTD, <a href="https://doi.org/10.5194/amt-2020-24">https://doi.org/10.5194/amt-2020-24</a> . Preliminary FIREX-AQ specifications.
NO <sub>2</sub>	Cavity enhanced absorbance (C	8.75" H 31 lbs 30 W 3 $\sigma$ @ 1 Hz: 0.5 ppbv	
NO <sub>2</sub>	LIF	Unk footprint 2 $\sigma$ @ 1 Hz: 1 pptv Accy: 5%	Bradshaw et al. 2000. <i>Review of Geophysics</i> ; Thornton, JA, et al. 1999. <i>Analytical Chemistry</i> .
NH <sub>3</sub>	Open path absorbance (OPALS)	0" (rack) 100 lbs 2 $\sigma$ precision: @ 10 Hz: 100 pptv @ 1 Hz: 35 pptv	No rack space required. Quoted weight requirement is for window mount. Wing pod installation could be lighter and smaller.

Considerations during inlet design phase as well as inlet and instrumentation characterization were presented to illustrate care is required to reduce uncertainty in sampling integrity and airborne measurement representativeness. In particular, the presentation focused on inlet characterization during flight tests conducted in the first year after acquisition of the NSF/NCAR Gulfstream-V. A detailed description of the objectives, experimental design, and results can be found at the following URL:

<https://archive.eol.ucar.edu/homes/dcrogers/ProgSci/PressureRake>.

The AAF is working to leverage the HIAPER modular inlet (HIMIL) inlet design and operational experience of the NSF/NCAR Gulfstream-V development and implementation to provide the same functionality on the AAF Challenger 850 platform.

Several sensors that take advantage of emerging measurement techniques were presented formally as white papers and during discussion periods. These represented sensor technologies covering a wide range of maturity, but all merit attention due to the natural evolutionary forces of technological advancements and shifts in scientific foci. Therefore, as time and budgets allow, one or all of these sensors may become attractive additions to the AAF gas-phase suite of measurements. The new instruments presented included a cavity enhanced phase shifted (CAPS) nitrogen dioxide sensor (aerosol precursor), open-path ammonia laser sensor (OPALS) (air mass characterization), and solid-phase dye chemiluminescence ozone sensors (aerosol processing and air mass characterization). During the discussion section, the advances in laser-induced fluorescence (LIF) techniques for  $\text{SO}_2$ ,  $\text{NO}$ , and  $\text{NO}_2$  were discussed as alternatives to existing instrumentation. Details of performance figures of merit, technology development status, and support requirements are included in Table 17.

### **3.3 Measurements from Tethered Balloon System (TBS)**

This session of the workshop was organized to introduce current ARM TBS capabilities, followed by short presentations on TBS-demonstrated or TBS-potential instrumentation and associated science drivers, operational requirements, and improvements over existing measurement capabilities.

#### **3.3.1 Current ARM TBS Capabilities**

ARM TBS deployments to the AMF3 at Oliktok Point, Alaska, have occurred from 2015 to 2020 with over 600 flight hours. Flights have been conducted in clouds, within Restricted Airspace R-2204, and cloud properties have been measured using supercooled liquid water sondes, a video ice particle sampler, a cloud droplet probe, a backscatter cloud probe, and a cloud droplet measurement system. Flights have been conducted at the SGP Central Facility (CF) and Extended Facilities 9 and 36 from 2019–2020 for over 150 flight hours. Flights are not conducted in clouds and reach a maximum flight altitude of 1.5 km above the surface. Aerosol properties have been observed with Handix printed optical particle spectrometers (POPS), TSI 3007 CPCs, SKC cascade impactors, and ADI Magic 200 CPCs. Gas-phase samples have been collected using a VOC gas sampler. Atmospheric state and aircraft state measurements have been collected using iMet RSB radiosondes and XQ2 sensors, Sensorsnet and Silixa distributed temperature sensing (DTS) systems, and NRG Systems 40C cup anemometers. A 3D sonic anemometer and Global Navigation Satellite Systems (GNSS) sensor for wind direction are in development. An Infrared Camera Inc. Mirage 640P cooled mid-wave infrared imager has been used for remote sensing of surface temperature.

The TBS (Figure 19) typically operates in a loitering mode, in which the balloon loiters at a fixed altitude for several hours, or in a profiling mode, in which it ascends and descends continuously. The loitering mode allows observations to be made at fixed altitudes for extended periods, while the profiling mode collects observations over a range of altitudes at a higher temporal frequency. Data from the POPS, TSI CPCs, iMet radiosondes and XQ2 sensors, anemometers, and DTS are available on ARM Data Discovery. Three ARM TBS trailers are in use and these platforms have undergone extensive capabilities

improvements from 2015 to 2020. The TBS employs three  $110\text{ m}^3$  aerostats with a maximum payload capacity of up to 36 kg depending on the surface altitude.



**Figure 19.** TBS in flight at the ARM SGP CF in 2019.

An image of the TBS winch is shown in Figure 20. Balloons are not launched or retrieved in wind speeds above 10 m/s and balloons are not flown in wind speeds aloft above 16 m/s. ARM TBSs are expected to be used during the Tracking Aerosol Convection Interactions ExpeRiment (TRACER) and Surface Atmosphere Integrated Field Laboratory (SAIL) campaigns in 2021 in Houston, Texas, and Crested Butte, Colorado, respectively, and at the future location of the AMF3 in the southeastern United States.



**Figure 20.** ARM TBS winch.

### 3.3.2 Proposed ARM TBS Capabilities

A summary of presented instrumentation is detailed in Table 19, along with their associated measurements, vendor sources, operational modes, and statuses.

**Table 19.** Summary of presented instrumentation and associated measurement, vendor source, operational modes, and status.

Measurement	Instrument	Source	Operational notes	Status
Particle maximum dimension, width, area, and aspect ratio	Sharkeye $\mu$ COPP	SPEC	<ul style="list-style-type: none"> <li>• <math>\mu</math>CPI: 1 <math>\mu</math>m–1mm</li> <li>• <math>\mu</math>2D-gray: 5–640 <math>\mu</math>m</li> <li>• <math>\mu</math>FCDP: 1–50 <math>\mu</math>m</li> </ul>	Flown on SPEC TBS and NASA high-altitude balloon.
Aerosol number concentration and size distribution	ADI MAGIC 200 CPC	ADI	<ul style="list-style-type: none"> <li>• Number: 1 nm–1 <math>\mu</math>m</li> <li>• Size: 1 nm–3 nm</li> </ul>	Flown on ARM TBS for 50 hours.
Aerosol mass and chemical composition (non-refractory)	High-resolution aerosol mass spectrometer (HR-AMS) for offline analysis	UC Davis	<ul style="list-style-type: none"> <li>• <math>&gt; \sim 100</math> nm</li> <li>• Filter extraction and liquid delivery</li> <li>• 10 hr. averaging to achieve adequate signal</li> </ul>	Not yet flown.
Refractory black carbon (rBC) number/mass loading, size distributions, and rBC mixing state Non-BC size number/mass	Single-particle soot photometer (SP2-XR)	DMT	<ul style="list-style-type: none"> <li>• BC: 50–800 nm (density = 1.8 g/cc)</li> <li>• Non BC: 100–500 nm</li> </ul>	Laboratory studies in 2019 at Paul Scherrer Institute.
Atmospheric $\text{SO}_2$ concentration (ppbv)	Single $\text{SO}_2$ sonde	U. Houston	<ul style="list-style-type: none"> <li>• Concentration range: 0.47–250 ppb</li> </ul>	Used on BlimpWorks 17' envelope in 2018.

The SPEC Sharkeye is an outgrowth of the  $\mu$ COPP (micro combined optical particle probe), which is an integration of the fast cloud droplet probe (FCDP), 2-dimensional stereo probe (2D-S), and cloud particle imager (CPI) that has been flown on the SPEC TBS and NASA high-altitude balloon. The Sharkeye is designed to mate with the ARM ArcticShark UAS with dimensions of 33.8 cm, 17.9 cm, and 6.14 kg, but is also suitable for deployment on the ARM TBS.

### 3.3.2.1 Vertically Resolved NPF

A compact, battery-operated, water-based CPC manufactured by Aerosol Dynamics Inc. (ADI; Hering et al. 2014) has recently been modified and adapted to detect aerosol particles with diameters down to 1 nm. This proposed 1-nm CPC targets a critical science gap not addressed by existing ARM aerial measurement capabilities: vertically resolved new particle formation (NPF). The ADI 1-nm CPC is a self-sustaining, water-based particle counter that enlarges ultrafine aerosol particles through the controlled condensation of water, after which they can be detected optically. The 1-nm CPC has no internal water reservoir, making it tolerant to tipping and vibration. For TBS deployment, there are no alternative approaches for the sizing and detection of 1-nm aerosol particles because of restrictions on weight, size, and power. The calibration procedure of the 1-nm ADI CPC is based on established protocols and involves the determination of the size-dependent counting efficiency via generation of electrical mobility-resolved, mono-disperse molecular ion standards and reference counting via an electrometer, shown in Figure 21.

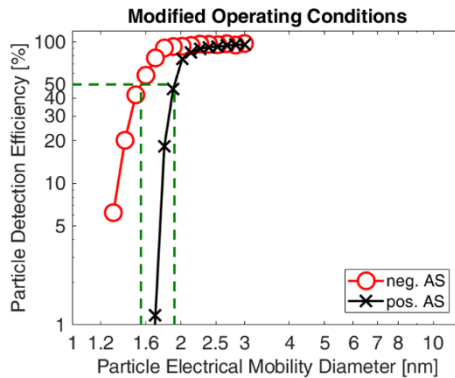


**Figure 21.** Size-dependent detection efficiency of ADI MAGIC 200 CPC using charged ammonium sulfate.

Current ARM aerial measurement capabilities for aerosol number concentration are limited to CPCs that measure aerosol particles with diameters  $> 3$  nm and  $> 10$  nm for manned aircraft,  $> 10$  nm for the TBS, and  $> 7$  nm for the UAS. Acquisition of a 1 nm CPC would address this critical measurement gap below 3 nm for potentially all three platforms (see Table 20 for CPC comparisons). The 1 nm ADI CPC was successfully deployed on the ARM TBS platform during the Vertically Resolved NPF and Transport Study at SGP during two periods in 2019; an image of the CPC enclosure is shown in Figure 22.

**Table 20.** Commercially available 1-nm CPC systems and relevant specifications and recommendations.

CPC model	Sizing Capability	Time Resolution	Weight	Power	Important considerations	Potential Platforms
TSI 3777	No	1 s (counting)	15 kg	200 W (max) 100 W (ss)	vacuum, booster CPC required	plane
Airmodus PSM	Yes	1 s (counting) 5 m (sizing)	22 kg	320 W (max)	vacuum, compressor, booster CPC required	plane
ADI MAGIC 200*	Yes	1 s (counting) 1 s (sizing)	2.4 kg	30 W (max) 15 W (ss)	potential water-depletion	plane; TBS
TSI 3789	No	1 s (counting)	8 kg	200 W (max) 80 W (ss)	low sensitivity to organics	plane

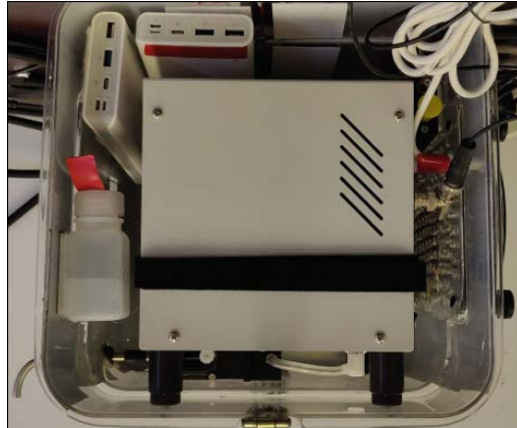


**Figure 22.** Enclosure with MAGIC CPC and system peripherals installed.

A particularly notable result from this campaign was the observation of a smoke plume on 7/25/2019. Prevailing winds were from the south. Figure 23 presents some observational highlights from that day, showing the number concentration of 1–3-nm aerosol (taken as the difference between the two CPC concentration readings) as a function of time (blue), and the altitude (above ground level) of the CPC measurements as a function of time (orange). This particular example points towards the strong vertical heterogeneity in nanoparticle concentrations that can be associated with biomass burning.

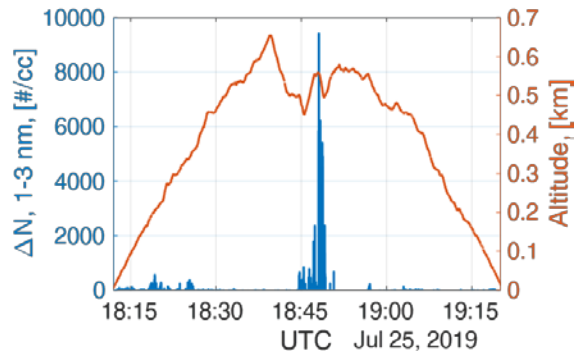


**Figure 23.** Vertically resolved number concentration (1–3 nm) and altitude at SGP.

Offline analysis of particulate matter (PM) samples collected from the TBS may provide aerosol chemical composition data with sufficient spatiotemporal resolution for process-level understanding of the highly dynamic atmospheric aerosol system. In order to obtain information on aerosol composition through TBS measurements, it is important to develop highly sensitive chemical analysis methods. Aerosol mass spectrometry (AMS), which has been a critical measurement technique for numerous field studies and long-term measurement projects, provides the requisite chemical sensitivity, making it an attractive tool for offline PM analysis to address physical and chemical characteristics and processes of atmospheric aerosols. Offline analysis proceeds with aerosol sample collection via filter impaction, followed by sample extraction via controlled atomization and drying, followed then by introduction into the AMS, as illustrated in Figure 24.

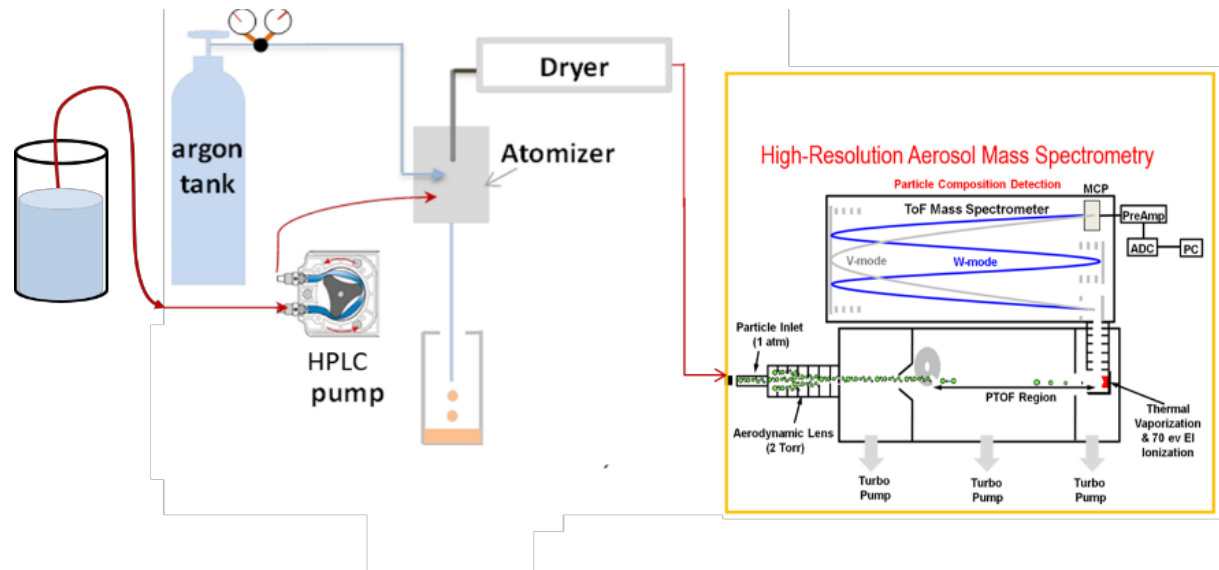


**Figure 24.** Schematic for offline AMS sample analysis.

This technique has been demonstrated in studies of chamber secondary organic aerosol experiments and ambient studies. For low-volume samples expected from TBS deployment, sample extraction proceeds via ultrasonic nebulization. Continuing work focuses on development of micro-nebulization techniques and quantitative methods for sample analysis.

### 3.3.2.2 SP2-XR

Quantification of the spatial and temporal variability of BC aerosol remains of great interest in understanding radiative forcing of climate, as BC is second only to CO<sub>2</sub> as a positive warming agent. Frequent, vertical profiles of BC in various environments over periods from days to seasons would provide insight into how representative ground-based measurements are for the depth of the boundary layer and serve as a significant metric for evaluation of BC loadings and transport in climate models.

The single-particle soot photometer – extended range (SP2-XR) from Droplet Measurement Technologies is a compact, lightweight version of the original single-particle soot photometer (SP2) for the measurement of BC aerosol. The SP2-XR, like the original SP2, directly detects and characterizes individual BC-containing particles using laser-induced incandescence. Any particle traversing the laser beam in the SP2-XR will scatter light, allowing a determination of its size. If the particle contains BC, the BC component will absorb some of the laser energy until its temperature is raised to the point at which it incandesces. The amplitude of the BC incandescence signal is directly proportional to the mass of BC contained in the illuminated particle. Binning individual incandescence signals per unit sample volume enables determination of the BC mass concentration, while binning the individual signals by volume-equivalent diameter enables determination of the size distribution.

The SP2-XR measures refractory Black Carbon (rBC) number/mass loading, size distributions (at sizes of 50–800 nm/1.8 g/cc density), and rBC mixing state. Non-BC size number and mass loading and size distribution (100–500 nm) are also reported. The SP2-XR achieves particle-resolved detection of rBC through laser-induced incandescence. Mixing state analysis couples particle scattering data with incandescence. Measurements of BC are needed to better constrain BC contribution to direct effect for

optical closures, to understand and quantify altitude-dependent contributions of BC to aerosol radiative forcing, and to assess the impact of rBC mixing state on optics. Furthermore, there is a paucity of BC measurements, particularly in the cryosphere. The SP2-XR is suitable for use on TBS or UASs and requires 25 W, weighs 13 kg, and is 40.4 cm long, 20 cm wide, and 21.5 cm high. The SP2-XR was operated on a King Air 300 and underwent laboratory studies at the Paul Scherrer Institute in 2019. The sample flow is user-selectable from 0.03–0.120 LPM. The SP2-XR uses the same calibration procedure as the SP2 (fullerene soot for incandescence channel and polystyrene latex (PSL) for the scattering channel) and achieves similar measurement uncertainty (25%).

### 3.3.2.3 SO<sub>2</sub>

The University of Houston has developed an SO<sub>2</sub> sonde based on a traditional electro-chemical cell (ECC) O<sub>3</sub> sonde system that uses an iodine/iodide redox reaction. A standard O<sub>3</sub> sonde has negative SO<sub>2</sub> interference, meaning 1 ppbv of SO<sub>2</sub> is measured as -1 ppbv O<sub>3</sub>. The previous SO<sub>2</sub> measurement method required two sondes, one with a SO<sub>2</sub> removal filter. SO<sub>2</sub> concentration was calculated based on the difference between the sondes. This methodology only worked when the O<sub>3</sub> concentration was greater than the SO<sub>2</sub> concentration, and also resulted in increased measurement uncertainty from the use of two sondes. University of Houston's new single SO<sub>2</sub> sonde method directly measures SO<sub>2</sub>, can measure SO<sub>2</sub> concentration much greater than concurrent O<sub>3</sub> concentration, and lowers the detection limit of SO<sub>2</sub> to below 1 ppbv. An operating schematic of the sonde is shown in Figure 25. The single SO<sub>2</sub> sonde has been flown on a Black Swift S2 fixed-wing UAS and 17'-long tethered balloon.

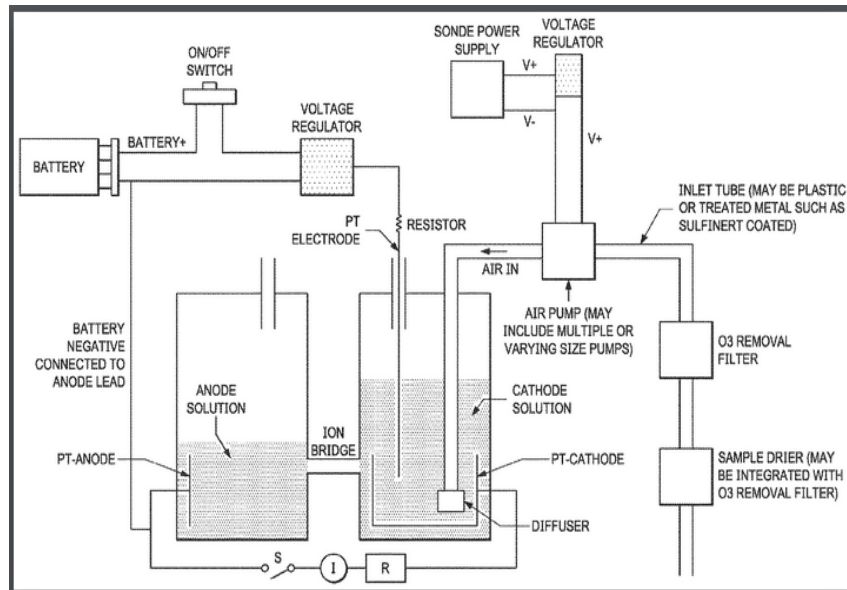


Figure 25. Component drawing of University of Houston SO<sub>2</sub> sonde.

## 3.4 Measurements from Unmanned Aerial System (UAS)

The ARM Airborne Instrumentation Workshop included presentations and discussion of the capabilities and status of the AAF ArcticShark UAS, the existing ArcticShark instrument suite, science drivers and

corresponding measurement needs, examples of other UAS measurement platforms, capabilities and campaigns, and descriptions of a number of recently developed instruments suitable for use with the ArcticShark. Science drivers for the ArcticShark are covered in Section 3.1 above. The following subsections provide a brief overview of the performance of the ArcticShark, the existing AAF ArcticShark instrument suite, details of several recently developed or proposed instruments for use with the ArcticShark, and a discussion of other potential measurement needs.

### **3.4.1 UAS Platform – ARM ArcticShark Versus Other Platforms**

The status and capabilities of the ARM AAF ArcticShark were presented. The ArcticShark is a highly capable, mid-sized UAS that has been modified (hardened) for cold-weather (e.g., arctic) operations. The platform has a payload capacity of up to 100 lbs total in two internal instrument bays and four under-wing hardpoints. Flight endurance ranges from 8 hours with a payload up to 75 lbs to 2.5 hours with a maximum payload of 150 lbs. The aircraft flies at a relatively slow airspeed of 30-40 m/s, which reduces some of the sampling complexities (e.g., ram heating) that are typically encountered with aircraft measurements.



**Figure 26.** The AAF's ArcticShark on the tarmac.

ArcticShark science missions will focus on supporting measurement campaigns at ARM observatories (e.g., Southern Great Plains) and mobile facility installations.

At present, science missions for the ArcticShark are limited to using instruments from the existing AAF instrument suite (see section 3.4.3). The next step will be to permit new instruments developed under the DOE SBIR program to integrate on the ArcticShark as “guest” instruments. In the future, it is expected that AAF will acquire additional instruments to extend the science capabilities of the ArcticShark and eventually develop protocols to allow integration of user-supplied instruments for science missions.

Many organizations, including ARM, have used smaller platforms for atmospheric studies from the tropics to the North Pole. Calmer overviewed those platforms and associated field studies as shown in Figure 27. Those field campaigns were conducted to study atmosphere-ocean-wave interactions, aerosol-cloud interactions, boundary-layer and cloud-base entrainment, and atmospheric properties in the arctic boundary layer.

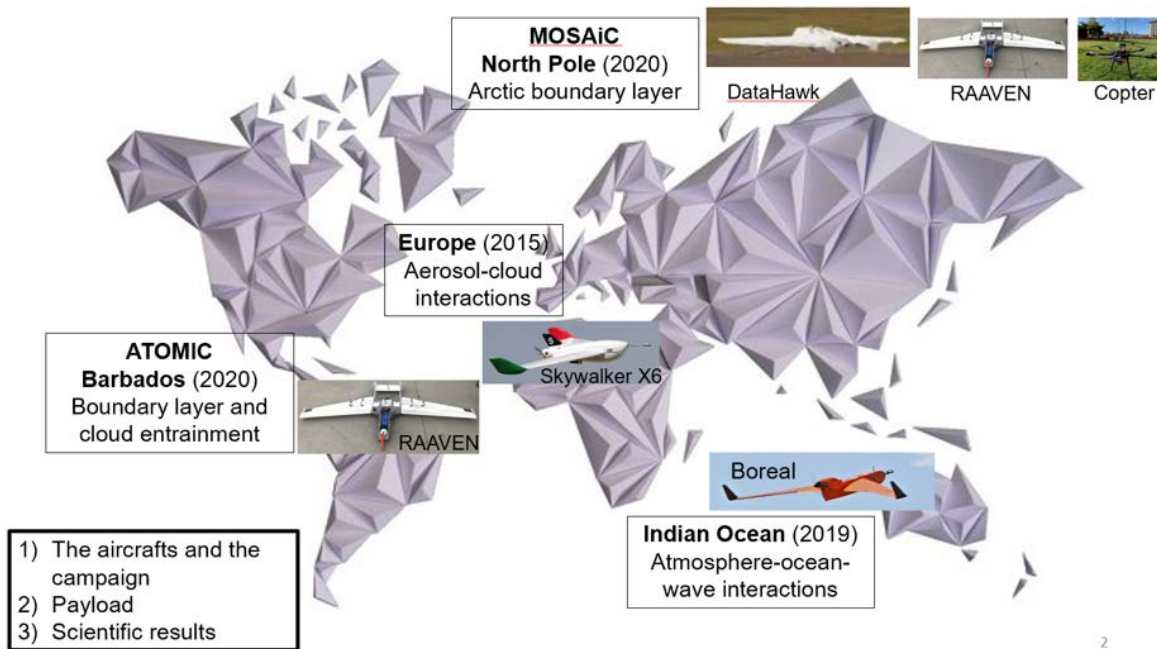


**Figure 27.** Overview of sUAS campaigns for the atmospheric studies by Radiance Calmer.

The Cooperative Institute for Research in Environmental Sciences (CIRES), Aerospace Department at the University of Colorado, Boulder, the University of Colorado Integrated Remote and in Situ Sensing (IRISS) Program, the University of Colorado, Denver, the University of Utah, and the NOAA Unmanned Aircraft Systems Program Office have worked together on the Nighttime Fire Observations eXperiment (NightFOX). They developed the UAS (Black Swift S2) capability to monitor wildfire in support of fire weather forecasting. The custom-built switchable payload packages include an in situ instrument package and a remote-sensing instrument package, as shown in Figures 28 and 29. Using two modular and easily exchangeable payloads, this sUAS can serve as an ideal platform for measurements of biomass burning emissions, plume distribution, fire extent and perimeter, and supporting meteorological data, especially at night when manned aircraft typically do not operate. One payload will provide in situ measurements of CO<sub>2</sub>, CO, and fine- and coarse-mode aerosol size distributions in biomass-burning plumes for characterization of fire combustion efficiency and emissions. A filter sampler will collect bulk aerosol samples for offline composition analysis. The second payload will be flown over the fire to make remote-sensing measurements of fire perimeter and fire radiative power using visible and short-, mid-, and long-wavelength IR observations. The multispectral remote-sensing data will be used to provide sub-pixel information for comparison with satellite fire observations, and along with measured meteorological parameters will be used to inform, test, and improve the WRF-SFIRE fire-atmosphere model.

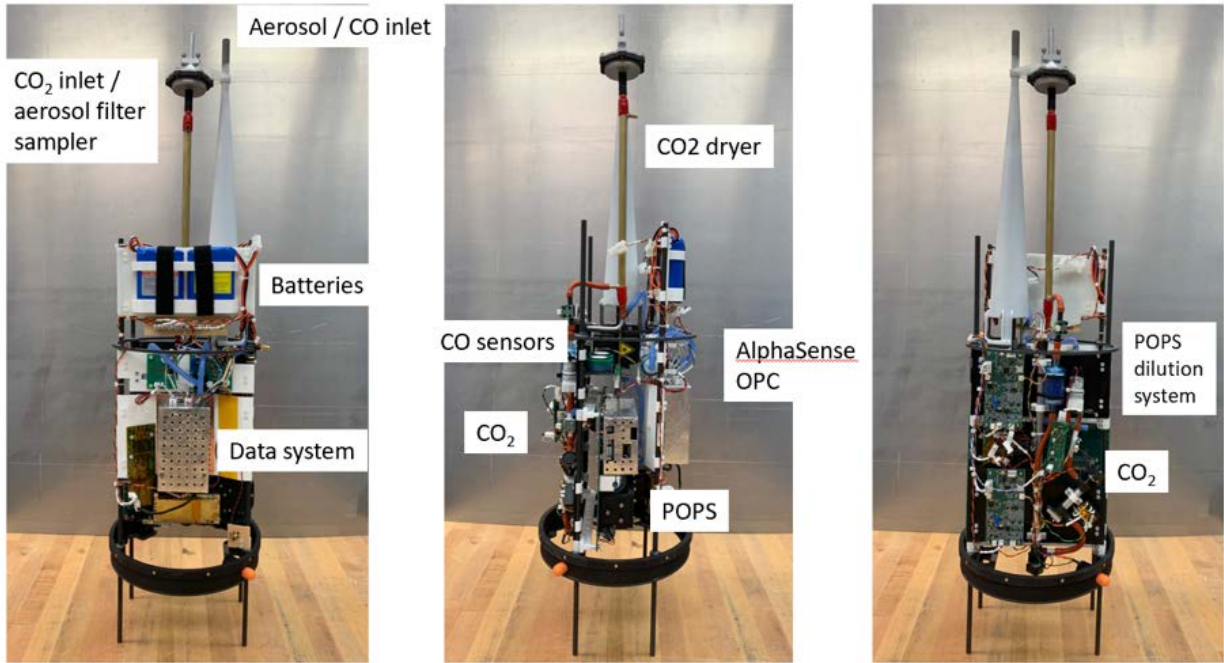


**Figure 28.** The NightFOX in situ instrument package payload.

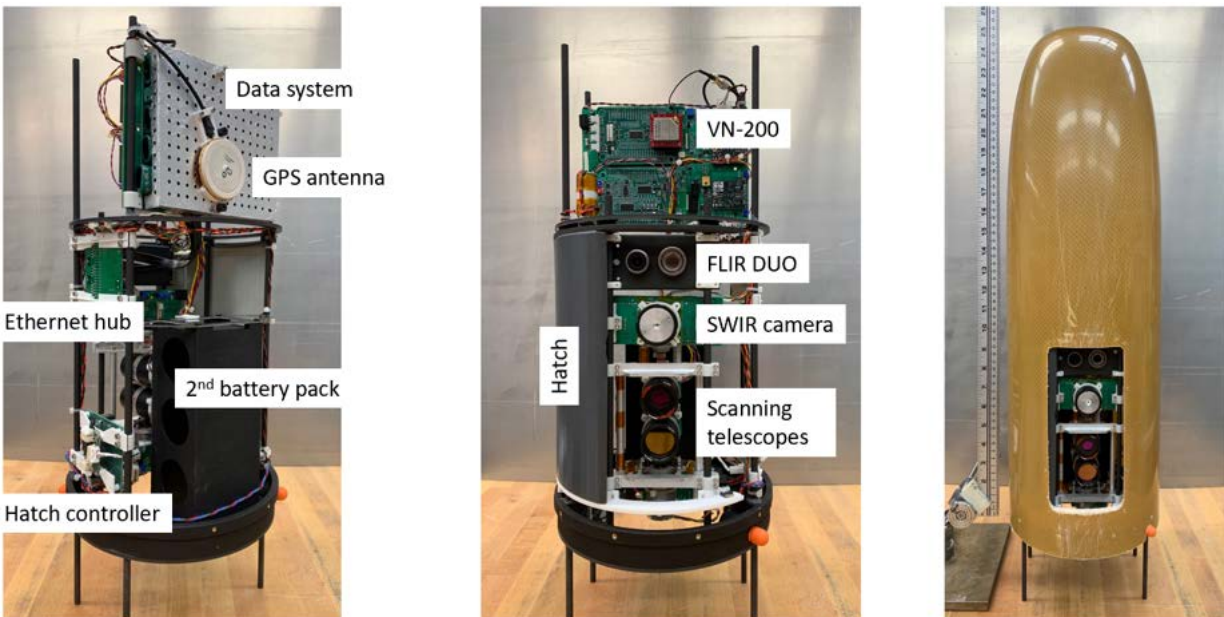


**Figure 29.** The NightFOX remote-sensing instrument package payload.

### 3.4.2 Current ARM UAS Instruments

The AAF has developed and integrated a number of instruments for the ArcticShark that provide a significant range of measurement capabilities. These instruments include in situ measurements of atmospheric state parameters, CO<sub>2</sub>, H<sub>2</sub>O, aerosols and cloud droplets, and remote sensing of the surface

with a multispectral camera and a surface temperature IR sensor. A broadband radiometer suite has also been developed but not yet integrated onto the aircraft. The existing AAF ArcticShark instruments are shown in Table 21.

**Table 21.** Existing AAF ArcticShark instruments.

Instrument		Measurement	Manufacturer
VN-300		Aircraft heading, position, attitude	VectorNav
AIMMS-30		Pressure, temperature, humidity, winds	Avantech Research Inc.
LI-840a		CO <sub>2</sub> and H <sub>2</sub> O	Li-Cor
POPS		Aerosol size distribution (0.14–3 μm)	Handix Scientific
ACCESS	MCPC	Aerosol concentration (> 7 nm)	Brechtel Manufacturing
	mOPC	Aerosol size distribution (0.18–10 μm)	
	STAP	Aerosol light absorption	
	Filter sampler	Aerosol collection for offline analysis	
CDP		Cloud droplet size distribution (2–50 μm)	Droplet Measurement Technologies
CT09		Surface temperature	Heitronics
Altum		Multispectral camera	MicaSense
SPN1		Broadband solar irradiance (0.4–2.7 μm)	Delta-T
MFR		Spectral solar irradiance discreet bands (415, 500, 615, 673, 870, and 940 nm, each 10 nm FWHM)	Yankee Environmental Systems
IR20		downward and upward longwave irradiance (4.5–40 μm)	Hukseflux

The majority of AAF instruments have been integrated onto the ArcticShark and have been evaluated during test flights.

### 3.4.3 Proposed ARM UAS Instruments

A number of new instruments have been developed under DOE SBIR grants for potential use with the ArcticShark. These include the SPEC, Inc. Sharkeye combination cloud probe and an open-path, tunable-diode laser hygrometer from Physical Science, Inc. Other instruments that have been developed for use on UAS, or could be adapted for use on the ArcticShark, include an open-path methane sensor, the DMT SP2-XR instrument for measuring BC aerosol, and the BNL fast chemiluminescence ozone instrument.

**Table 22.** Proposed instruments for the ArcticShark UAS.

Instrument	Measurement	Location, weight and power	Developer
Sharkeye	Cloud particle number, size distribution, ice habit	Wing mount, 6.2 kg, < 200 W	SPEC, Inc.
UAS laser hygrometer	H <sub>2</sub> O mixing ratio	Wing mount, 0.9 kg, 49 W	Physical Sciences, Inc.
Mid-IR methane sensor	CH <sub>4</sub> mixing ratio	Wing mount, 1.6 kg, 30 W	Mark Zondlo, Princeton University
SP2-XR	BC aerosol number and mass	Payload bay, 13 kg, 25 W	Droplet Measurement Technologies
Fast chemiluminescence ozone instrument	O <sub>3</sub> mixing ratio	Payload bay, 4 kg, 15 W	DOE Brookhaven National Lab

### 3.4.3.1 Sharkeye Combination Cloud Probe

Due to their large spatial extent, persistence and radiative properties, mixed-phase clouds in the Arctic have a major impact on surface radiative fluxes and energy balance, which are critical to climate change. Net warming from mixed-phase cloud cover over the Arctic promotes melting and increases the amount of open water, which absorbs more incoming solar radiation than ice surfaces, setting up a positive feedback process that leads to more melting and additional warming.

The Sharkeye Combination Cloud Probe developed for the ArcticShark under an SBIR grant by SPEC, Inc., represents a significant improvement in cloud measurement capability (see Table 23) over the current AAF CDP. The Sharkeye combines a  $\mu$ FCDP (improved version of the CDP) forward-scattering detector, a  $\mu$ 2D-Gray imaging detector, and  $\mu$ CPI high-resolution camera and will provide improved cloud particle number and size distribution measurement from 1  $\mu$ m to 640  $\mu$ m diameter. The Sharkeye will also allow determination of cloud particle phase and characterization of ice habits, critical information for determining cloud microphysical processes and radiative properties.

**Table 23.** Sharkeye combination cloud probe measurement specifications.

Instrument	Measurement type	Sensor specifications	Target resolution	Measurement range	Sampling speed	Laser wavelength
$\mu$ CPI	Camera	1024*1280 8-bit gray scale	1 $\mu$ m per pixel	1 $\mu$ m to 1 mm	~30 Hz	905 nm
$\mu$ 2D-Gray	Imaging	128-photodiode array	5 $\mu$ m per pixel	5–640 $\mu$ m	Continuous	830 nm
$\mu$ FCDP	Forward scattering	Signal and qualifier photodiode	1 $\mu$ m	1–50 $\mu$ m	Continuous	785 nm

### **3.4.3.2 High-Performance UAS Laser Hygrometer**

Mixed-phase clouds play a significant role in the radiative balance of the Arctic, and improved understanding of their formation and stability is an ARM research priority. Achieving this goal requires the ability to accurately and precisely measure supersaturation conditions near and within the clouds.

A lightweight, high-performance laser hygrometer for use on mid-sized UAS has been developed under a DOE SBIR by Physical Sciences, Inc. in collaboration with Princeton University. The sensor is an open-path design that measures water vapor in the free airstream via optical absorption at 2.7  $\mu\text{m}$ . The sensor has an accuracy and precision of 1 ppmv at a reporting rate of 1 Hz. Size, weight, and power (SWaP) values for the payload are 5675  $\text{cm}^3$ , 0.9 kg, and 49 W. These values are well within the payload resources of the ArcticShark, where integration would be in an underwing pod.

The UAS laser hygrometer measures in situ water vapor via tunable-diode laser absorption spectroscopy. The sensor has a very high dynamic range (4 to 5 orders of magnitude in absorption) achieved by using both direct absorption and wavelength modulation spectroscopy, with the mode automatically based on the magnitude of the absorption in real time. The sensor is characterized by high precision and accuracy that it achieves through its data processing routines. The open-path design of the instrument eliminates issues of water absorption/desorption from inlet surfaces that can degrade the accuracy of closed-path (extractive) water measurements, reduces weight by eliminating the need for a pump, and enables a fast measurement response necessary in the spatially heterogeneous conditions in and near clouds. Simultaneous in situ temperature and pressure measurements are made from the hygrometer instrument pylon in order to process the data and calculate mixing ratio.

### **3.4.3.3 Compact, Mid-IR Methane Sensor**

A capable, UAS-deployable methane instrument would enable ARM to use the ArcticShark for science missions to study CH<sub>4</sub> emissions from sources like melting arctic permafrost, methane clathrates, wetland ecosystems, concentrated animal feeding operations, and oil and gas facilities at Prudhoe Bay or the Southern Great Plains site.

A compact, low-power, laser-based sensor has been developed and deployed to measure methane from airborne platforms, and the system is particularly designed for lower-power and lightweight platforms such as the ArcticShark UAS (and TBS). Performance specifications for the current system are shown in Table 24. The system has been flown on various UAS as well as a manned Cessna aircraft, and the measurements have been validated against tower measurements from commercial methane sensors. The open-path design allows the sampling cell to be directly exposed to the ambient air, which helps to minimize power draw and mass by avoiding pumps and a sampling system.

**Table 24.** Compact, mid-IR methane sensor performance.

Parameter	Value
Precision	5 ppbv $\text{Hz}^{-1/2}$
Mass	0.68 kg (sensor head), 4.00 kg (control box)
Dimensions	24 cm $\times$ 10 cm $\times$ 10 cm (sensor head) 20 cm $\times$ 26 cm $\times$ 11 cm (control box)
Frequency	1–10 Hz
Power	30 W

By replacing the DFB laser with an interband cascade laser (ICL) at an appropriate mid-IR wavelength, the system could be readily adapted to measure carbon monoxide (CO, 4.61  $\mu\text{m}$ , expected precision 2 ppbv at 1 Hz) or nitrous oxide (N<sub>2</sub>O, 4.54  $\mu\text{m}$ , 0.3 ppbv precision expected at 1 Hz). The CO and N<sub>2</sub>O open-path precisions are based upon past open-path systems for these gases using quantum cascade lasers (QCL). The adaptation for CO measurements would be useful as a tracer of combustion for pollution or wildfire emissions studies. N<sub>2</sub>O measurements would be of interest in studies ranging from agricultural emissions to natural ecosystems (e.g., tropical soils).

#### 3.4.3.4 Fast Chemiluminescence Ozone Instrument

Ozone is an important atmospheric trace species and a human health concern and plays a significant role in processing secondary organic aerosol (SOA). BNL has recently developed a lightweight, low-power, fast ozone instrument to measure the concentration of ozone through its chemiluminescence reaction with a dye-impregnated silica plate. The resultant luminescence is linear over 0–200 ppbv of ozone, and the reaction is sufficiently rapid that a response of 2–10 Hz has been demonstrated. The instrument delivers sufficient temporal resolution to be used for both eddy-correlation flux measurements and spatial mapping of rapidly changing atmospheric features encountered during aircraft-based sampling. The instrument has so far been operated only in the laboratory. Aircraft operation was simulated by restricting the inlet flow to 500 hPa (18,000 ft) with no change in response detected.

The instrument weight and power consumption, 4 kg and 15 W, are easily accommodated by the ArcticShark, but the instrument would need to be repackaged from the prototype configuration in order to fit into the volume of the ArcticShark payload bay. For UAS operation, the instrument would be calibrated pre and post-flight via the commercial ozone analyzer.

## 4.0 Recommendations

During the two-day workshop, participants discussed in depth the current AAF capabilities and potential future capabilities AAF can implement. Several recommendations were also made throughout the workshop.



**Figure 30.** Sebastien Biraud speaks with colleagues at the AAF Instrumentation Workshop.

## 4.1 Recommendations for Measurements from Piloted Aircraft

### 4.1.1 Atmospheric State Measurements

A high-priority recommendation is to obtain reliable high-time-resolution temperature and water vapor measurements at frequencies greater than currently available from radiosondes (at least 10 Hz). Such measurements are needed to coincidentally exist with the ARM surface-based measurements with extended high spatial resolution. Additionally, the time synchronization between the high-time-resolution measurement of the meteorological properties with the aerosol and cloud properties was emphasized during the discussion.

### 4.1.2 Radiation Measurements

Two primary recommendations came out of the presentations and discussion in the Radiation Measurements section:

1. **Broadband and spectral airborne measurement needs.** A combination of both broadband and spectral aircraft measurements of the downwelling and upwelling solar and IR radiation would provide the most powerful instrument package for characterizing the radiative properties and effects of aerosols and clouds throughout the atmospheric column, and of the surface.
  - The incorporation of spectral radiometric instrumentation, with the more established broadband instrumentation, would represent the largest extension of scientific utility of ARM's airborne radiation measurement capability, enabling research related to atmospheric structure and composition including cloud and aerosol properties and their radiative interactions.

2. **Importance of the correction for non-level platform.** Downwelling broadband and spectral solar irradiance measurements require a method to correct for the attitude of the aircraft, by either an actively stabilized level platform or the application of correction techniques using the aircraft navigational and attitude data combined with auxiliary solar radiation measurements.

#### 4.1.3 Aerosol and Gas-phase Measurements

Aerosol number concentration, size distribution, composition, and mixing state are key parameters affecting aerosol optical properties and cloud nucleating properties. Also, the collocated measurements of aerosols and their trace gas precursors reveal the insight of the aerosol processing and air mass characterization; therefore, measurements of these quantities are critical to better understand the aerosol life cycle. The recommendation from the discussion in the Aerosol and Trace Gas Measurement sections include:

1. **Enhancing Gas-Phase Oxidants and Aerosol Precursors.** The AAF has kept improving the current capability and enhancing the measurements under challenging environmental conditions. It is also important to measure gas-phase oxidants and aerosol precursor concentrations to fully understand the mechanisms controlling the formation, growth, and decay of aerosols and represent those mechanisms in models.
2. **A well-characterized inlet system** will ensure the accuracy of the measurement and is critical for airborne sampling. For future missions, two types of aerosol inlets – isokinetic and CVI – are desired to serve as the basic inlet system. The AAF is working to leverage the HIMIL inlet design and operational experience of the NSF/NCAR Gulfstream-V development and implementation to provide the same functionality on the AAF Challenger 850 platform. All of the inlet systems mentioned above will be characterized both in the wind tunnel and during testing flights.
3. **Increasing frequent and routine airborne sampling.** Airborne platforms can sample the vertical and horizontal variability of aerosol properties over local, regional, and even global scales needed to develop and evaluate Earth System Models. For example, measurements from global aircraft transects from recent HIAPER Pole-to-Pole Observations (HIPPO) and Atmospheric Tomography Mission (ATOM) campaigns are now being used to evaluate the performance of Earth System Models in predicting aerosol properties and variability. Thus, more routine and frequent airborne sampling will provide statistically desired data products.
4. **Strengthen the remote sensing capability with Lidar.** Several types of aerosol lidars and meteorological lidars can be deployed on an aircraft. Aerosol lidars, such as HRSL, provide the accurate high spatial and temporal resolution of aerosol information, such as the aerosol attenuated backscatter and depolarization profiles, aerosol extinction and aerosol optical thickness. Meteorological lidars, such as Raman lidar, provide temperature, and moisture profiles at high spatial and temporal resolution.

#### 4.1.4 Cloud Measurements

Two primary recommendations came out of the presentations and discussion in the Cloud Measurements section:

1. **Next-generation instruments.** Several new instruments were introduced that will improve cloud particle sizing and shape determination, ice and liquid phase characterization, and information desired

- on mass-based ice/water phase partitioning within a given volume. Those instruments will strengthen the AAF capability for mixed-phase clouds measurements.
2. **Co-located in situ measurements and cloud radar and/or lidar measurements** are recommended for providing the in situ statistical characterization of ice mass and evaluating multi-wavelength retrieval algorithms.

## 4.2 Recommendations for Measurements from Unmanned Platforms

While airborne measurements from aircraft, TBS, and UAS platforms do not provide the spatial and long-term coverage that can be obtained from satellites, they provide more detailed characterization of aerosol properties than are available from satellite remote-sensing instruments and are thus better suited to develop and evaluate the representation of aerosol processes in Earth System Models.

Discussions of articulated measurement platforms/measurement strategies included: tethered unmanned aerial systems for an extended operation period, a balanced measurement considerations of TBS profiles versus loiters (i.e., virtual tower allowing for extended sampling to achieve better measurement signal), and how loiters are needed to decouple aerosol transport from aerosol growth. Additionally, although the collection of measurements could be obtained by multiple platforms during intensive operational periods, it is very challenging to assure collocation of the properties measured and enable study of their covariations. Further engineering practices may provide valuable lessons on how to conduct such operations in the future.

Discussions of articulated measurement needs included: distributed temperature sensing and 3D wind speed for turbulence, vertically resolved water vapor, vertically resolved aerosol chemical composition (potentially using TRAC or filter-based samplers), vertically resolved aerosol optical properties, use of water CPC droplet impaction for offline analysis of aerosol droplets (but perhaps not enough mass for studying NPF chemical composition), and how the thermal desorption chemical ionization mass spectrometer (TDCIMS) can provide offline chemical composition as it is not currently viable for online TBS deployment. These emerging capabilities require smaller-scale field studies to ensure the measurement accuracy and comparability to the ground measurements.

## 5.0 References

- D'Alessandro, JJ, M Diao, C Wu, X Liu, M Chen, H Morrison, T Eidhammer, JB Jensen, A Bansemer, MA Zondlo, and JP DiGangi. 2017. "Dynamical conditions of ice supersaturation and ice nucleation in convective systems: A comparative analysis between in situ aircraft observations and WRF simulations." *Journal of Geophysical Research – Atmospheres* 122(5): 2844–2866, <https://doi.org/10.1002/2016JD025994> <http://doi.wiley.com/10.1002/2016JD025994>
- D'Alessandro, JJ, M Diao, C Wu, X Liu, JB Jensen, and B Stephens. 2019. "Cloud phase and relative humidity distributions over the Southern Ocean in austral summer based on in situ observations and CAM5 simulations." *Journal of Climate* 32(10): 2781–2805, <https://doi.org/10.1175/JCLI-D-18-0232.1>

Diao, M, L Jumbam, J Sheffield, EF Wood, and MA Zondlo. 2013a. “Validation of AIRS/AMSU-A water vapor and temperature data with in situ aircraft observations from the surface to UT/LS from 87°N-67°S.” *Journal of Geophysical Research – Atmospheres* 118(12): 6816–6836, <https://doi.org/10.1002/jgrd.50483>

Diao, M, MA Zondlo, AJ Heymsfield, SP Beaton, and DC Rogers. 2013b. “Evolution of ice crystal regions on the microscale based on in situ observations.” *Geophysical Research Letters* 40(13): 3473–3478, <https://doi.org/10.1002/grl.50665>

Diao, M, MA Zondlo, AJ Heymsfield, and SP Beaton. 2014. “Hemispheric comparison of cirrus cloud evolution using in situ measurements in HIAPER Pole-to-Pole Observations.” *Geophysical Research Letters* 41(11): 4090–4099, <https://doi.org/10.1002/2014GL059873>

Diao, M, JB Jensen, LL Pan, CR Homeyer, S Honomichl, JF Bresch, and A Bansemer. 2015. “Distributions of ice supersaturation and ice crystals from airborne observations in relation to upper tropospheric dynamical boundaries.” *Journal of Geophysical Research – Atmospheres* 120(10): 5101–5121, <https://doi.org/10.1002/2015JD023139>

Diao, M, JB Jensen, GH Bryan, H Morrison, and DP Stern. 2015. “Sensitivity of ice supersaturated region’s characteristics to spatial resolution in an idealized squall-line scenario.” Recorded presentation at American Meteorological Society Annual Meeting.

<https://ams.confex.com/ams/27WAF23NWP/webprogram/Paper273665.html>

Heymsfield, AJ, LM Avallone, ME Paige, SP Beaton, T Campos, and DC Rogers. 2014. “Cloud-scale ice-supersaturated regions spatially correlate with high water vapor heterogeneities.” *Atmospheric Chemistry and Physics* 14(5): 2639–2656, <https://doi.org/10.5194/acp-14-2639-2014>

Kanji, ZA, LA Ladino, H Wex, Y Boose, M Burkert-Kohn, DJ Cziczo, and M Kramer. 2017. “Overview of ice nucleating particles.” *American Meteorological Society Monograph* 58: 1.1–1.33, <https://doi.org/10.1175/AMSMONOGRAPH-D-16-0006.1>

Long, CN, A Bucholtz, H Jonsson, B Schmid, A Vogelmann, and J Wood. 2010. “A method of correcting for tilt from horizontal in downwelling shortwave irradiance measurements on moving platforms.” *The Open Atmospheric Science Journal* 4(1): 78–87, <https://doi.org/10.2174/1874282301004010078>

Patnaude, R, and M Diao. 2020. “Aerosol indirect effects on cirrus clouds based on global aircraft observations.” *Geophysical Research Letters* 47(10): e2019GL086550, <https://doi.org/10.1029/2019GL086550>

Schmid, B, RG Ellingson, and GM McFarquhar. 2016. “ARM Aircraft Measurements.” *Meteorological Monographs* 57: 10.1–10.13, <https://doi.org/10.1175/AMSMONOGRAPH-D-15-0042.1>

Schmid, B, JM Tomlinson, JM Hubbe, JM Comstock, F Mei, D Chand, MS Pekour, CD Kluzek, E Andrews, SC Biraud, and GM McFarquhar. 2014. “The DOE ARM Aerial Facility.” *Bulletin of the American Meteorological Society* 95: 723–742, <https://doi.org/10.1175/BAMS-D-13-00040.1>

Schnaiter, M, E Järvinen, A Abdelmonem, and T Leisner. 2018. “PHIPS-HALO: The airborne particle habit imaging and polar scattering probe—Part 2: Characterization and first results.” *Atmospheric Measurement Techniques* 11(1): 341–357, <https://doi.org/10.5194/amt-11-341-2018>

Tan, X, Y Huang, M Diao, A Bansemer, MA Zondlo, JP DiGangi, R Volkamer, and Y Hu. 2016. “An assessment of the radiative effects of ice supersaturation based on in situ observations.” *Geophysical Research Letters* 43(20): 11039–11047, <https://doi.org/10.1002/2016GL071144>

Wang, Z, J French, G Vali, P Wechsler, S Haimov, A Rodi, M Deng, D Leon, J Snider, L Peng, and AL Pazmany. 2012. “Single Aircraft Integration of Remote Sensing and In Situ Sampling for the Study of Cloud Microphysics and Dynamics.” *Bulletin of the American Meteorological Society* 93(5): 653–668, <https://doi.org/10.1175/BAMS-D-11-00044.1>

Wu, C, X Liu, M Diao, K Zhang, A Gettelman, Z Lu, JE Penner, and Z Lin. 2017. “Direct comparisons of ice cloud macro- and microphysical properties simulated by the Community Atmosphere Model version 5 with HIPPO aircraft observations.” *Atmospheric Chemistry and Physics* 17(7): 4731–4749, <https://doi.org/10.5194/acp-17-4731-2017>

Zondlo, MA, ME Paige, SM Massick, and JA Silver. 2010. “Vertical cavity laser hygrometer for the National Science Foundation Gulfstream-V aircraft.” *Journal of Geophysical Research* 115(D20): D20309, <https://doi.org/10.1029/2010JD014445>

## Appendix A

### Workshop Advisees and Invitees

#### A.1 Advisees

Last name	First name	Role	Affiliation	Email
<b>ARM</b>				
Mather	Jim	Technical Director	PNNL	<a href="mailto:Jim.Mather@pnnl.gov">Jim.Mather@pnnl.gov</a>
Hickmon	Nicki	Associate Director of Operations	ANL	<a href="mailto:nhickmon@anl.gov">nhickmon@anl.gov</a>
Comstock	Jennifer	Science Products and Measurements	PNNL	<a href="mailto:Jennifer.Comstock@pnnl.gov">Jennifer.Comstock@pnnl.gov</a>
Wasem	Mike	Communication	PNNL	<a href="mailto:Michael.Wasem@pnnl.gov">Michael.Wasem@pnnl.gov</a>
Theisen	Adam	IMB	ANL	<a href="mailto:atheisen@anl.gov">atheisen@anl.gov</a>
Prakash	Giri	IMB	ORNL	<a href="mailto:palanisamyg@ornl.gov">palanisamyg@ornl.gov</a>
Hardesty	Jasper	IMB	SNL	<a href="mailto:joharde@sandia.gov">joharde@sandia.gov</a>
<b>DOE –Program Management</b>				
McFarlane	Sally	DOE Program Manager	DOE BER	<a href="mailto:sally.mcfarlane@science.doe.gov">sally.mcfarlane@science.doe.gov</a>
Petty	Rick	DOE Program Manager	DOE BER	<a href="mailto:rick.petty@science.doe.gov">rick.petty@science.doe.gov</a>
Nasiri	Shaima	DOE Program Manager	DOE BER	<a href="mailto:Shaima.nasiri@science.doe.gov">Shaima.nasiri@science.doe.gov</a>
Stehr	Jeff	DOE Program Manager	DOE BER	<a href="mailto:jeff.stehr@science.doe.gov">jeff.stehr@science.doe.gov</a>
<b>ARM Aerial Facility – AAF</b>				
Schmid	Beat	Manager	PNNL	<a href="mailto:beat.schmid@pnnl.gov">beat.schmid@pnnl.gov</a>
Mei	Fan	Data Manager & Instrument Mentor	PNNL	<a href="mailto:fan.mei@pnnl.gov">fan.mei@pnnl.gov</a>
Tomlinson	Jason	Director of Engineering & Instrument Mentor	PNNL	<a href="mailto:jason.tomlinson@pnnl.gov">jason.tomlinson@pnnl.gov</a>
Matthews	Alyssa	Instrument Mentor	PNNL	<a href="mailto:alyssa.matthews@pnnl.gov">alyssa.matthews@pnnl.gov</a>
Mendoza	Albert	Instrument Mentor	PNNL	<a href="mailto:albert.mendoza@pnnl.gov">albert.mendoza@pnnl.gov</a>
Nelson	Dan	Instrument Mentor	PNNL	<a href="mailto:Danny.Nelson@pnnl.gov">Danny.Nelson@pnnl.gov</a>

Last name	First name	Role	Affiliation	Email
Newburn	Matt	Instrument Mentor	PNNL	<a href="mailto:matt.newburn@pnnl.gov">matt.newburn@pnnl.gov</a>
Carroll	Peter	UAV Operator	PNNL	<a href="mailto:peter.carroll@pnnl.gov">peter.carroll@pnnl.gov</a>
Goldberger	Lexie	Instrument Mentor	PNNL	<a href="mailto:lexie.goldberger@pnnl.gov">lexie.goldberger@pnnl.gov</a>
Glienke	Susanne	Instrument Mentor	PNNL	<a href="mailto:susanne.glienke@pnnl.gov">susanne.glienke@pnnl.gov</a>
Geffen	Charlotte	Sector Leader	PNNL	<a href="mailto:ca.geffen@pnnl.gov">ca.geffen@pnnl.gov</a>
<b>AAF External Mentors</b>				
Springston	Steven	Instrument Mentor	BNL	<a href="mailto:srs@bnl.gov">srs@bnl.gov</a>
Sedlacek	Art	Instrument Mentor	BNL	<a href="mailto:sedlacek@bnl.gov">sedlacek@bnl.gov</a>
Biraud	Sebastien	Instrument Mentor	LBL	<a href="mailto:scbiraud@lbl.gov">scbiraud@lbl.gov</a>
Riihimaki	Laura	Instrument Mentor	NOAA	<a href="mailto:laura.riihimaki@noaa.gov">laura.riihimaki@noaa.gov</a>
<b>ARM TBS Facility</b>				
Dexheimer	Darielle	Manager	SNL	<a href="mailto:ddexhei@sandia.gov">ddexhei@sandia.gov</a>
Longbottom	Casey	Instrument Mentor	SNL	<a href="mailto:cmlongb@sandia.gov">cmlongb@sandia.gov</a>
Rohr	Garth	Instrument Mentor	SNL	<a href="mailto:gdrohr@sandia.gov">gdrohr@sandia.gov</a>
Slad	George	Aviation Safety	SNL	<a href="mailto:gwslad@sandia.gov">gwslad@sandia.gov</a>
Parrott	Lori	Manager of the Atmospheric Sciences Division	SNL	<a href="mailto:lkparro@sandia.gov">lkparro@sandia.gov</a>
Ivey	Mark	Manager	SNL	<a href="mailto:mdivey@sandia.gov">mdivey@sandia.gov</a>

## A.2 Invitees

Last name	First name	Affiliation	Scientific expertise	Web link
Worsnop	Doug	Aerodyne	Aerosol: AMS	<a href="http://www.aerodyne.com/employees/dr-douglas-r-worsnop">http://www.aerodyne.com/employees/dr-douglas-r-worsnop</a>
Lewis	Gregory	Aerosol Dynamics	Aerosol: mini-SMPS and water-based CPC	<a href="https://aerosol.us/staff">https://aerosol.us/staff</a>
Jensen	Mike	BNL	Cloud: life cycle and microphysical properties	<a href="https://www.bnl.gov/envsci/bio/jensen-mike.php">https://www.bnl.gov/envsci/bio/jensen-mike.php</a>
Kuang	Chongai	BNL	Aerosol: ultrafine aerosol properties	<a href="https://www.bnl.gov/envsci/bio/kuang-chongai.php">https://www.bnl.gov/envsci/bio/kuang-chongai.php</a>
McComiskey	Allison	BNL	Aerosol: radiative forcing	<a href="https://www.bnl.gov/envsci/bio/mccomiskey-allison.php">https://www.bnl.gov/envsci/bio/mccomiskey-allison.php</a>
Brechtel	Fred	Brechtel	Aerosol: UAS/aircraft instrumentation, aircraft inlets	<a href="https://www.brechtel.com/staff-member/fred-j-brechtel">https://www.brechtel.com/staff-member/fred-j-brechtel</a>
Sullivan	Amy	Colorado State U.	Aerosol: organic aerosol markers	<a href="http://collett.atmos.colostate.edu/people/Sullivan.html">http://collett.atmos.colostate.edu/people/Sullivan.html</a>

Last name	First name	Affiliation	Scientific expertise	Web link
Atwood	Alexis	DMT	Aerosol (bioaerosol)	<a href="http://www.dropletmeasurement.com/dmt-staff">http://www.dropletmeasurement.com/dmt-staff</a>
Badder				
Roden	Chris	Handix	Cloud instrumentation	<a href="http://www.specinc.com/node/156">http://www.specinc.com/node/156</a>
Lambrightsen	Bjorn	NASA JPL	Microwave remote sensing	<a href="https://science.jpl.nasa.gov/people/Lambrightsen/">https://science.jpl.nasa.gov/people/Lambrightsen/</a>
Ziemba	Luke	NASA Langley	Aerosol: inlet, remote sensing	<a href="https://airbornescience.nasa.gov/person/Luke_D_Ziemba">https://airbornescience.nasa.gov/person/Luke_D_Ziemba</a>
Bansemter	Aaron	NCAR	Cloud and rain droplets	<a href="https://staff.ucar.edu/users/bansemter">https://staff.ucar.edu/users/bansemter</a>
Bailey	Adriana	NCAR	Co-chair of the US CLIVAR Working Group on Water Isotopes	<a href="https://staff.ucar.edu/users/abailey">https://staff.ucar.edu/users/abailey</a>
Campos	Teresa	NCAR	Gas phase: inlet	<a href="https://staff.ucar.edu/users/campos">https://staff.ucar.edu/users/campos</a>
Thornberry	Troy	NOAA	UAS: composition measurements	<a href="https://www.esrl.noaa.gov/csd/staff/troy.thornberry">https://www.esrl.noaa.gov/csd/staff/troy.thornberry</a>
Bucholtz	Anthony	NPS	Radiation, aircraft measurements	<a href="https://airbornescience.nasa.gov/person/Anthony_Bucholtz">https://airbornescience.nasa.gov/person/Anthony_Bucholtz</a>
Flynn	Connor	U. Oklahoma	Aerosol/radiation	<a href="https://meteorology.ou.edu/member/flynn-connor/">https://meteorology.ou.edu/member/flynn-connor/</a>
Berg	Larry	PNNL	Turbulence and BL clouds	<a href="https://www.pnnl.gov/atmospheric/staff/staff_info.asp?staff_num=5718">https://www.pnnl.gov/atmospheric/staff/staff_info.asp?staff_num=5718</a>
Fast	Jerome	PNNL	Aerosol modeling, cloud chemistry and aerosol-cloud interaction	<a href="https://www.pnnl.gov/science/staff/staff_info.asp?staff_num=5717">https://www.pnnl.gov/science/staff/staff_info.asp?staff_num=5717</a>
Diao	Minghui	San Jose State U.	Gas phase: water vapor and aerosols	<a href="http://www.sjsu.edu/people/minghui.diao/">http://www.sjsu.edu/people/minghui.diao/</a>
Lawson	Paul	SPEC	Cloud: measurements and instruments	<a href="http://www.specinc.com/about-us">http://www.specinc.com/about-us</a>
Small-Griswold	Jennifer	U. Hawaii	Cloud: microphysics and remote sensing	<a href="http://jenniferdsmallphd.com/CV.html">http://jenniferdsmallphd.com/CV.html</a>
Garron	Jessica	U. Alaska, Fairbanks	UAS: ACUASI science lead	<a href="https://people.alaska.edu/search?q=jessica+garron">https://people.alaska.edu/search?q=jessica+garron</a>
Calmer	Radiance	U. Colorado	Turbulence	<a href="https://cires.colorado.edu/directory/radiance-calmer">https://cires.colorado.edu/directory/radiance-calmer</a>
Geerts	Bart	U. Wyoming	Cloud: cloud radar	<a href="https://www.uwyo.edu/atsc/directory/faculty/geerts/">https://www.uwyo.edu/atsc/directory/faculty/geerts/</a>
Zhang	Qi	U. Cal., Davis	Aerosol: chemistry and single-particle analysis	<a href="http://etox.ucdavis.edu/directory/faculty/zhang-qi/">http://etox.ucdavis.edu/directory/faculty/zhang-qi/</a>
Wang	Jian	Washington U., St. Louis	Aerosol: properties, distribution, and evolution	<a href="https://engineering.wustl.edu/Profiles/Pages/Jian-Wang.aspx">https://engineering.wustl.edu/Profiles/Pages/Jian-Wang.aspx</a>

## Appendix B

# ARM Aerial Instrumentation Workshop Agenda

### PNNL, Richland, Washington March 2 and 3, 2020

Conveners: Beat Schmid, Fan Mei, Darielle Dexheimer

Monday, March 2		
8:30-9:00	Arrive at Pacific Northwest National Laboratory 3400 Discovery Hall, 650 Horn Rapids Road, Richland, WA 99354 <b>All speakers please load your presentations!</b> <i>Refreshments provided</i>	
9:00-9:03	Welcome remarks by Malin Young, Associate Lab Director, EBSD	Young
9:03-9:18 (15 min)	<b>PL1:</b> ARM facility overview	Mather
9:18-9:40 (22 min)	<b>PL2:</b> ARM Aerial Facility (AAF) introduction and workshop objectives	Schmid
9:40-10:45 (65 mins)	Research infrastructure, aircraft and atmospheric state measurements (Challenger 850) <ul style="list-style-type: none"> <li>Current AAF capabilities – Tomlinson(<b>MS1.1</b>) / Goldberger (<b>MS1.2</b>) (15 min)</li> <li>New capabilities <ul style="list-style-type: none"> <li><b>MS1.3:</b> Laboratory calibration and applications of water vapor measurements from the surface to UT/LS using VCSEL – Diao (10 min)</li> <li><b>MS1.4:</b> Microwave soundings from aircraft (HAMSR<sup>1</sup>, PAMR<sup>2</sup>) – Lambrightsen (10 min)</li> <li><b>MS1.5:</b> Desired capability to Host Lidars, Radars, Radiometers, and Imagers<sup>3</sup> – Tomlinson (10 min)</li> </ul> </li> <li>Discussion (20 min)</li> </ul>	Geerts (chair) Goldberger (co-chair)
10:45-11:00	Coffee break (refreshments provided)	
11:00-12:00 (60 mins)	Radiation measurements (Challenger 850) <ul style="list-style-type: none"> <li><b>MS2.1:</b> Current AAF capabilities – Riihimaki (10 min)</li> <li>New capabilities <ul style="list-style-type: none"> <li><b>MS2.2:</b> Broadband radiometers +INFLAME<sup>4</sup> – Bucholtz (10 min)</li> </ul> </li> </ul>	Bucholtz (chair) Riihimaki (co-chair)

<sup>1</sup> Marian Klein et al., Profiling Airborne Microwave Radiometer – PAMR

<sup>2</sup> Bjorn Lambrightsen et al., An Airborne Microwave Sonde for ARM

<sup>3</sup> Joseph C. Hardin et al., Capability to Host Lidars, Radars, Radiometers and Imagers on the New AAF Bombardier Challenger 850

<sup>4</sup> Martin G. Mlynczak et al., In-situ Net Flux within the Atmosphere of the Earth (INFLAME)

	<ul style="list-style-type: none"> <li>○ <b>MS2.3:</b> 4STAR<sup>5</sup>, Spectral SPN<sup>6</sup> – Flynn (10 min)</li> <li>○ <b>MS2.4:</b> Imaging camera<sup>7</sup> – Riihimaki (6 min)</li> <li>○ <b>MS2.5:</b> IR soundings from aircraft<sup>8</sup> – Lambrightsen (S-HIS) (6 min)</li> <li>● Discussion (18 min)</li> </ul>	
12:00-12:10	Get working lunch (provided) and return to the meeting room	
12:10-14:50 (160 mins)	<p><i>Working Lunch</i></p> <p>Aerosol measurements (Challenger 850)</p> <ul style="list-style-type: none"> <li>● <b>MS3.1:</b> Current AAF capabilities – Mei (10 min)</li> <li>● New capabilities <ul style="list-style-type: none"> <li>○ <b>MS3.2:</b> Modifications to the NASA HU-25 Falcon Aircraft for aerosol-cloud interaction observations – Ziembka (15 min)</li> <li>○ <b>MS3.3:</b> Isokinetic and CVI inlets – Brechtel (12 min)</li> <li>○ <b>MS3.4:</b> FIMS<sup>9</sup> and TRAC2<sup>10</sup> – Wang (12 min)</li> <li>○ <b>MS3.5:</b> On- and offline PILS measurements – Sullivan (12 min)</li> <li>○ <b>MS3.6:</b> HR-ToF-AMS<sup>11</sup>, Vocus PTR-ToF-AMS<sup>12</sup>, ToF-CIMS<sup>13</sup> – Worsnop (15 min)</li> <li>○ <b>MS3.7:</b> WIBS<sup>14</sup> – Attwood (6 min)</li> <li>○ <b>MS3.8:</b> CAPS-SSA<sup>15</sup>, PTI<sup>16</sup>, NAIS<sup>17</sup>, LED-based nephelometer<sup>18</sup> – Sedlacek (18 min)</li> <li>○ <b>MS3.9:</b> Imaging polar neph<sup>19</sup> – Schmid (6 min)</li> <li>○ <b>MS3.10:</b> Remote sensing via lidar<sup>20</sup> – Fast (12 min)</li> </ul> </li> <li>● Discussion (42 min)</li> </ul>	Fast (chair) Mei (co-chair)
14:50-15:05	Coffee break (refreshments provided)	
15:05-17:20 (135 mins)	Cloud measurements (Challenger 850) <ul style="list-style-type: none"> <li>● <b>MS4.1:</b> Current AAF capabilities – Glienke (15 min)</li> <li>● New capabilities</li> </ul>	Geerts (chair) Matthews (co-chair)

<sup>5</sup> Samuel LeBlanc et al., 4STAR/Airborne Sun-Sky photometry

<sup>6</sup> Sebastian Schmidt et al., Airborne Spectral Radiometry

<sup>7</sup> Duli Chand et al., Remote Sensing by Hyperspectral Imaging Camera

<sup>8</sup> Joe K. Taylor et al., The scanning high-resolution interferometer sounder (S-HIS)

<sup>9</sup> Jian Wang, High time resolution measurements of aerosol size distribution onboard Bombardier Challenger 850 regional jet

<sup>10</sup> Alexander Laskin et al., A New Time-Resolved Aerosol Collector (TRAC2) for automated sampling aboard ARM's aerial observation platforms

<sup>11</sup> Manjula Canagaratna et al., Aerodyne Aerosol Mass Spectrometer

<sup>12</sup> Jordan Krechmer et al., Vocus Proton Transfer Reaction Time-of-Flight Mass Spectrometer (Vocus PTR-MS)

<sup>13</sup> Joel Thornton et al., Versatile Time-of-flight Chemical Ionization Mass spectrometer (ToF-CIMS)

<sup>14</sup> Darrel Baumgardner, Wideband Integrated bioaerosol sensor (WIBS)

<sup>15</sup> Art J. Sedlacek, CAPS-SSA/Aerosol Optical Extinction and SSA

<sup>16</sup> Art J. Sedlacek, 2 wavelength PTI/Aerosol Absorption and Scattering

<sup>17</sup> Janek Uin, Neutral cluster and air Ion Spectrometer

<sup>18</sup> Janek Uin, Neutral cluster and air Ion Spectrometer

<sup>19</sup> Janek Uin et al., LED-based Nephelometer

<sup>20</sup> Jerome Fast et al., Remote Sensing via Lidars

	<ul style="list-style-type: none"> <li>○ <b>MS4.2:</b> Airborne aerosol and cloud lidar measurements (MPL<sup>21</sup>, AECL<sup>22</sup>, HSRL<sup>23</sup>) – Flynn (15 min)</li> <li>○ <b>MS4.3:</b> Airborne cloud radar measurements – Geerts (15 min)</li> <li>○ <b>MS4.4:</b> In situ instruments: HVPS-4<sup>24</sup>, CDS<sup>25</sup>, and 2D-Gray<sup>26</sup> – Lawson (15 min)</li> <li>○ <b>MS4.5:</b> In situ instruments: BCPD<sup>27</sup> – Attwood (6 min)</li> <li>○ <b>MS4.6:</b> In situ instruments: PHIPS<sup>28</sup>, HOLODEC<sup>29</sup> – Glienke (10 min)</li> <li>○ <b>MS4.7:</b> Multi-phase water isotopic measurements<sup>30</sup> – Bailey (15 min)</li> <li>○ <b>MS4.8:</b> Ice nuclei measurements (CFDC - Handix)<sup>31</sup> – Roden (6 min)</li> <li>○ <b>MS4.9:</b> Ice nuclei measurements (CFDC - PNNL<sup>32</sup> - Mei (6 min)</li> </ul> <ul style="list-style-type: none"> <li>● Discussion (32 min)</li> </ul>	
18:00	No-host dinner at LU Craft Bar + Kitchen, 606 Columbia Point Dr., Richland, WA 99352	
<b>Tuesday, March 3</b>		
8:00-9:20 (80 mins)	Trace gas measurement (Challenger 850) <ul style="list-style-type: none"> <li>● Current AAF capabilities – Biraud(TS1.1)/Springston (TS1.2)(6/12 min)</li> <li>● New capabilities <ul style="list-style-type: none"> <li>○ <b>TS1.3:</b> Gas-phase airborne measurements: Characterizations to add confidence in the representativeness of in situ observations – Campos (15 min)</li> <li>○ <b>TS1.4:</b> CAPS NO<sub>2</sub><sup>33</sup> – Worsnop (6 min)</li> <li>○ <b>TS1.5:</b> Open-path atmospheric ammonia sensor<sup>34</sup> – Diao (6 min)</li> <li>○ <b>TS1.6:</b> Fast chemiluminescent measurement of ozone<sup>35</sup> – Springston (6 min)</li> </ul> </li> <li>● Discussion (29 min)</li> </ul>	Campos (chair) Springston (co-chair)
9:20-9:35	Coffee break (refreshments provided)	
9:35-11:20 (105 mins)	Science drivers and miniaturized instrumentation for TBS <ul style="list-style-type: none"> <li>● <b>TS2.1:</b> Current ARM capabilities – Dexheimer (15 min)</li> <li>● Science drivers and new capabilities</li> </ul>	Kuang (chair) Dexheimer (co-chair)

<sup>21</sup> Connor Flynn et al., MiniMPL<sup>22</sup> Perry Wechsler et al., The Alenglow Airborne Elastic Lidar<sup>23</sup> Ed Eloranta et al., High Spectral Resolution Lidar<sup>24</sup> Paul Lawson, High Volume Precipitation Spectrometer Version 4<sup>25</sup> Paul Lawson, Cloud Drop Spectrometer (CDS)<sup>26</sup> Paul Lawson, An Improved 2D-Gray Probe<sup>27</sup> Darrel Baumgardner, Backscatter Cloud probe with Polarization Detection (BCPD)<sup>28</sup> David Delene et al., Particle Habit Imaging and Polar Scattering Probe (PHIPS)<sup>29</sup> Raymond Shaw et al., Digital Holographic Measurement of Cloud Hydrometeors<sup>30</sup> David Noone et al., Multi-phase water isotopic measurements<sup>31</sup> Paul DeMott et al., Continuous Flow Diffusion Chamber (CFDC) for measuring Ice<sup>32</sup> Gourihar Kulkarni et al., Airborne Ice Nucleating Particle Measurements<sup>33</sup> Timothy Onasch et al., CAPS Fast Response NO<sub>2</sub> monitor<sup>34</sup> Mark A. Zondlo et al., Open-path atmospheric ammonia sensor for the Bombardier Challenger 850<sup>35</sup> Stephen Springston, Fast Chemiluminescent Measurement of Ozone/Atmospheric Ozone

	<ul style="list-style-type: none"> <li>○ <b>TS2.2:</b> Science drivers for TBS and Sharkeye<sup>36</sup> – <b>Lawson</b> (12 min)</li> <li>○ <b>TS2.3:</b> Vertically resolved new particle formation (incl 1 nm CPC)<sup>37</sup> – <b>Kuang</b> (12 min)</li> <li>○ <b>TS2.4:</b> Chemical analysis of PM samples collected from unmanned aerial platforms<sup>38</sup> – <b>Zhang</b> (12 min)</li> <li>○ <b>TS2.5:</b> SP2-XR<sup>39</sup> – <b>Sedlacek</b> (6 min)</li> <li>○ <b>TS2.6:</b> SO<sub>2</sub> sonde for balloon and UAS platforms<sup>40</sup> – <b>Springston</b> (6 min)</li> <li>● Discussion (42 min)</li> </ul>	
11:20-11:30	Get working lunch (provided) and return to the meeting room	
11:30-13:40 (130 mins)	<p><i>Working Lunch</i></p> <p>Science drivers and miniaturized instrumentation for UAS</p> <ul style="list-style-type: none"> <li>● <b>TS3.1:</b> Current capabilities ArcticShark platform and science infrastructure – <b>Carroll/Newburn</b> (15 min)</li> <li>● <b>TS3.2:</b> Current capabilities ArcticShark instruments – <b>Schmid</b> (12 min)</li> <li>● Science drivers and new capabilities <ul style="list-style-type: none"> <li>○ <b>TS3.3:</b> Science drivers for UAS in the Arctic – <b>Garron</b> (12 min)</li> <li>○ <b>TS3.4:</b> Science questions and related instrumentation needs for UAS platforms – <b>Brechtel</b> (12 min)</li> <li>○ <b>TS3.5:</b> From the tropics to the North Pole: Atmospheric measurements using small UAS – <b>Calmer</b> (12 min)</li> <li>○ <b>TS3.6:</b> Opportunities and challenges of airborne science with small SWaP payloads – <b>Thornberry</b> (12 min)</li> <li>○ <b>TS3.7:</b> Compact, mid-IR methane sensor<sup>41</sup> – <b>Diao</b> (6 min)</li> <li>○ <b>TS3.8:</b> High-performance UAS laser hygrometer<sup>42</sup> – <b>Diao</b> (6 min)</li> </ul> </li> <li>● Discussion (43 min)</li> </ul>	<b>Thornberry</b> (chair) <b>Mei</b> (co-chair)
13:40-14:00 (20 mins)	<p>Wrap-up</p> <ul style="list-style-type: none"> <li>● Action items (workshop report, breakout session at ARM/ASR meeting)</li> </ul>	<b>Dexheimer,</b> <b>Mei, Schmid</b>

<sup>36</sup> Paul Lawson, The Sharkeye: A Combination Optical Particle Probe for Installation on the ARM ArcticShark UAV

<sup>37</sup> Chongai Kuang, 1-nm Condensation Particle Counter: Number Concentration of Aerosol > 1 nm

<sup>38</sup> Qi Zhang, Chemical Analysis of PM Samples Collected from Unmanned Aerial Platforms

<sup>39</sup> Art J. Sedlacek, SP2-XR/refractory black carbon

<sup>40</sup> James Flynn et al., SO<sub>2</sub> sonde for balloon and UAV platforms

<sup>41</sup> Mark Zondlo et al., Compact, Mid-IR Methane Sensor for the ArcticShark UAS and Tethered Balloon Systems

<sup>42</sup> D. Sonnenfroh et al., High Performance UAS Laser Hygrometer

## Appendix C

### White Papers

Barnes, John E. Imaging Polar Nephelometer.

[https://www.arm.gov/capabilities/observatories/aaf/workshop-march2020/Barnes\\_nephelometer.pdf](https://www.arm.gov/capabilities/observatories/aaf/workshop-march2020/Barnes_nephelometer.pdf)

Baumgardner, Darrel. Backscatter Clouprobe with Polarization Detection (BCPD).

[https://www.arm.gov/capabilities/observatories/aaf/workshop-march2020/Baumgardner\\_BCPD.pdf](https://www.arm.gov/capabilities/observatories/aaf/workshop-march2020/Baumgardner_BCPD.pdf)

Baumgardner, Darrel. Wideband Integrated Bioaerosol Sensor (WIBS).

[https://www.arm.gov/capabilities/observatories/aaf/workshop-march2020/Baumgardner\\_WIBS.pdf](https://www.arm.gov/capabilities/observatories/aaf/workshop-march2020/Baumgardner_WIBS.pdf)

Canagaratna, Manjula, Timothy Onasch, John Shilling, Joel Thornton, John Jayne, and Douglas Worsnop. Aerodyne Aerosol Mass Spectrometer (AMS).

[https://www.arm.gov/capabilities/observatories/aaf/workshop-march2020/Canagaratna\\_AMS.pdf](https://www.arm.gov/capabilities/observatories/aaf/workshop-march2020/Canagaratna_AMS.pdf)

Chand, Duli, and Jerry Tagesad. Remote Sensing by Hyperspectral Imaging Camera.

[https://www.arm.gov/capabilities/observatories/aaf/workshop-march2020/Chand\\_remote\\_sensing.pdf](https://www.arm.gov/capabilities/observatories/aaf/workshop-march2020/Chand_remote_sensing.pdf)

Delene, David, Emma Jarvinen, Martin Schnaiter, Greg McFarquhar, and Wei Wu. Particle Habit Imaging and Polar Scattering (PHIPS) Probe.

[https://www.arm.gov/capabilities/observatories/aaf/workshop-march2020/Delene\\_PHIPS.pdf](https://www.arm.gov/capabilities/observatories/aaf/workshop-march2020/Delene_PHIPS.pdf)

DeMott, Paul, JM Creamean, EJT Levin, and GR McMeeking. Continuous Flow Diffusion Chamber (CFDC) for Measuring Ice Nucleating Particles (INPs).

[https://www.arm.gov/capabilities/observatories/aaf/workshop-march2020/DeMott\\_CFDC](https://www.arm.gov/capabilities/observatories/aaf/workshop-march2020/DeMott_CFDC)

Eloranta, Ed. High-Spectral-Resolution Lidar.

[https://www.arm.gov/capabilities/observatories/aaf/workshop-march2020/Eloranta\\_airborne\\_hsrl.pdf](https://www.arm.gov/capabilities/observatories/aaf/workshop-march2020/Eloranta_airborne_hsrl.pdf)

Fast, Jerome D, Rich A Ferrare, Chris Hostetier, Dave Turner, Volker Wulfmeyer, Duli Chand, Rob Newsom, Alma Hodzic, and Po-Lun Ma. Remote Sensing via Lidars.

[https://www.arm.gov/capabilities/observatories/aaf/workshop-march2020/Fast\\_Remote\\_Sensing\\_via\\_Lidars.pdf](https://www.arm.gov/capabilities/observatories/aaf/workshop-march2020/Fast_Remote_Sensing_via_Lidars.pdf)

Flynn, Connor. MiniMPL. [https://www.arm.gov/capabilities/observatories/aaf/workshop-march2020/C\\_Flynn\\_Mini\\_MPL.pdf](https://www.arm.gov/capabilities/observatories/aaf/workshop-march2020/C_Flynn_Mini_MPL.pdf)

Flynn, James, and Rebecca Sheesley. SO<sub>2</sub> Sonde for Balloon and UAV Platforms.

[https://www.arm.gov/capabilities/observatories/aaf/workshop-march2020/J\\_Flynn\\_SO2\\_sonde.pdf](https://www.arm.gov/capabilities/observatories/aaf/workshop-march2020/J_Flynn_SO2_sonde.pdf)

Hardin, Joseph C, Adam Varble, Stephen Nesbitt, P:aquita Zuidema, Alessandro Battaglia, Jennifer Comstock, Susan Crewell, Jiwen Fan, Zhe Feng, Ann Fridlind, Bart Geerts, Virendra Ghate, William Gustafson, Samuel Haimov, Michael Jensen, Stefan Kneifel, Maximilian Maahn, Jim Marquis, David Mechem, Alain Protat, Angela Rowe, Courtney Schumacher, Matthew Shupe, Frederic Tridon, Zhien Wang, Christopher Williams, and Edward Zipser. Capability to Host Lidars, Radars, Radiometers, and Imagers on the New AAF Bombardier Challenger 850.

[https://www.arm.gov/capabilities/observatories/aaf/workshop-march2020/Hardin\\_capability\\_to\\_host.pdf](https://www.arm.gov/capabilities/observatories/aaf/workshop-march2020/Hardin_capability_to_host.pdf)

Klein, Marian. Profiling Airborne Microwave Radiometer–PAMR.

[https://www.arm.gov/capabilities/observatories/aaf/workshop-march2020/Klein\\_PAMR.pdf](https://www.arm.gov/capabilities/observatories/aaf/workshop-march2020/Klein_PAMR.pdf)

Krechmer, Jordan, Manjula Canagaratna, Timothy Onasch, John Shilling, Joel Thornton, and Douglas Worsnop. Vocus Proton Transfer Reaction Time-of-Flight Mass Spectrometer (Vocus PTR-MS).

[https://www.arm.gov/capabilities/observatories/aaf/workshop-march2020/Krechmer\\_Vocus\\_PTR-MS.pdf](https://www.arm.gov/capabilities/observatories/aaf/workshop-march2020/Krechmer_Vocus_PTR-MS.pdf)

Kuang, Chongai. 1-nm Condensation Particle Counter: Number Concentration of Aerosol > 1 nm.

[https://www.arm.gov/capabilities/observatories/aaf/workshop-march2020/Kuang\\_1\\_nm\\_CPC.pdf](https://www.arm.gov/capabilities/observatories/aaf/workshop-march2020/Kuang_1_nm_CPC.pdf)

Kulkarni, Gourihar, and Xiaohong Liu. Airborne Ice Nucleating Particle Measurements.

[https://www.arm.gov/capabilities/observatories/aaf/workshop-march2020/Kulkarni\\_Airbone\\_INP.pdf](https://www.arm.gov/capabilities/observatories/aaf/workshop-march2020/Kulkarni_Airbone_INP.pdf)

Lambrigtsen, Bjorn. An Airborne Microwave Sounder for ARM.

[https://www.arm.gov/capabilities/observatories/aaf/workshop-march2020/Lambrigtsen\\_airborne\\_microwave.pdf](https://www.arm.gov/capabilities/observatories/aaf/workshop-march2020/Lambrigtsen_airborne_microwave.pdf)

Laskin, Alexander. A New Time-Resolved Aerosol Collector (TRAC2) for Automated Sampling Aboard ARM’s Aerial Observation Platforms. [https://www.arm.gov/capabilities/observatories/aaf/workshop-march2020/Laskin\\_TRAC2.pdf](https://www.arm.gov/capabilities/observatories/aaf/workshop-march2020/Laskin_TRAC2.pdf)

Lawson, Paul. An Improved 2D-Gray Probe.

[https://www.arm.gov/capabilities/observatories/aaf/workshop-march2020/Lawson\\_2D\\_Gray\\_Probe.pdf](https://www.arm.gov/capabilities/observatories/aaf/workshop-march2020/Lawson_2D_Gray_Probe.pdf)

Lawson, Paul. Cloud Drop Spectrometer (CDS).

[https://www.arm.gov/capabilities/observatories/aaf/workshop-march2020/Lawson\\_Cloud\\_Drop\\_Spec.pdf](https://www.arm.gov/capabilities/observatories/aaf/workshop-march2020/Lawson_Cloud_Drop_Spec.pdf)

Lawson, Paul. High-Volume Precipitation Spectrometer Version 4 (HVPS-4).

[https://www.arm.gov/capabilities/observatories/aaf/workshop-march2020/Lawson\\_HVPS4.pdf](https://www.arm.gov/capabilities/observatories/aaf/workshop-march2020/Lawson_HVPS4.pdf)

Lawson, Paul. The Sharkeye: A Combination Optical Particle Probe for Installation on the ARM ArcticShark UAV. [https://www.arm.gov/capabilities/observatories/aaf/workshop-march2020/Lawson\\_Sharkeye.pdf](https://www.arm.gov/capabilities/observatories/aaf/workshop-march2020/Lawson_Sharkeye.pdf)

LeBlanc, Samuel, Connor Flynn, Meloë Kacenelenbogen, Kristina Pistone, Michal Segal-Rosenheimer, Steven Broccardo, Steve Dunagan, Roy Johnson, Robert Dahlgren, Conrad Esch, Jens Redemann, and K Sebastian Schmidt. 4STAR/Airborne Sun-Sky Photometry.

[https://www.arm.gov/capabilities/observatories/aaf/workshop-march2020/LeBlanc\\_4STAR.pdf](https://www.arm.gov/capabilities/observatories/aaf/workshop-march2020/LeBlanc_4STAR.pdf)

Mlynczak, Martin G, David G Johnson, and Daniel R Feldman. In Situ Net Flux within the Atmosphere of the Earth (INFLAME). [https://www.arm.gov/capabilities/observatories/aaf/workshop-march2020/Mlynczak\\_In\\_situ\\_Net\\_Flux.pdf](https://www.arm.gov/capabilities/observatories/aaf/workshop-march2020/Mlynczak_In_situ_Net_Flux.pdf)

Murphy, Margaret. The Incorporation of AI within Infrared Radiation Detection Technology.

[https://www.arm.gov/capabilities/observatories/aaf/workshop-march2020/Murphy\\_AI\\_within\\_IRDT.pdf](https://www.arm.gov/capabilities/observatories/aaf/workshop-march2020/Murphy_AI_within_IRDT.pdf)

Noone, David, Adriana Bailey, and Darin Toohey. Multi-Phase Water Isotopic Measurements.

[https://www.arm.gov/capabilities/observatories/aaf/workshop-march2020/Noone\\_multi-phase.pdf](https://www.arm.gov/capabilities/observatories/aaf/workshop-march2020/Noone_multi-phase.pdf)

Onasch, Timothy, and Andrew Freedman. CAPS Fast Response NO<sub>2</sub> Monitor.

[https://www.arm.gov/capabilities/observatories/aaf/workshop-march2020/Onasch\\_CAPS.pdf](https://www.arm.gov/capabilities/observatories/aaf/workshop-march2020/Onasch_CAPS.pdf)

Schmidt, K Sebastian, Connor Flynn, and Samuel LeBlanc. Airborne Spectral Radiometry.

[https://www.arm.gov/capabilities/observatories/aaf/workshop-march2020/Schmidt\\_airborne\\_spectral.pdf](https://www.arm.gov/capabilities/observatories/aaf/workshop-march2020/Schmidt_airborne_spectral.pdf)

Sedlacek, Art J. 2-wavelength PTI/Aerosol Absorption and Scattering.

[https://www.arm.gov/capabilities/observatories/aaf/workshop-march2020/Sedlacek\\_PTI\\_Aerosol.pdf](https://www.arm.gov/capabilities/observatories/aaf/workshop-march2020/Sedlacek_PTI_Aerosol.pdf)

Sedlacek, Art J. CAPS-SSA/Aerosol Optical Extinction and SSA.

[https://www.arm.gov/capabilities/observatories/aaf/workshop-march2020/Sedlacek\\_CAPS-SSA.pdf](https://www.arm.gov/capabilities/observatories/aaf/workshop-march2020/Sedlacek_CAPS-SSA.pdf)

Sedlacek, Art J. SP2-XR/Refractory Black Carbon.

[https://www.arm.gov/capabilities/observatories/aaf/workshop-march2020/Sedlacek\\_SP2-XR.pdf](https://www.arm.gov/capabilities/observatories/aaf/workshop-march2020/Sedlacek_SP2-XR.pdf)

Shaw, Raymond. Digital Holographic Measurement of Cloud Hydrometeors.

[https://www.arm.gov/capabilities/observatories/aaf/workshop-march2020/Shaw\\_Digital\\_Holography.pdf](https://www.arm.gov/capabilities/observatories/aaf/workshop-march2020/Shaw_Digital_Holography.pdf)

Sonnenfroh, D, and Mark Zondlo. High-Performance UAS Laser Hygrometer.

[https://www.arm.gov/capabilities/observatories/aaf/workshop-march2020/Sonnenfroh\\_UAS\\_laser\\_hygrometer.pdf](https://www.arm.gov/capabilities/observatories/aaf/workshop-march2020/Sonnenfroh_UAS_laser_hygrometer.pdf)

Springston, Stephen R. Fast Chemiluminescent Measurement of Ozone/Atmospheric Ozone.

[https://www.arm.gov/capabilities/observatories/aaf/workshop-march2020/Springston\\_Fast\\_Chemiluminescent.pdf](https://www.arm.gov/capabilities/observatories/aaf/workshop-march2020/Springston_Fast_Chemiluminescent.pdf)

Tao, Lei, Hongming Yi, and Mark Zondlo. Compact, Mid-IR Methane Sensor for the ArcticShark UAS and Tethered Balloon Systems. [https://www.arm.gov/capabilities/observatories/aaf/workshop-march2020/Tao\\_compact\\_Mid-IR.pdf](https://www.arm.gov/capabilities/observatories/aaf/workshop-march2020/Tao_compact_Mid-IR.pdf)

Taylor, Joe K, Henry Revercomb, Fred Best, P Jonathan Gero, Robert Knuteson, William Smith Sr, David Tobin, David Turner, and Elisabeth Weisz. The Scanning High-Resolution Interferometer Sounder (S-HIS). [https://www.arm.gov/capabilities/observatories/aaf/workshop-march2020/Taylor\\_S-HIS.pdf](https://www.arm.gov/capabilities/observatories/aaf/workshop-march2020/Taylor_S-HIS.pdf)

Thornton, Joel, and John Shilling. Versatile Time-of-Flight Chemical Ionization Mass Spectrometer (ToF-CIMS) Guest Instrument. [https://www.arm.gov/capabilities/observatories/aaf/workshop-march2020/Thornton\\_UW\\_ToFCIMS.pdf](https://www.arm.gov/capabilities/observatories/aaf/workshop-march2020/Thornton_UW_ToFCIMS.pdf)

Uin, Janek. LED-based Nephelometer. [https://www.arm.gov/capabilities/observatories/aaf/workshop-march2020/Uin\\_LED\\_based\\_nephelometer.pdf](https://www.arm.gov/capabilities/observatories/aaf/workshop-march2020/Uin_LED_based_nephelometer.pdf)

Uin, Janek, and Chongai Kuang. Neutral Cluster and Air Ion Spectrometer.  
[https://www.arm.gov/capabilities/observatories/aaf/workshop-march2020/Uin\\_Neutral\\_Cluster.pdf](https://www.arm.gov/capabilities/observatories/aaf/workshop-march2020/Uin_Neutral_Cluster.pdf)

Wang, Jian. High-Time-Resolution Measurements of Aerosol Size Distribution Onboard Bombardier Challenger 850 Regional Jet. [https://www.arm.gov/capabilities/observatories/aaf/workshop-march2020/Wang\\_high\\_time\\_resolution\\_measurements.pdf](https://www.arm.gov/capabilities/observatories/aaf/workshop-march2020/Wang_high_time_resolution_measurements.pdf)

Wechsler, Perry, Nick Mahon, Zhien Wang, and David Leon. The Alpenglow Airborne Elastic Lidar.  
[https://www.arm.gov/capabilities/observatories/aaf/workshop-march2020/Wechsler\\_Alpenglow.pdf](https://www.arm.gov/capabilities/observatories/aaf/workshop-march2020/Wechsler_Alpenglow.pdf)

Yi, Hongming, Lei Tao, and Mark Zondlo. Open-Path Atmospheric Ammonia Sensor for the Bombardier Challenger 850 Aircraft. [https://www.arm.gov/capabilities/observatories/aaf/workshop-march2020/Yi\\_OPALS.pdf](https://www.arm.gov/capabilities/observatories/aaf/workshop-march2020/Yi_OPALS.pdf)

Zhang, Qi. Chemical Analysis of PM Samples Collected from Unmanned Aerial Platforms.  
[https://www.arm.gov/capabilities/observatories/aaf/workshop-march2020/Zhang\\_chemical\\_analysis.pdf](https://www.arm.gov/capabilities/observatories/aaf/workshop-march2020/Zhang_chemical_analysis.pdf)



[www.arm.gov](http://www.arm.gov)

U.S. DEPARTMENT OF  
**ENERGY**

Office of Science